TURUN
YLIOPISTO
UNIVERSITY
OF TURKU

EPIGENETIC REGULATION OF BONE FORMATION

Effects of LSD1 and RCOR2 on osteoblast differentiation

Petri Rummukainen

TURUN YLIOPISTON JULKAISUJA – ANNALES UNIVERSITATIS TURKUENSIS
SARJA – SER. D OSA – TOM. 1869 | MEDICA – ODONTOLOGICA | TURKU 2025

TURUN
YLIOPISTO
UNIVERSITY
OF TURKU

EPIGENETIC REGULATION OF BONE FORMATION

Effects of LSD1 and RCOR2 on osteoblast differentiation

Petri Rummukainen

TURUN YLIOPISTON JULKAISUJA – ANNALES UNIVERSITATIS TURKUENSIS
SARJA – SER. D OSA – TOM. 1869 | MEDICA – ODONTOLOGICA | TURKU 2025

University of Turku

Faculty of Medicine
Institute of Biomedicine
Medical Biochemistry and Genetics
Turku Doctoral Programme of Molecular Medicine

Supervised by

Adjunct Professor Riku Kiviranta, MD, PhD
Institute of Biomedicine
University of Turku,
Turku, Finland

Adjunct Professor Terhi Heino, PhD
Institute of Biomedicine
University of Turku,
Turku, Finland

Adjunct Professor Kaisa Ivaska, PhD
Institute of Biomedicine
University of Turku,
Turku, Finland

Reviewed by

Professor Marie Lagerquist, PhD
Institute of Medicine
University of Gothenburg,
Gothenburg, Sweden

Adjunct Professor Kirsi Ketola, PhD
Institute of Biomedicine
University of Eastern Finland,
Kuopio, Finland

Opponent

Professor Claes Ohlsson, MD, PhD
Institute of Medicine
University of Gothenburg,
Gothenburg, Sweden

The originality of this publication has been checked in accordance with the University of Turku quality assurance system using the Turnitin OriginalityCheck service.

ISBN 978-952-02-0104-3 (PRINT)
ISBN 978-952-02-0105-0 (PDF)
ISSN 0355-9483 (Print)
ISSN 2343-3213 (Online)
Painosalama, Turku, Finland 2025

To you who have been there for me

UNIVERSITY OF TURKU
Faculty of Medicine
Institute of Biomedicine
Medical Biochemistry and Genetics
PETRI RUMMUKAINEN: Epigenetic regulation of bone formation - Effects of LSD1 and RCOR2 on osteoblast differentiation
Doctoral Dissertation, 138 pp.
Turku Doctoral Programme of Molecular Medicine (TuDMM)
May 2025

ABSTRACT

Bone remodelling is regulated by a complex network of pathways and factors where multiple cell types coordinate to maintain bone strength. Different regulatory mechanisms controlling the transcription of cell type specific genes have been previously identified. The traditional transcription regulation model has been complemented through studies on mechanisms modifying chromatin availability for transcription, called epigenetic regulation. One essential epigenetic regulator modifying the accessibility of DNA is Lysine-specific demethylase 1, LSD1. LSD1 was first found in an epigenetic regulator complex with REST corepressor 1 (RCOR1). RCOR2, a paralogue of RCOR1, was later shown to replace RCOR1 in some complexes with LSD1. LSD1 has been shown to regulate differentiation of mesenchymal and hematopoietic stem cells *in vitro* and *in vivo.* However, data on the effects of LSD1 expression or loss of function on bone tissue homeostasis are conflicting between different studies and experimental models.

In this thesis, the roles of LSD1 and RCOR2 in osteoblast differentiation and function were studied using both pharmacological inhibition of LSD1 and shRNA-mediated downregulation of LSD1 and RCOR2 mRNA expression *in vitro*. The roles were further investigated *in vivo* using global and mesenchymal cell targeted conditional knockout mouse models and applying ovariectomy and closed tibial fracture healing models to highlight the effects of RCOR2 on bone formation in adult mice. Loss of LSD1 demethylation activity through pharmacological inhibition or mRNA expression led to loss of osteoblast activity both *in vitro* and *in vivo*, resulting also in the loss of growth plate chondrocyte organization and in a bone phenotype resembling osteogenesis imperfecta. The downregulation of RCOR2 *in vitro* led to inhibition of osteoblast differentiation, which was not replicated to the same extent in the mouse models *in vivo*.

These results emphasize the importance of epigenetic regulation on mesenchymal cell differentiation and bone remodelling through the histone demethylation effects of RCOR2 expression and LSD1 activity. Further understanding of various epigenetic mechanisms could lead to new therapeutic approaches for bone diseases, expanding beyond the current treatment methods.

KEYWORDS: Bone tissue, epigenetic regulation, LSD1, mesenchymal stromal cell, osteoblast, RCOR2

TURUN YLIOPISTO
Lääketieteellinen tiedekunta
Biolääketieteen laitos
Lääketieteellinen biokemia ja genetiikka
PETRI RUMMUKAINEN: Luunmuodostuksen epigeneettinen säätely – LSD1:n ja RCOR2:n vaikutus osteoblastien erilaistumiseen
Väitöskirja, 138 s.
Molekyylilääketieteen tohtoriohjelma (TuDMM)
Toukokuu 2025

TIIVISTELMÄ

Luukudoksen uudelleenmuodostusta säädellään monimutkaisella signalointireittien ja -tekijöiden verkostolla, jossa useat solutyypit toimivat yhdessä ylläpitääkseen luun lujuutta. Useita solutyypeille ominaisten geenien luentaa säätteleviä mekanismeja on tunnistettu aiemmin. Perinteistä geenien luennan säätelymallia on uuden tutkimustiedon valossa täydennetty DNA:n luettavuutta säätelevillä mekanismeilla, joita kutsutaan epigeneettiseksi säätelyksi. Yksi tärkeä DNA:n luettavuutta muokkaava epigeneettinen säätelytekijä on LSD1 (Lysine-specific demethylase 1). LSD1 tunnistettiin alun perin yhdessä RCOR1:n (REST corepressor 1) kanssa. RCOR2:n, joka on RCOR1:n geeniperheen jäsen, on osoitettu korvaavan RCOR1 joissain proteiinikomplekseissa. LSD1:n on osoitettu säätelevän muun muassa mesenkymaalisten ja hematopoieettisten kantasolujen erilaistumista. LSD1:n toiminnan tai hiljentämisen vaikutuksista luukudoksessa on kuitenkin saatu ristiriitaisia tuloksia eri tutkimusten ja koemallien välillä.

Tutkimuksessamme selvitettiin LSD1:n ja RCOR2:n merkitystä luuta muodostavien osteoblastien erilaistumisessa ja toiminnassa estämällä LSD1:n aktiivisuutta ja toisaalta hiljentämällä LSD1:n ja RCOR2:n luentaa *in vitro*. Lisäksi käytettiin mesenkymaalisiin soluihin kohdennettuja ja kohdentamattomia poistogeenisiä hiirimalleja. RCOR2:n vaikutusta tutkittiin hiirillä myös sekä murtuman paranemisen että estrogeenivajeen aikaansaaman luunmenetyksen aikana. LSD1:n aktiivisuuden ja luennan väheneminen vähensivät osteoblastien aktiivisuutta ja luunmuodostusta, saaden lisäksi aikaan kasvulevyn rustosolujen epäjärjestyksen ja luusairaus osteogenesis imperfectaa muistuttavan luuilmiasun. RCOR2:n hiljentäminen puolestaan vähensi osteoblastien aktiivisuutta *in vitro*, mutta tätä vaikutusta ei nähty samassa laajuudessa poistogeenisissä hiirimalleissa.

Väitöstutkimus korostaa epigeneettisen säätelyn ja erityisesti RCOR2:n ja LSD1:n tärkeyttä mesenkymaalisten solujen erilaistumisessa ja luun lujuuden säätelyssä. Epigeneettisten mekanismien ymmärtäminen voi tulevaisuudessa mahdollistaa uusien hoitomuotojen kehittämisen luusairauksien hoitoon.

AVAINSANAT: Luukudos, epigeneettinen säätely, LSD1, mesenkymaalinen stroomasolu, osteoblasti, RCOR2

Table of Contents

Abbreviations

ALP	Alkaline phosphatase
AOD	Amine-oxidase domain
AR	Androgen receptor
ATF	Activating transcription factor 4
BMP	Bone morphogenic protein
bp	Base pair
BV/TV	Bone volume / Tissue volume ratio
C/EBP	CCAAT/enhancer-binding protein
CBF	Core binding factor
ChIP-seq	Chromatin immunoprecipitation sequencing
cKO	Conditional knockout
COL1A1	Collagen type 1, alpha 1
CTX	C-terminal telopeptides of type I collagen
DE	Differentially expressed
DKK	Dickkopf
DLX	Distal-less homeobox
DNMT	DNA methyltransferase
ECM	Extracellular matrix
ELM	Egl-27 and MTA homology
EZH	Enhancer of zeste
FAD	Flavin adenine dinucleotide
FZD	Frizzled
HAT	Histone acetyltransferase
HDAC	Histone deacetylase
HE	Haematoxylin and eosin
HSC	Hematopoietic stem cell
IL	Interleukin
KDM	Lysine demethylase
KO	Knockout
LRP	Low-density lipoprotein receptor-related protein
LSD	Lysine-specific histone demethylase

μCT	Micro-computed tomography
MAPK	Mitogen-activated protein kinase
M-CSF	Macrophage Colony-stimulating factor
miRNA	MicroRNA
mRNA	Messenger RNA
MSC	Mesenchymal stem/stromal cell
MTA	Metastasis tumor antigen
NFAT1	Nuclear factor associated with T-cells 1
NF-κB	Nuclear factor kappa B
NuRD	Nucleosome remodelling and deacetylase complex
OCN	Osteocalcin
OM	Osteogenic medium
OPG	Osteoprotegerin
OSX	Osterix/SP7
OVX	Ovariectomy
PBS	Phosphate buffered saline
PCP	Planar cell polarity
PPARγ	Peroxisome proliferator-activated receptor-γ
PRRX1	Paired related homeobox 1
PTH	Parathyroid hormone
PTHrP	Parathyroid hormone related protein
RANKL	Receptor Activator of NF-κB ligand
RCOR	REST corepressor
REST	Repressor element-1 silencing transcription factor
RNA-seq	RNA-sequencing
ROI	Region of interest
RT-qPCR	Reverse transcription quantitative polymerase chain reaction
RUNX	Runt-related Transcription Factor
SANT	Swi3, Ada2, N-CoR, TFIIIB
SD	Standard deviation
SEMA	Semaphorin
shRNA	Small hairpin RNA
SMAD	SMA and MAD family
SSC	Skeletal stem cells
SWIRM	Swi3p, Rsc8p and Moira
TGF	Transforming growth factor
TNF	Tumor necrosis factor
TRACP	Tartrate-resistant acid phosphatase
TSS	Transcription start site
WNT	Wingless-related integration site

List of Original Publications

This dissertation is based on the following original publications, which are referred to in the text by their Roman numerals:

I Rummukainen P, Tarkkonen K, Dudakovic A, Al-Majidi R, Nieminen-Pihala V, Valensisi C, Hawkins R.D, van Wijnen A.J and Kiviranta R. Lysine-Specific Demethylase 1 (LSD1) epigenetically controls osteoblast differentiation. *PLoS ONE* 17(3): e0265027. 2022, DOI:10.1371/journal.pone.0265027

II Rummukainen P, Tarkkonen K, Al-Majidi R, Puolakkainen T, Nieminen-Pihala V, Valensisi C, Hawkins R.D, Heino T.J, Ivaska K and Kiviranta R. The Complex Role of Rcor2: Regulates Mesenchymal Stromal Cell Differentiation *in vitro* But Is Dispensable *in vivo*. *Bone,* 2024; Volume 187, 117180, https://doi.org/10.1016/j.bone.2024.117180

1 Introduction

Regulation of bone metabolism is a complex network of pathways and factors. Multiple cell types derived from stem cells of different origins work together to maintain the optimal balance of bone volume and structural integrity. The traditional model of gene expression regulation, which focuses on transcription factor expression, has later been complemented with epigenetic regulation, which involves managing chromatin accessibility, allowing transcription factors to bind without altering the DNA structure.

Osteoporosis, the loss of bone density and mass leading to increased risk of fractures is a disorder diagnosed in 18.3% of people worldwide, especially in women over the age of 50 years (Salari et al., 2021). The increased fracture risk has been linked to increased post-fracture mortality rate. Treatment of osteoporosis includes exercise, nutritional supplements, hormone therapies (selective estrogen receptor modulators and estrogen), bisphosphonates, romosozumab, a sclerostin inhibitor and denosumab, a RANKL inhibitor. Treatment options available are still limited and novel therapeutic targets to treat osteoporosis are needed. One promising approach could be utilizing the epigenetic regulation of key transcription factors in osteoblasts to enhance bone formation. However, the mechanisms of epigenetic regulation in bone cells are not yet fully elucidated and this area is currently a topic of active research (Sharma et al., 2024).

One strong epigenetic regulator is the lysine-specific demethylase 1, LSD1. LSD1 was first discovered together with REST corepressor 1 (RCOR1) as a member of an epigenetic regulator complex, which was further identified as a REST binding regulatory complex (Andrés et al., 1999; You et al., 2001). LSD1 and its family member LSD2 are members of the AOD-containing subfamily of lysine demethylases (Polticelli et al., 2005). LSD1 has since been investigated in bone remodelling and was found to regulate the differentiation of mesenchymal stem cells to adipocytes, chondrocytes and osteoblasts as well as hematopoietic stem cells to osteoclasts (Doi et al., 2022; Rodova et al., 2011; Sun et al., 2018). LSD1 expression and activity is necessary for normal differentiation and activity of osteoblasts *in vitro* and *in vivo* (Sun et al., 2018). However, the data on the effects of LSD1 across different studies are complex, ranging from support of osteoclast differentiation (Doi

et al., 2022) to enabling callus formation during endochondral bone formation (Sun et al., 2020).

RCOR2 (also known as CoREST2) was found in a complex with histone deacetylases 1 and 2 (HDAC1/2), BHC80 and LSD1 similarly to CoREST/RCOR1 and capable of facilitating the nucleosomal demethylation activity of LSD1. RCOR2 is most studied in the context of embryonic stem cell maintenance and reprogramming of somatic cells (P. Yang et al., 2011). The role of RCOR2 in osteoblasts has previously remained unstudied. Our preliminary RNA-sequencing data collected during MC3T3-E1 osteoblast differentiation suggested that both LSD1 and RCOR2 were expressed in osteoblasts.

Previous data has demonstrated that LSD1 activity is essential to the long bone development and growth plate organization (Sun et al., 2018, 2020), however the mechanism behind the effects of targeting LSD1 in osteoblasts remains to be studied in more detail. Especially, the discrepancies between different mouse models remain to be elucidated.

The aim of this study was to investigate the expression, demethylation activity and roles of LSD1 and RCOR2 in bone. Based on our preliminary studies, we decided to study in depth the role of RCOR2 and LSD1 in differentiating osteoblasts. To achieve this, we inhibited LSD1 demethylation activity and downregulated the expression of LSD1 and RCOR2 in osteoblasts differentiated from the MC3T3-E1 cell line, as well as in primary calvarial osteoblasts collected from newborn mice. To further study the role of LSD1 in a more clinically translatable model than the cell culture models, we treated wild type mice with a selective LSD1 inhibitor and investigated the bone effects. Finally, we created knockout mouse models by deleting LSD1 or RCOR2 globally or conditionally using targeted deletion in limb bud mesenchymal cells and applying ovariectomy and closed tibial fracture healing models to highlight the effects of RCOR2 on bone regulation.

2 Review of the Literature

2.1 Bone, a complex tissue with multiple functions

Bone as a rigid, mineralized connective tissue has various important functions; bones protect our vital organs from damage by forming a protective cage, enable our movement together with muscles and cartilage, and harbour our blood cell formation. Bone is also an active endocrine organ, which stores minerals to be released as a response to parathyroid hormone (PTH) as well as secretes hormone-like molecules, such as osteocalcin (OCN) in the circulation (Guntur & Rosen, 2012; Jilka et al., 2010).

Bone tissue undergoes constant renewal as changes in mechanical loading, microdamage and other external stimuli direct the remodelling of bone. As Wolff's Law proposed already in 1892 describes, bones adapt to the mechanical loading they bear and respond to it by increased strength of the inner spongy bone called trabecular bone, followed by thickening of the outer layer called cortical bone. Similarly, decrease in loading leads to loss of strength in both trabecular and cortical bone (Frost, 1994). Response to changes in loading is proposed to be detected by the mechanosensing osteocytes embedded inside the bone matrix, which further signal to the cells on the bone surface to meet the changed needs, forming a signalling loop of different cell types performing remodelling cycles where and when necessary (Mullender et al., 2004).

2.1.1 Bone cells

Bone tissue consists of extracellular matrix (ECM) and four different cell types: bone resorbing osteoclasts, bone forming osteoblasts, bone lining cells and bone signalling osteocytes (Florencio-Silva et al., 2015). Osteoclasts originate from hematopoietic stem cells (HSCs) whereas osteoblasts and osteocytes are derived from mesenchymal stem/stromal cells (MSCs). Chondrocytes (fundamental cells in growth plate, articular cartilage and forming the cartilage intermediate for indirect bone formation) and actively signalling and energy storing adipocytes are also of MSC-origin and can be found both near and within bone tissue (Kolf et al., 2007). HSCs also give rise to a multitude of other cell types, such as red blood cells, myeloid

and lymphoid white blood cells and platelets (Cheng et al., 2020). Both HSCs and MSCs are maintained in niches, which are specific molecular and cellular environments surrounding the stem cells, aiming to maintain the naïve state (Kolf et al., 2007; Morrison & Scadden, 2014). The MSC and HSC niches are located near the vasculature in the bone marrow and comprises different cell types, such as pericytes (Kolf et al., 2007) and mesenchymal stromal cells (Morrison & Scadden, 2014). The HSC niches in adults are found in the bone marrow of long bones (Frisch, 2019), while MSC niches or MSC-like cell niches are found perivascularly in different tissues throughout the body (Blashki et al., 2006; Meirelles et al., 2006).

Osteoblast differentiation originates from the mesenchymal stem/stromal cell. Mesenchymal stem cells differentiate into osteoblasts, adipocytes and chondrocytes, but they can also transdifferentiate into cells of the ectoderm (epithelial cells, neurons) and endoderm layer (myocytes, gut epithelia), among others (Uccelli et al., 2008). Cells extracted from different tissues and cultured *in vitro* with proliferation and differentiation capacity were previously collectively called mesenchymal stem cells. As the potential of mesenchymal stem cells as a research target was established, different protocols for extraction and *in vitro* culture were published, some with great variability (Marote et al., 2023; Salerno et al., 2020; A. Wilson et al., 2019; A. J. Wilson et al., 2023). To improve the reproducibility and standardize the nomenclature in MSC research, the International Society for Cell & Gene Therapy coined the name Mesenchymal stromal cell to cells which are plastic-adherent, possess a specific surface antigen pattern and have differentiation capability to osteoblasts, adipocytes and chondrocytes (Dominici et al., 2006). Recently another subpopulation of mesenchymal stem cells has been defined, residing in the adult skeleton and capable of differentiation into osteoblasts, adipocytes and chondrocytes: the skeletal stem cells (SSCs) (Melis et al., 2024). SSCs are mesenchymal cells with self-renewal and multipotency capabilities. They are a subpopulation of the skeletal stem and/or progenitor cells (SSPCs), and pure populations of SSCs have been difficult to identify (Melis et al., 2024). In this study, the primary cells extracted from newborn mouse calvarias, cultured and differentiated are considered mesenchymal stromal cells.

Differentiation of a mesenchymal stem cell towards a bone forming cell is gatekept by transcription factors and growth factors, such as bone morphogenic proteins (BMP) and wingless-related integration site (WNT) proteins (**Figure 1**) (Ponzetti & Rucci, 2021; Zhu et al., 2024). The osteo-chondroprogenitor cell further commits to osteoblast lineage through expression of master transcription factors, such as osterix (OSX/SP7), runt-related transcription factor 2 (RUNX2) and distal-less homeobox 5 (DLX5) (Ponzetti & Rucci, 2021; Rutkovskiy et al., 2016). The committed osteoprogenitor cell then progresses to a pre-osteoblast expressing osteoblast markers such as alkaline phosphatase (ALP) and type 1 collagen (COL1) (Ponzetti & Rucci,

2021; Rutkovskiy et al., 2016). Expression of these markers continue throughout the lifespan of the osteoblast, but different levels can be expressed depending on the functional activity of mature osteoblasts before terminal differentiation (Ponzetti & Rucci, 2021; Zhu et al., 2024). Osteoblasts can have three different fates: maturing into mechanosensing osteocytes buried inside the bone ECM during active bone formation, becoming inactive bone lining cells protecting the surface of the bone from osteoclast activity, or dying by apoptosis at the end of the lifespan (**Figure 1**) (Ponzetti & Rucci, 2021; Rutkovskiy et al., 2016; Zhu et al., 2024).

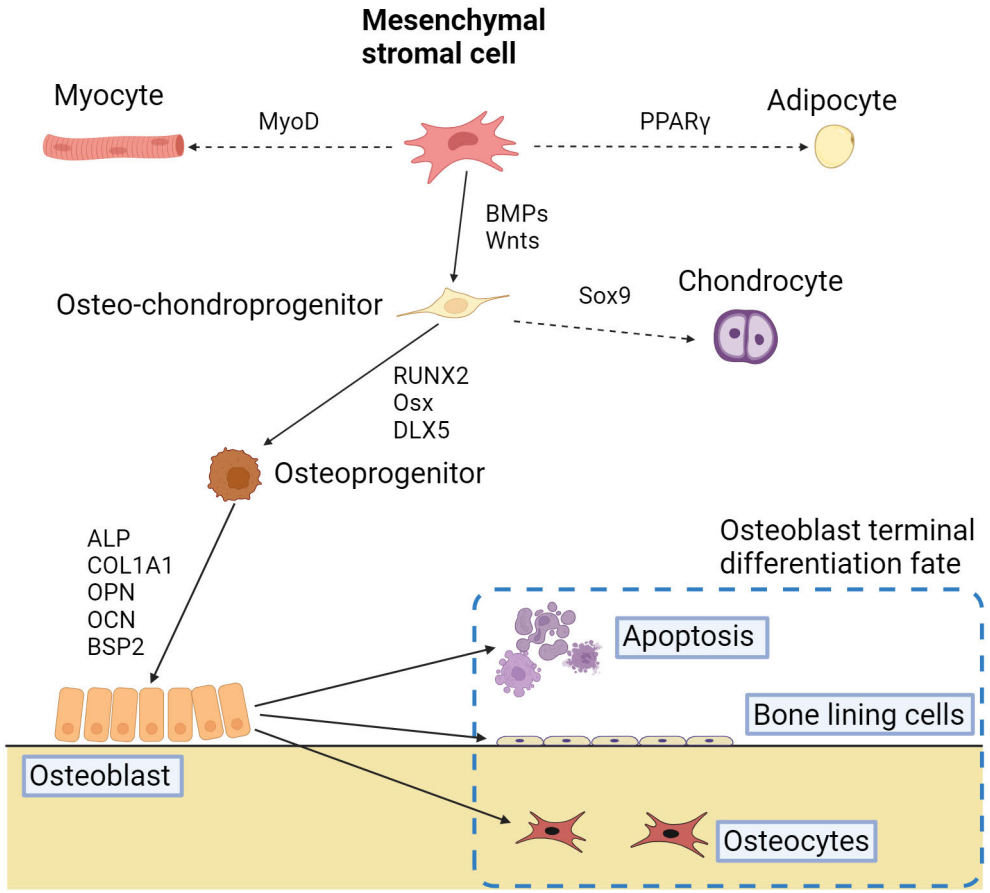

Figure 1. Differentiation of mesenchymal stem/stromal cells to osteoblasts and other cell types. Mesenchymal stem cell differentiation into osteo-chondroprogenitors is induced by BMP and WNT signalling. Further commitment and differentiation into osteoblasts leads either to apoptosis, or terminal differentiation into bone lining cells or osteocytes. PPARγ, peroxisome proliferator-activated receptor gamma; MyoD, myoblast determination protein 1; Sox9, SRY-box transcription factor 9; OPN, osteopontin; OCN, osteocalcin; BSP2, bone sialoprotein 2. Modified from Ponzetti & Rucci 2021 & Rutkovskiy et al., 2016. Created in BioRender.com

Osteoclasts differentiate from HSCs via the myeloid committed precursors and macrophage/dendritic cell precursors. After osteoclast precursors have differentiated to mononucleated osteoclasts, further activation/maturation leads to fusion of mononucleated osteoclasts into multinucleated osteoclasts, which after attachment to bone matrix and formation of resorption canopy are active, bone-resorbing osteoclasts (Edwards & Mundy, 2011; Kim et al., 2020). Commitment of HSCs and early differentiation of osteoclasts is driven by macrophage colony-stimulating factor (M-CSF) and receptor activator of NF-κB ligand (RANKL) (**Figure 2**) (Edwards & Mundy, 2011; Kim et al., 2020; Long & Humphrey, 2012). After activation and resorption activity, murine multinucleated osteoclasts can fission into mono- or multinucleated osteomorphs or undergo apoptosis (Jansen et al., 2012; McDonald et al., 2021).

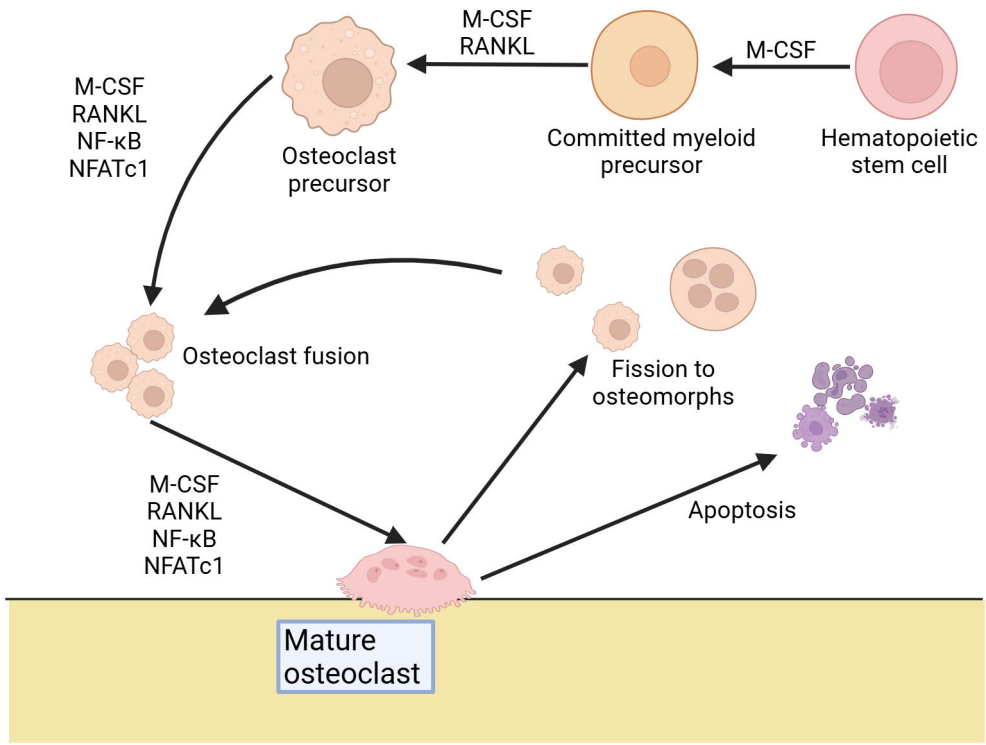

Figure 2. Osteoclast differentiation and life cycle. Osteoclast early differentiation from hematopoietic stem cell is induced by macrophage colony-stimulating factor (M-CSF) and receptor activator of NF-κB ligand (RANKL). Differentiation, fusion and maturation is seen as osteoclast marker gene expression. Mature osteoclast inactivation and detachment can result in apoptosis or fission to mononuclear osteoclasts through the osteomorph intermediate. NF-κB, nuclear factor kappa B; NFATc1, nuclear factor associated with T-cells 1. Modified from Edwards & Mundy 2011 & Long & Humphrey 2012. Created in BioRender.com

Bone renewal is a constant physiological process which is seen continuously in normal bone. The interplay of osteoclasts, osteoblasts and their precursors is normally orchestrated into a balanced process of controlled bone resorption followed by bone formation, called bone remodelling cycle (**Figure 3**) (Bhardwaj et al., 2022; Kim et al., 2020). The cycle begins with the recruitment of osteoclast precursors maturing into functional osteoclasts in the resorption phase. Osteoclasts resorb the mineralized matrix at the remodelling site through the release of hydrogen ions and proteolytic enzymes such as cathepsin K and collagenase into the resorption pit formed between cells and the bone ECM surface, thus degrading the previously formed inorganic and organic matrix. After resorption, osteoclasts are detached from the bone surface and undergo apoptosis or fission to osteomorphs (Bhardwaj et al., 2022). Thereafter osteoblast precursors are attracted to the remodelling site, and osteoblast differentiation begins in the reversal phase. The exact mechanisms of the reversal phase are still poorly understood, although some details have been discovered. The key phenomenon of the phase is reversing the conditions from osteolytic to osteogenic, connected to the recruitment of a macrophage subtype called osteomacs (Bhardwaj et al., 2022; Delaisse, 2014). The balance between resorption and formation results only in small changes in bone mass or strength after each remodelling cycle in mature, healthy bone is finished (Kim et al., 2020).

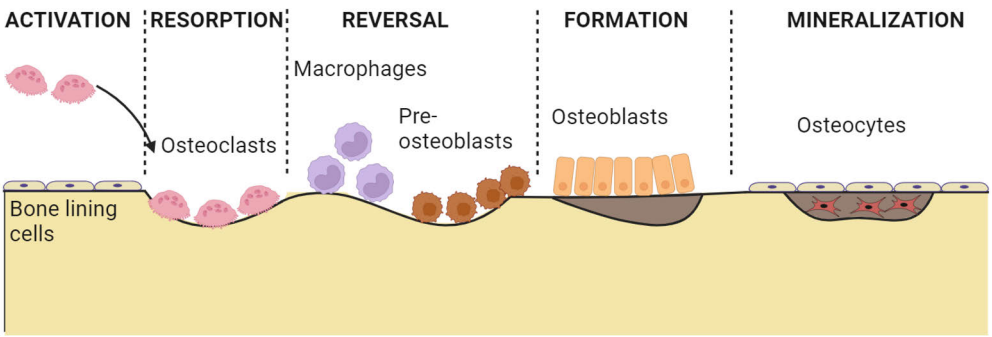

Figure 3. Simplified representation of the bone remodelling cycle: Osteoclasts are recruited to replace the bone lining cells on the bone surface, mature into multinuclear cells and resorb the bone. Reversal phase begins with detachment of osteoclasts and replacement with maturing osteoblasts, followed by bone formation by osteoblasts producing new bone matrix (osteoid) and this matrix is mineralized. Modified from Bhardwaj et al., 2022. Created in BioRender.com

The delicate balance of bone remodelling requires crosstalk between osteoclasts, osteoblasts and osteocytes (**Figure 4**). Osteocytes, in response to changes in mechanical stimuli and shear stress, signal to osteoclasts through RANKL, osteoprotegerin (OPG), interleukin-1 beta (IL-1β), and insulin-like growth factor 1

(IGF-1) and to osteoblasts through sclerostin (SOST), IL-6 and IGF-1, among others (Kitaura et al., 2020). Osteoclast differentiation is stimulated also by osteoblasts through factors like M-CSF, RANKL and WNT5a. After bone resorption has ended, osteoclast differentiation is suppressed by osteoblast-derived OPG and WNT16 (Edwards & Mundy, 2011; Kim et al., 2020). Osteoclasts on the other hand can signal back to osteoblasts through sphingosine 1-phosphate (S1P), collagen triple helix repeat containing-1 (CTHRC1) and complement component C (C3) secretion to promote and through semaphorin 4D (SEMA4D) to suppress their differentiation (Kim et al., 2020). Osteoblasts and osteoclasts also signal using direct juxtacrine cell-cell interactions through e.g. Ephrin B2, FS-7-associated surface antigen (FAS) and SEMA3A (Kim et al., 2020). The OPG–RANKL–RANK cross-signalling is of key importance to the regulation of bone remodelling, where most regulators which upregulate RANKL expression simultaneously downregulate OPG expression or upregulate it significantly less (Kitaura et al., 2020). These regulators affect the OPG/RANKL ratio, which drives the balance from bone resorption to bone formation or vice versa.

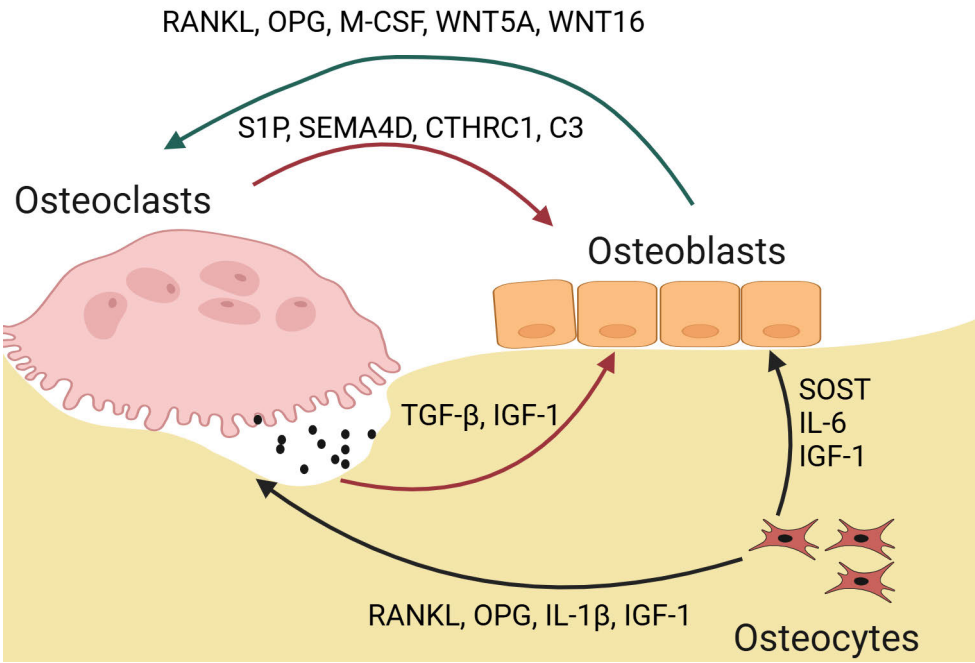

Figure 4. Crosstalk of osteoclasts, osteoblasts and osteocytes and various factors identified in this context. Osteoblasts and osteoclasts can signal with each other through soluble signalling molecules and growth factors. Bone-embedded osteocytes can both induce and repress osteoblast and osteoclast differentiation. Osteoclasts signal to osteoblasts also through signals secreted and released from the ECM during the resorption. TGF-β, transforming growth factor beta. Modified from Kim et al., 2020 & Kitaura et al., 2020. Created in BioRender.com

2.1.2 *In vivo* models of bone research

Multiple different *in vitro* models are used to study remodelling and crosstalk between different cell types. However, for bone research, the complexity of the remodelling cycle including different cell types and metabolic regulators as well as endocrine regulation via remote organs limits the translatability of *in vitro* results with current technologies. This directs the most complex experiments on crosstalk and cross-regulation towards *in vivo* experiments.

The basis of ethical research when planning to use live animals is to when applicable, always 1) use either *in vitro* experimentation, or 2) use the least developed models applicable to the experiment setting or 3) use primary cells (Replacement in 3R) (NC3Rs, 2024). Among the available animal species, *Mus musculus* (the house mouse) is currently the preferred model organism in research applying genetically modified models. The choice is largely due to the similarities of bone formation process compared to humans, combined with the vast knowledge of the mouse genome. Other animal models applied in bone research are zebrafish, rats, rabbits, dogs, sheep, goats, pigs or non-human primates. Similarly to other research fields, key models of *in vivo* bone research nowadays include genetically modified models. In addition, hormonal interference, surgical procedures, pharmaceutical treatments or limitation of movement can be used to adjust the bone microenvironment and thereby remodelling (Schafrum Macedo et al., 2019).

With the introduction of modification of embryonal DNA, global gene knockout (KO) and conditional gene knockout (cKO) models have been established. Since the establishment of the Cre-LoxP system (Sauer & Henderson, 1988), sections of DNA can be removed from either all cells of an organism, or from a specific cell type or at a specific point of differentiation, depending on the gene promoter of choice. For example, the target gene can be excised from osteoblast DNA in the limb bud development phase (Prrx1-Cre), in early osteoblast development phase (OSX-Cre) or in mature osteoblasts (OCN-cre) (Kitase & Prideaux, 2023). More recent technologies, such as CRISPR/Cas9, allow for instance modification or introduction of the target DNA sequence *in vitro* or *ex vivo* (Redman et al., 2016).

The main focus of bone research revolves around the cellular and molecular mechanisms leading to osteoporosis and finding possible therapeutic targets through osteoblast activation or osteoclast inactivation. In humans, significant risk factors of developing osteoporosis are aging, changes in estrogen and testosterone production, immobility and poor nutrition as well as certain medications or diseases (secondary osteoporosis) (National Institute of Arthritis and Musculoskeletal and Skin Diseases, 2024). To model the effect of changes in reproductive hormone levels on bone, animals can be subjected to surgical removal of ovaries (ovariectomy) or testicles (orchidectomy) or be administered drugs to inhibit the production or effects of reproductive hormones. Bone loss can also be modelled in animals by

immobilization or limiting load of a limb. The nutritional state of animals can be adjusted using a specific diet and aging can be taken into account when selecting time points for sampling and/or treatment (Schafrum Macedo et al., 2019). Another similarly complex modality of accelerated bone remodelling is fracture healing, which includes multiple phases from inflammation, stem cell recruitment, callus formation and eventually bone remodelling and modelling. Due to the interplay and differentiation of nearly all cell types of MSC-lineage as well as various other cell types, fracture healing and osteoporosis are complex phenomena (Y. Li et al., 2018; Schafrum Macedo et al., 2019).

2.2 Molecular regulation of bone formation

The balance between bone formation and resorption is regulated through a network of signalling mechanisms and their downstream effectors. While allowing remodelling to adapt to changes in mechanical loading and structural micro- and macrodamage, also the integrity of the skeleton, mineral deposits and stable levels of calcium ions in blood have to be maintained. Some of the most important bone regulating transcription factors, growth factors and hormones are discussed below, focusing on the primary cell type studied, osteoblasts.

2.2.1 Transcription factors regulating osteoblast differentiation

Transcription factors are proteins regulating the transcription of genes with their common features: the DNA-binding domain, which is necessary for the recognition of the binding motif (a specific target sequence), the regulatory domain facilitating the repression or induction of transcription and the dimerization domain. Not all transcription factors harbour all these domains, but a combination of these is seen in most transcription factors (Slack, 2014). Differentiation of MSCs to osteoblasts is regulated by numerous transcription factors (**Figure 1**), some of which are described here (**Table 1**).

RUNX2

RUNX2 (also known as core binding factor alpha, CBFα and polyomavirus enhancer binding protein PEBP2), is expressed in the late stage of mesenchymal condensation and directs osteo-chondroprogenitors to differentiate into osteoblasts. RUNX2 is highly expressed in osteoblasts and less in chondrocytes. RUNX2 is vital for osteoblast differentiation and skeletal development, since no mature osteoblasts or mineralized bone matrix are found in RUNX2 knockout mice (Komori et al., 1997).

In addition, induced RUNX2 expression leads to ectopic bone formation and expression of osteoblast-specific genes in cells of non-osteoblast background (X. Yang & Karsenty, 2002). In turn, decreased RUNX2 expression in osteo-chondroprogenitors directs differentiation to chondrocytes, while in maturing chondrocytes RUNX2 expression is restored (Rashid et al., 2021; Rutkovskiy et al., 2016). RUNX2 binds with core binding factor beta (CBFβ) and controls the expression of several genes required for osteoblast function, such as *OSX,* osteocalcin, osteopontin, bone sialoprotein and *COL1A1*. RUNX2/CBFβ heterodimers have a DNA-recognition sequence TGTGGT, a property preserved in all three RUNX family members (Chan et al., 2021; Zhu et al., 2024). In osteoblasts, RUNX2 also upregulates glucose transporter 1 expression, thus supporting osteoblast differentiation as glucose is the main energy source for osteoblasts (Wei et al., 2015).

RUNX1, which is another member of the RUNX transcription factor family and plays a major role in hematopoiesis, is also important for osteoblast differentiation. Expression of RUNX1 in progenitor cells inhibits the differentiation into adipocytes and induces early differentiation to both osteoblasts and chondrocytes (Lian et al., 2003; Tang et al., 2020), while loss of RUNX1 impairs differentiation of both osteoblasts and chondrocytes (Y. Wang et al., 2005). The last family member, RUNX3 is expressed in osteoblasts and chondrocytes (Yamashiro et al., 2002). Knockout studies have shown that RUNX3 controls chondrocyte differentiation in both early and late stages (Soung et al., 2007) and that the loss of RUNX3 leads to osteopenia (Bauer et al., 2015).

Osterix

Osterix is a member of the Krüppel-like family of proteins expressed specifically in osteoblasts. RUNX2 controls OSX expression, demonstrated by RUNX2 knockout mice lacking OSX expression, while RUNX2 is expressed in OSX knockout mice. Similarly to RUNX2 knockout mice, OSX knockout mice also lack osteoblasts (Nakashima et al., 2002). Osterix expression has been found to overlap and succeed RUNX2 expression in osteoblasts during commitment and differentiation, controlling the maturation of osteoblasts. Interestingly, treatment of osteoblasts lacking RUNX2 with BMP2 induced the expression of OSX, suggesting an alternative pathway for OSX induction not normally seen in osteoblasts (M.-H. Lee et al., 2003). Osterix has multiple known and suggested downstream targets, such as early B cell factor 1 (EBF1), zinc finger and BTB domain-containing 16 (ZBTB16), fibrillin-2 (FBN2) and periostin (POSTN) (S.-J. Lee et al., 2017; Nieminen-Pihala et al., 2021; Onizuka et al., 2016).

Other transcription factors

The family of SMADs, named as a fusion of SMA and MAD families, mediates the downstream effects of the transforming growth factor beta (TGF-β) superfamily. SMADs are categorized into three different types: Receptor-regulated SMADs, co-SMADs and inhibitory SMADs (Massagué et al., 2005). Receptor-regulated SMADs are activated by TGF-βs (SMAD2/3) or BMPs (SMAD1/5/8) and trimerize with the co-SMAD SMAD4 to become activated as transcription factors, translocate to the nucleus and bind their SMAD-binding element sequence, GTCTAGAC (Derynck et al., 1998; Massagué et al., 2005; Zawel et al., 1998). Inhibitory SMADs (SMAD6/7) repress the activity of receptor-regulated SMADs with SMAD6 showing more targeted activity towards inhibiting BMP signalling and SMAD7 towards TGF-β signalling (Derynck et al., 1998; Massagué et al., 2005; Zawel et al., 1998). SMADs control mouse osteoblast differentiation and chondrocyte maturation through the regulation of RUNX1/2 activity as well as by functioning directly as transcription factors (Canalis et al., 2003; D. Chen et al., 2004; Valcourt et al., 2002).

Activating transcription factor 4 (ATF4) dimerizes with various transcription factors to modulate the regulation of bone formation. For example, ATF4 induces osteocalcin expression by first forming a dimer with CCAAT-enhancer-binding protein beta (C/EBPβ) (St-Arnaud & Hekmatnejad, 2011). This facilitates the binding of ATF4 and RUNX2 to the osteoblast-specific cis-acting elements 1 and 2 in the osteocalcin gene promoter and induces gene expression (St-Arnaud & Hekmatnejad, 2011; G. Xiao et al., 2005; Zhu et al., 2024).

Table 1. Key transcription factors controlling osteoblast commitment, differentiation and maturation.

FAMILY	MEMBERS	FUNCTION
RUNX	RUNX1	Promotes osteoblast and chondrocyte differentiation
	RUNX2	Promotes osteoblast differentiation and chondrocyte maturation Inhibits chondrocyte differentiation and osteoblast maturation
	RUNX3	Promotes chondrocyte differentiation
OSTERIX		Promotes osteoblast differentiation and maturation
SMAD	SMAD2/3	TGFβ-activated SMADs, promote early osteoprogenitor proliferation and inhibit osteoblast maturation
	SMAD1/5/8	BMP-activated SMADs, promote early osteoprogenitor proliferation and chondrocyte maturation
	SMAD4	Co-activator SMAD
	SMAD6/7	Inhibitory SMADs
ATF4		Promotes terminal differentiation of osteoblasts and osteocalcin expression

2.2.2 Growth factors regulating osteoblast differentiation

Growth factors are typically secreted proteins or hormones capable of inducing the growth, proliferation and differentiation of cells. Growth factors influence bone metabolism in multiple different ways during both skeletal development and bone remodelling during tissue maintenance, response to changes of mechanical loading and repair of damage on bone tissue (**Figure 1**, **Table 2**).

TGF-β superfamily

The TGF-β superfamily of growth factors includes the BMPs, TGF-βs, growth differentiation factor (GDF), activin, inhibin and left-right determination factor (LEFTY) subfamilies, of which the BMP and TGF-β subfamilies will be discussed in this context.

The BMP subfamily consists of 13 proteins. BMPs 2, 4, 6, 7 and 9 have been demonstrated to have stimulatory effects on bone formation while BMPs 3 and 12 suppress bone formation. BMPs effecting bone regulation are secreted by mesenchymal cells (Daluiski et al., 2001; Peng et al., 2003). BMPs can signal downstream through SMAD1/5/8, for example SMAD1 drives the degradation of β-catenin through interaction with Dishevelled-1, an inhibitor of glycogen synthase kinase-3 beta (GSK-3β). This leads to repression of canonical Wnt-signalling (Liu et al., 2006; Zhu et al., 2024). BMPs are also able to signal through pathways other than SMADs. For example, BMP-2 induces RUNX2 and Osterix expression through the activation of MAPK pathway and DLX5 in human MSCs (Celil et al., 2005) and mouse C2C12 cells (Celil et al., 2005; K.-S. Lee et al., 2002). Due to the strong capacity of BMP-2 and BMP-7 to induce and enhance bone formation, they are used in clinical practice in orthopaedic and dental surgeries to promote bone healing and regeneration (Friedlaender et al., 2001; Govender et al., 2002).

The TGF-β subfamily has 3 members, TGF-β 1-3, all of which are expressed widely in different cell types, including osteoblasts, chondrocytes and membranes surrounding cartilage and bone. TGF-βs are stored in ECM and released during osteoclastic bone resorption and they act as important coupling factors of bone resorption and formation (**Figure 4**). TGF-βs are key regulators of osteoblast proliferation and early differentiation but suppress late differentiation. TGF-βs signal through SMAD2/3 and SMAD4. In addition, TGF-βs can signal through SMAD1/5/8 by binding anaplastic lymphoma kinase 1 (Wu et al., 2016; Zhu et al., 2024). The activation of SMAD2/3 leads to direct inhibition of RUNX2 expression, as well as recruitment of histone deacetylases (HDACs) 4 and 5 to repress RUNX2 (J. S. Kang et al., 2005). Independent of SMADs, TGF-βs induce RUNX2 and OSX expression through activating the MAPK pathway (K.-S. Lee et al., 2002).

WNT signalling

The WNT family of glycoproteins is divided into two sub-families based on their downstream pathways: canonical signalling sub-family (Wnt ligands 1, 2, 2b, 3, 8a, 8b, 9a, 9b, 10a, 10b and 16) and non-canonical signalling subfamily (Wnt ligands 2b, 3a, 4, 5a, 5b, 6, 7a, 7b, 9a, 9b, 11 and 16), both of which signal through the frizzled (FZD) receptor family (Chae & Bothwell, 2018). There are 19 family members which can be either membrane-bound or secreted, but all require activation through FZD for downstream effects (J. Liu et al., 2022).

The canonical signalling pathway activation includes binding of WNT ligands to FZD and recruitment of the low-density lipoprotein receptor-related protein 5/6 (LRP5/6) to the receptor. The activated receptor then inactivates the GSK-3β inhibitor Dishevelled, allowing β-catenin to escape ubiquitination and degradation and to accumulate in the nucleus activating the transcription factors T-cell factor (TCF) and lymphoid enhancer factor 1 (LEF1) (Hu et al., 2024; Zhu et al., 2024). In osteoblasts, canonical WNT-signalling induces osteoblast differentiation and inhibits adipocyte and chondrocyte differentiation through upregulation of RUNX2, DLX5, Osterix and downregulation of adipocyte master regulator PPARγ gene expression (Hu et al., 2024).

Non-canonical WNT signalling includes two pathways, the WNT/planar cell polarity (PCP) pathway and the WNT/Ca^{2+} pathway. The WNT/PCP pathway induces the polarization of epithelial cells to apical and basal axis, regulating processes of cell morphology and movement as well as cell fate determination. The WNT ligands for WNT/PCP pathway signal through FZD receptors, but instead of LRP5/6, recruit other co-receptors such as receptor tyrosine kinase–like orphan receptor 1/2 (ROR1/2) and related to receptor tyrosine kinase (RYK) to the cell surface. The receptor activation leads to recruitment of Dishevelled, further activating c-JUN-N-terminal kinase and Rho kinase (Kobayashi et al., 2008; Zhu et al., 2024). Activation of the WNT/PCP pathway has been described to stimulate the abnormal mineralization in osteoblasts collected from osteoarthritis patients (Martineau et al., 2017) and to regulate the expression of adipocyte markers through histone methylation of *PPARγ* in murine MSCs (Takada et al., 2007).

The WNT/Ca^{2+} pathway raises intracellular calcium concentration after receptor activation followed by inositol 1,4,5-triphosphate and diacylglycerol production and inactivation of protein kinase G. The increase of intracellular calcium activates calcineurin, protein kinase C and Ca^{2+}/calmodulin-dependent protein kinase II (Hu et al., 2024), leading to transcription of factors regulating osteoclast differentiation, such as nuclear factor κB (NF-kB), nuclear factor associated with T cells (NFAT) and cAMP-responsive element-binding protein in osteoclasts (Sato et al., 2006). WNT/Ca^{2+} pathway has not been reported to regulate osteoblast differentiation directly but increase of intracellular calcium has been reported to effect β-catenin

translocation to the nucleus in human prostate cancer cells (Thrasivoulou et al., 2013).

The different modalities of WNT signalling are regulated by multiple other proteins. Dickkopf (DKK) family members DKK1, DKK2 and DKK4 are inhibitors of canonical WNT signalling. DKK1/2/4 inhibit the binding of LRP with FZD both by directly binding the co-receptors LRP5/6 and through the recruitment of Kremen 1 and Kremen 2 (Niehrs, 2006). Secreted frizzled-related proteins inhibit both canonical and non-canonical WNT signalling through competitive binding of WNT ligands (Zhang et al., 2023). Another WNT inhibitor sclerostin inhibits both BMP signalling by binding the BMP receptors (Winkler et al., 2003) and canonical WNT signalling by binding LRP5/6 and inhibiting the interaction of the co-receptor and FZD (X. Li et al., 2005). Anti-sclerostin antibodies are used in treatment of osteoporosis of postmenopausal women, both suppressing bone resorption and enhancing bone formation (Rauner et al., 2021).

Table 2. Key growth factors regulating osteoblast differentiation.

FAMILY	MEMBERS	FUNCTION
TGF-β	TGF-β1-3	Promotes osteoblast proliferation and early osteoblast differentiation, inhibits late osteoblast differentiation
	BMP-2, BMP-4, BMP-6, BMP-7, BMP-9	Promote bone formation
	BMP-3, BMP-12	Suppress bone formation
WNT	Canonical Wnt-signalling: Wnt1, 2, 3, 8a, 8b, 10a and 10b	Induce osteoblast differentiation, inhibit osteoclast differentiation, increase bone mass
	Non-canonical Wnt-signalling: Wnt3a, 4, 5a, 5b, 6, 7a, 7b and 11	Promote osteoclast differentiation

2.2.3 Hormonal regulation of bone formation and maintenance

Bone remodelling is regulated by hormones, such as parathyroid hormone (PTH), testosterone, estrogen, growth hormone, insulin, IGF-1 and thyroid hormone. The hormonal regulation of bone remodelling is influenced by various external stimuli, such as serum calcium levels, age, nutrition and sex hormone binding globulin (SHBG) levels (Mallorie & Shine, 2022; Narla & Ott, 2018).

Parathyroid hormone family is a family of two proteins, parathyroid hormone (PTH) and parathyroid hormone related protein (PTHrP). PTH is an 84 amino-acid peptide released from the parathyroid glands in response to decreased blood calcium

levels. PTH regulates calcium levels through its effects on kidneys, small intestine and bone (Silva & Bilezikian, 2015; Wein & Kronenberg, 2018). PTHrP is a 141-amino-acid peptide released from various cell types, such as osteoblasts, neuronal tissues and chondrocytes among others (Datta & Abou-Samra, 2009). Two receptors have been discovered, of which parathyroid hormone type 1 receptor is expressed highly in bone and kidneys and recognizes both PTH and PTHrP, while the type 2 receptor expressed in pancreas and kidneys only has one ligand, PTH (Mannstadt et al., 1999).

Multiple pathways have been discovered downstream of PTH binding to its receptor PTH1R in bone. One key pathway is the PTH–ATF4–OSX axis, where ATF4 binds to a response element in the proximal *OSX* promoter after PTH-induced activation, leading to anabolic bone activity (S. Yu et al., 2009). Another important mechanism is the regulation of OPG–RANKL–RANK system, where PTH regulates the expression of both OPG and RANKL, modulating the activation of RANK and subsequently osteoclastogenesis (Kanzawa et al., 2000; Silva & Bilezikian, 2015). Increased PTH level is however not directly predictive of the bone remodelling balance. In cases of extended treatment with PTH or its analogues, anabolic effects on bone are lost and replaced with catabolic effects due to the reversed ratio of OPG/RANKL (Silva & Bilezikian, 2015).

Sex hormones estrogen and testosterone play important roles in both male and female physiology. The previously assumed, more traditional gender-dependent model of hormone preference, where testosterone regulates bone formation in men and estrogen in women, has been refined over time. An updated model (Narla & Ott, 2018) suggests that the maintenance of cortical bone is controlled by estrogen in both males and females, while the preferential hormone in the maintenance of trabecular bone depends on gender, where testosterone plays a more dominant role in males and estrogen in females.

Sex hormones have an anabolic effect on bone and their production is controlled by the release of gonadotropin-releasing hormone from the hypothalamus followed by follicle stimulating hormone and luteinizing hormone release from the anterior pituitary gland. The amount of estrogen and testosterone in the blood stream is maintained by the production of SHBG and albumin from the liver. Testosterone can also be converted to estrogen by the aromatase enzyme (Khosla & Monroe, 2018; Narla & Ott, 2018). There are two main nuclear receptors for estrogen, estrogen receptor alpha and beta, both expressed in bone (Dahlman-Wright et al., 2006; Vanderschueren et al., 2004) , while there is only one known androgen receptor (AR) in humans.

Multiple pathways by which sex hormones mediate their effects on bone tissue have been found. Estrogen inhibits the expression of inflammatory cytokines such as tumor necrosis factor alpha (TNFα) and interleukins 1 and 6 (IL-1 and IL-6) in

osteoclasts and osteoblasts (Narla & Ott, 2018; Weitzmann & Pacifici, 2006). Estrogen also induces the Wnt/β-catenin pathway both through induction of TGF-β signalling and by repressing the expression of Wnt inhibitor sclerostin (Niziolek et al., 2015). Increased Wnt signalling also contributes at least partly to the estrogen-mediated increase in OPG expression and decrease in RANKL expression in osteoblasts (Bord et al., 2003; Streicher et al., 2017). Similar findings of decreased RANKL and IL-6 expression and induction of TGF-signalling have also been observed after testosterone exposure (Shigehara et al., 2021).

2.3 Epigenetic regulation

All our diploid cells, from the primordial stem cells to the mature tissue-specific cells carry the same genetic code in their nuclei. Although all the genetic code is available, only the essential genes for the function of the specific cell type are translated. Similarly, the passage of parental environment effects is inexplainable by genetic traits. This phenomenon has been explained with epigenetic regulation (Waddington, 1957).

The definition of epigenetic regulation is not yet entirely established. It has been agreed that epigenetic regulation is a mechanism of gene expression changes not dependent on changes in the DNA sequence itself (Rakyan et al., 2001). In most fields the epigenetics is defined as being mitotically or meiotically heritable, for example from the progenitor cells to the differentiated cells. The definition has also been suggested to be expanded to non-hereditary changes, due to findings of similar changes in non-dividing cells (Bird, 2007).

Three types of epigenetic regulation have been discovered and will be described here: post-translational histone tail modifications (acetylation, methylation, phosphorylation, ubiquitinylation and ADP-ribosylation), DNA methylation and RNA interference (**Figure 5**). These types, in their different modi operandi, affect the availability of genetic code to be transcribed by either affecting the density of packaging of DNA between open-state euchromatin and densely packed heterochromatin or by subjecting the messenger-RNA (mRNA) to degradation instead of translation.

The key functions, where epigenetic regulation plays an important role are genomic imprinting, X chromosome inactivation and gene expression. Genomic imprinting is dependent on DNA methylation as well as histone modifications, while X chromosome inactivation depends on RNA interference by long non-coding RNA, whereas all three levels are crucial in regulation of gene expression (Y. Li & Sasaki, 2011; Moore et al., 2013; Rakyan et al., 2001).

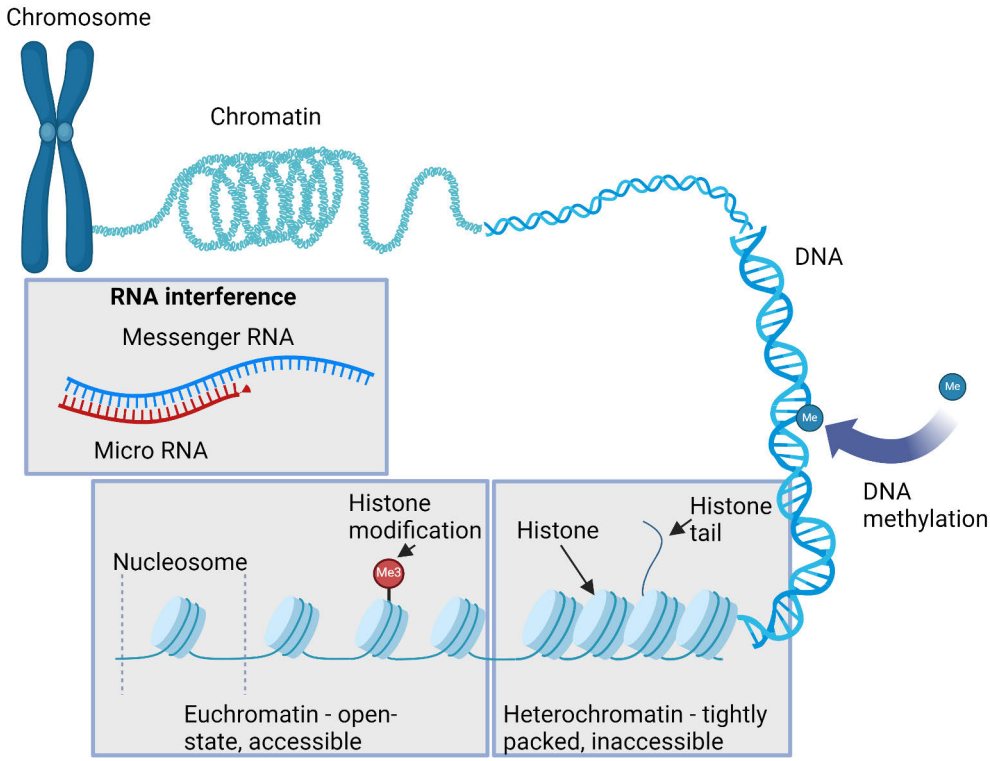

Figure 5. The three types of epigenetic regulation: Histone modifications (trimethylation, Me3), DNA methylation (Me) and RNA interference. Figure modified from Moore et al., 2013. Created in BioRender.com

2.3.1 Histone modifications

Histones are a five-member small-molecule protein family (H1, H2A, H2B, H3 and H4), which share a structural motif consisting of three α-helices connected by two loops, known as a histone fold domain. The histone fold motif allows the heterodimerization of H2A with H2B and H3 with H4. Histones form an octamer by binding first two H2A-H2B dimers and H3-H4 dimers separately into tetramers, which are then associated to form an octamer. This octamer, together with the 146 base pairs (bp) DNA strand surrounding it, then forms the nucleosome (Luger et al., 1997). Nucleosomes are organized and connected through linker histones (H1 subtypes) and linker DNA (Fyodorov et al., 2018).

Histones are rich in arginine and lysine, which are positively charged and can interact with the negatively charged DNA. The N-terminal tail of histone proteins protrudes from the globular histone fold domain and can be chemically modified, especially on histones H3 and H4, as well as the globular bodies (Xu et al., 2021). There are over ten different types of modifications identified taking place in at least

100 different amino acid residues (Bridi & Abel, 2013) and these modifications are crucial for various histone functions, including the regulation of gene expression and chromatin structure. Of these modifications, acetylation, methylation, ubiquitinylation and phosphorylation are the best known. Histone modification mechanisms also work hand-in-hand with other epigenetic mechanisms (Wolffe & Hayes, 1999).

2.3.1.1 Histone methylation

Histone methylation occurs on -$NH3^+$ group of lysine and -$NH3^+$ and NH2 groups of arginine residues, most commonly taking place on histone tails of histone 3 and 4. Lysine can be either mono-, di- or trimethylated and arginine either mono- or dimethylated (Sweatt et al., 2013). Histones are methylated by methyltransferases (either lysine methyltransferase, KMT or protein arginine methyltransferase, PRMT) and demethylated by demethylases. Lysines are demethylated by lysine demethylases, KDMs, but only one demethylase has been discovered for arginine, Jumonji domain-containing 6 (Poulard et al., 2016).

Lysine methyl transferase activity relies on one of the two known domains, the SET domain or the seven-beta-strand domain (7βS). There are at least 55 proteins with an identified SET domain, half of which are enzymatically active. There are approximately 160 members in the 7βS family, with varying target specificity of methylation activity (Clarke, 2013; Husmann & Gozani, 2019). Canonical histone methylation targets are found on H3K4, H3K9, H3K27, H3K36, H3K56 and H3K79, as well as on H4K20 (Murn & Shi, 2017).

Histone lysine demethylase family consists of eight subfamilies (KDM1-8) with structural differences. All subfamilies share some properties, such as the structural support providing Jumonji N domain (Husmann & Gozani, 2019). KDM1 is different from KDM2-8 by its amine-oxidase domain, dependence of flavin adenine dinucleotide (FAD) and capability of erasing mono- and dimethylation marks (Shi, 2007). Subfamilies KDM2-8 are capable of removing mono-, di- and trimethylation marks utilizing their Jumonji C domain (Tsukada et al., 2006). There are numerous different domains that some of the subfamilies incorporate, including protein-protein binding tetratricopeptide, Leu-rich repeat and F-box domains, as well as DNA and histone binding domains the Swi3p, Rsc8p and Moira (SWIRM) domain, AT-rich interacting domain, plant homeodomain, zinc fingers and the Tudor domain. Some subfamilies include multiple copies of the same domain, such as the plant homeodomain, of which there are two or three copies in KDM5s (Husmann & Gozani, 2019).

The methylation status of histone tails can either have a transcription activating, suppressing or elongating effect, depending on the methylation site and methylation level, as well as the arginine methylation configuration. The effects of methylation

on histone targets are listed in **Table 3** (Husmann & Gozani, 2019; Jack et al., 2013; J.-Y. Kang et al., 2018; Sterling et al., 2021).

Table 3. Histone methylation targets, their effectors and effects.

TARGET	HISTONE METHYLASES	HISTONE DEMETHYLASES	METHYLATION EFFECT, RELATED PROCESS
H3K4	SET1, MLL1-5	LSD1, KDM1B, KDM2B, KDM5A-D	Activation, self-renewal and differentiation.
H3K9	Suv39H1/2, SETDB1, EHMT1/2	LSD1, KDM3A-C, KDM4A-E, KDM7-C	Repression, cell fate transition, senescence, heterochromatin maintenance
H3K27	EZH1/2	KDM6A/B, KDM7A/B	Repression, Silencing of lnc-RNA, transcriptional elongation, heterochromatin maintenance
H3K36	SETD2, NSD1-3, ASH1L	KDM2A, KDM2B, KDM4A-C, KDM8	Activation, dsDNA break repair and chromatin structure control
H3K56	G9a/KMT1C	KDM4E	Repression, chromatin state maintenance and DNA replication
H3K79	hDOT1L	KDM2B	Activation, DNA re-replication control
H4K20	SET8, Suv420H1/2	KDM7A/B	Repression, chromatin organization after mitosis and DNA replication limitation

Histone methylation has been shown to regulate bone metabolism in various ways. H3K27 is mono-, di- and trimethylated by enhancer of zeste 2 (EZH2) and demethylated by KDM6A. EZH2 has been shown to target *RUNX2* and osteocalcin transcription start sites, repressing their gene expression and leading to decreased bone formation (Hemming et al., 2014). The methylation status of H3K4 has also been shown to regulate osteoblast differentiation, where enrichment of monomethylation of H3K4 leads to transcriptional repression of RUNX2 and osterix and decrease of osteoblast differentiation, while the accumulation of trimethylation of H3K4 on the same targets results in transcriptional activation and increased bone formation (Aguilar et al., 2021; Sepulveda et al., 2017).

2.3.1.2 Histone acetylation

Histone acetylation is a reversible process of transferring an acetyl group from acetyl coenzyme A to the -$NH3^+$ group of a histone lysine residue by histone acetyl transferases (HAT). This addition is reversed by histone deacetylases (HDAC) (Kao et al., 2000). Histone acetyl transferases can be divided to two groups, type A and type B, based on their localization and thereby their function (**Table 4**). Type A HATs contain a bromodomain and function in the nucleus, where they add acetyl groups to

assembled nucleosomes to regulate gene expression. There are multiple type A HATs identified, such as $hTAF_{II}250$, p300/CBP and PCAF (Mizzen et al., 1996; Shiama, 1997; X.-J. Yang et al., 1996). Type B HATs lack the bromodomain of type A HATs and are localized in the cytoplasm, where they acetylate the newly formed histone subunits, enabling the identification and assembly of nucleosomes. There is only one known type B HAT, Histone acetyltransferase 1 (Verreault et al., 1998).

Table 4. Key histone acetylases and deacetylases.

	TYPE / CLASS	**PROTEIN**	**SUBSTRATES**
HISTONE ACETYL-TRANSFERASES	TYPE A	$hTAF_{II}250$	H3 (K14), TFIIEb
	TYPE A	p300/CBP	All histones, K5, 9, 12, 16 of H4 pep, TFIIEβ (K52), TFIIF, p53 (K373, 382, peptide)
	TYPE A	PCAF	H3
	TYPE B	HAT1	H4 (K12, K5)
	TYPE / CLASS	**PROTEIN**	**NOTES**
HISTONE DEACETYLASES	CLASS I	HDAC1, 2, 3 and 8	Target both histone / non-histone proteins
	CLASS IIa	HDAC4, 5, 7 and 9	Shuttle between cytoplasm and nucleus, low activity
	CLASS IIb	HDAC6 and 10	Found typically cytoplasmically, both histone and non-histone protein targets
	CLASS III	SIRT1-7	Both deacetylase and other activities, found in different compartments of the cell
	CLASS IV	HDAC11	Histone / non-histone proteins, regulates mRNA splicing

Histone deacetylases (HDACs) are divided into two families, the histone deacetylase family and the sirtuin protein family and into five classes (**Table 4**). Class I HDACs include proteins HDAC1, 2 3 and 8 and harbour a highly homologous deacetylase domain with differences mainly in the C-terminal end (Park & Kim, 2020). Class I HDACs deacetylate both histones and other protein targets (Xiong et al., 2010). Class II HDACs are divided into two subclasses due to their different domain compositions, class IIa harbouring a Myocyte Enhancer Factor-2 binding site (HDAC4, 5, 7 and 9) and class IIb, which characteristically contains a long C-terminus domain (HDAC6 and 10). Class IIa HDACs have a distinctively low enzymatic activity, while activity of class IIb HDACs remains poorly understood (Kuo & Allis, 1998; Muslin & Xing, 2000). The sirtuin family forms class III of HDACs with seven family members (SIRT1-7). Class III HDACs are dependent of the cofactor nicotinamide adenine dinucleotide (NAD^+) for their

catalytic functions but additionally exhibit other enzymatic activities towards various functional groups (Buck et al., 2004; Du et al., 2011). Class IV of HDACs includes only HDAC11, which shares the catalytic domain of Class I and II HDACs. HDAC11 has been reported to associate with the survival of motor neurons (SMN) complex and regulate mRNA splicing (Gao et al., 2002; Joshi et al., 2013).

Histone acetylation and deacetylation have at least three different functions: nucleosome assembly, chromatin condensation and transcription factor recruitment. In the lifespan of histones, first subunit acetylation happens during the nucleosome assembly and is important for chaperone recognition, followed by rapid deacetylation after nucleosomes are formed (Shahbazian & Grunstein, 2007; Smith & Stillman, 1991). In chromatin condensation HDACs remove negatively charged acetyl group which increases the interactions between histones and negatively charged phosphate groups of DNA. The interactions behind chromatin condensation take place between histone tails and linker DNA, leading to a more closed conformation (Angelov et al., 2001; Shahbazian & Grunstein, 2007). In transcription regulation, acetylated histones both open the conformation of nucleosomes, attracting transcription factors to their binding sites and enabling the passage of RNA polymerase on chromatin. The acetylation of most lysines in N-terminal tails of histones 3 and 4 have been associated with increased gene expression (Marushige, 1976; Pokholok et al., 2005). This can be explained with transcription factor complexes containing bromodomains, such as the SWI/SNF complex, which prefers binding to acetylated histone marked sites (Hassan et al., 2002).

Histone deacetylation functions opposite to acetylation, counteracting the neutralization of lysine residues in histones. Histone deacetylation has also unique roles where deacetylation of histone tails attracts repressive complexes such as the CoREST or SMRT complexes through the Swi3, Ada2, N-CoR, TFIIIB (SANT) domain. Both of these complexes also include HDAC proteins (Song et al., 2020; J. Yu et al., 2003). HDACs are recruited to histones both globally and site-specifically leading to transcription repression (Shahbazian & Grunstein, 2007).

Both HDAC1 and HDAC2 function in bone and affect osteoblast differentiation. While HDAC1 has been shown to negatively impact osteoblast differentiation through deacetylation of *OSX*, osteocalcin and *RUNX2* promoter areas, HDAC2 has instead been linked to osteoclast maturation and differentiation through Akt/FoxO1 mediated RANKL expression in mice (Dou et al., 2016; McGee-Lawrence & Westendorf, 2011).

2.3.1.3 Other histone modifications

Histone proteins are not only subject to methylation and acetylation, but also to other post-translational modifications, such as phosphorylation, ubiquitinylation and

ADP-ribosylation. Additional known modifications include deamination, β-N-acetylglucosamination, sumoylation, proline isomerization and subunit exchange. As more research is performed on histone modifications, even more mechanisms are most likely to be found.

Histone phosphorylation is regulated by kinases and phosphatases at a high turnover rate. The N-terminal serines, threonines and tyrosines are the most common targets for phosphorylation. Phosphorylation of histone amino acid residues brings a significant negative charge to the protein but the detailed mechanisms of complex recruitment in histone phosphorylation remains unknown. The overall effect of histone phosphorylation has been associated with transcriptional activation. The best described target of activation through histone phosphorylation has been reported on H3S10 in combination with the acetylation of H3K9 (Pal et al., 2015).

Histone ubiquitinylation is a more substantial change to the nucleosomes than the other previously mentioned modifications. In ubiquitinylation, a 76 amino acid polypeptide known as ubiquitin is attached to the lysine residues of proteins, most commonly histones H2A and H2B, through the actions of three key enzymes: E1 (ubiquitin-activating enzyme), E2 (ubiquitin-conjugating enzyme), and E3 (ubiquitin ligase). Multiple ubiquitins can be attached to the same target, depending on the enzyme constitution. Ubiquitins are removed by de-ubiquitin enzymes and the modification is highly dynamic (Hershko & Ciechanover, 1998).

Histone mono- and poly-ADP-ribosylation takes place on the glutamate and arginine residues. The modification is reversible, where ADP-ribosylation depends on poly-ADP-ribose polymerase and mono-ADP-ribose polymerase families of proteins and is reversed by the poly-ADP-ribose-glycohydrolase family. ADP-ribosylation is linked to an open chromatin state and has also been associated with acetylation of histones (Cohen-Armon et al., 2007; O et al., 2006).

2.3.2 DNA methylation

DNA methylation can take place on the fifth carbon of the aromatic ring of a cytosine base, and usually occurs when cytosine is followed by guanine in DNA through the phosphate backbone in between, called a CpG site (Fuggle et al., 2022). CpG islands are ~500-1000 bp long stretches of DNA enriched with CpG sites (>55% G/C content). Even though the CpG islands are promoter-rich, they are often not enriched with common promoter elements such as TATA-boxes. Genes harbouring CpG islands include in particular genes expressed universally in different tissues, commonly conserved between vertebrates. CpG islands are GC rich, similarly to the binding sites of transcription factors targeting the promoter areas (Carninci et al., 2006; Gardiner-Garden & Frommer, 1987; Hamilton, 2011; Moore et al., 2013). CpG shores are regions located 0-2 kb from CpG islands and CpG shelves are regions 2-4 kb from

CpG islands (Rechache et al., 2012). 80% of CpG nucleotides outside of CpG islands are methylated in normal physiological conditions (Hamilton, 2011).

CpG sites are methylated by DNA methyltransferases (DNMT1/3A/3B) and their coregulators ubiquitin-like, containing PHD and RING finger domains 1 (UHRF1) and Dnmt3-Like protein (DNMT3L) among others (Hashimoto et al., 2012). DNA methyltransferases are divided to two subsets, *de novo* methyltransferases DNMT3A and 3B and maintenance methyltransferase DNMT1. *De novo* methyltransferases are capable of methylating CpG sites where neither of the strands have a methyl group previously attached. DNMT1 instead methylates a CpG site based on the template of the other strand during DNA replication. DNMT1 can also recruit histone deacetylases (HDACs) during cell division to propagate the existing acetylation patterns (Moore et al., 2013).

Demethylation of CpG sites in the absence of DNMT enzymes is performed passively by cell division or actively by DNA demethylases, such as the Growth Arrest and DNA Damage 45 combined with DNA repair-like processes (Ma et al., 2009). The amount of tissue-specific DNA methylation is relatively low in CpG islands (4-8%), compared to the tissue-specificity of CpG shores (76%) (Irizarry et al., 2009).

Genomic imprinting is the phenomenon of expressing only either paternal or maternal copy of a gene contributing to embryogenesis, gametogenesis and reproduction. Imprinting is seen only on a subset of genes and can be complete or partial. Imprinted genes are usually found in imprinting control regions. Loss of imprinting on previously completely imprinted genes usually have negative effects on fetal development (Elhamamsy, 2017; Morcos et al., 2011). The parental DNA methylation pattern is erased between embryonic days 10.5 and 12.5, followed by re-establishing according to the gender of the individual (Y. Li & Sasaki, 2011).

Genomic imprinting is also tissue specific, where only a maternal copy is expressed in some tissues and biallelic expression is found in other tissues (Rougeulle et al., 1997). Biallelicity has also been found to be temporally limited on some genes (Wilkinson et al., 2007).

The ten-eleven translocases (TET) proteins oxidize 5-methylcytosines, priming them for demethylation by DNMTs. RUNX2 has been shown to recruit TET proteins to their complex and regulate its own activity through the demethylation of the promoter's CG region, resulting in increased gene expression (L. Wang et al., 2022).

2.3.3 Non-coding RNAs

There is increasing interest and understanding on the role of long non-coding RNAs and small non-coding RNAs. Long non-coding RNAs are known to play a key role in X-chromosomal inactivation and imprinting as well as affecting transcription through regulation of histone methylation and acetylation along with limiting the

association of transcription factor II D to its promoter area targets (Mercer et al., 2009; Nagano & Fraser, 2009).

Small non-coding RNAs are categorized into microRNAs (miRNA), small inhibitory RNAs, PIWI-interacting RNAs, small nuclear RNAs and small nucleolar RNAs. Of these, the importance and function of miRNAs is best known (Guennewig & Cooper, 2014). miRNAs are 19-24 nucleotides long sequences processed in the cytoplasm by a Dicer-including complex, which bind the 3' untranslated region of target genes in the presence of the RNA-induced silencing complexes, leading to degradation of the target mRNA (Hensley & McAlinden, 2021).

Recent studies have also identified a multitude of miRNAs, which affect both osteoblasts and osteoclasts either by increasing or inhibiting their activity. There is a growing list of miRNA targets, highlighting the importance of non-coding RNAs also in the field of bone research. These targets include several key regulators of bone formation, such as upstream and downstream signalling of the WNT pathway, RUNX1/2, BMPs and Osterix/SP7. For example, RUNX2 activity alone has been reported to be affected by miR-137-3p, miR-155 and miR-23a-5p (Hensley & McAlinden, 2021).

2.4 LSD1/RCOR2 complex

Epigenetic regulation of bone metabolism has been a topic of interest ever since the methodology has allowed for investigation of bone cell epigenetic markers. The epigenetic effects of BMP-2 were published already in 2009 (Pan et al., 2009), and many other proteins with epigenetic regulation capabilities have since been revealed, with novelty either in the newly found mechanism of a known protein or as an entirely new regulator in the field of bone research (Sharma et al., 2024).

The LSD1/RCOR complex was originally discovered as a HDAC2 binding complex in human HeLa and HEK293 cell lines, distinct from the previous known mSin3 and nucleosome remodelling and deacetylating (NuRD) transcription repression complexes. First, a protein was discovered as a binding partner of HDAC2 named p110 (Tong et al., 1998), later to be named LSD1. Another study discovered that the core protein CoREST (also known as RCOR1, KIAA0071) was capable of binding to the known repressor of transcription Repressor element-1 silencing transcription factor (REST) (Andrés et al., 1999). These findings were followed by discovery of CoREST interaction with ZNF217, HDAC1/2 and the previously found amine oxidase p110b (or LSD1), in a complex first named CoREST/HDAC complex and later the CoREST transcription repression complex (You et al., 2001). LSD1 (also known as KDM1a, AOF2, KIAA0601, BHC110 or p110b) has been later found in also other complexes. LSD1 and BRAF35 were found in the BRAF–histone deacetylase (BHC) complex together with HDAC1/2, BHC80, C-terminal-binding protein 1 and CoREST in HeLa cells (Hakimi et al., 2002), among other complex

members (Maiques-Diaz & Somervaille, 2016; Maksour et al., 2020). Lastly, RCOR2 (also known as CoREST2) was found in a similar complex with HDAC1/2, BHC80 and LSD1 as CoREST/RCOR1 and capable of facilitating the nucleosomal demethylation activity of LSD1. This suggests similar repressive action of RCOR2 to RCOR1 (P. Yang et al., 2011).

One proposed mechanistic cycle of action of the CoREST/RCOR2 transcription repression complex includes a) the recruitment to target DNA by REST and Brahma-related gene 1 (BRG1), b) priming of the repression site by deacetylation and c) repression by methylation/demethylation of histone tails leading to d) chromatin condensation (**Figure 6**, representing the LSD1/RCOR2 complex).

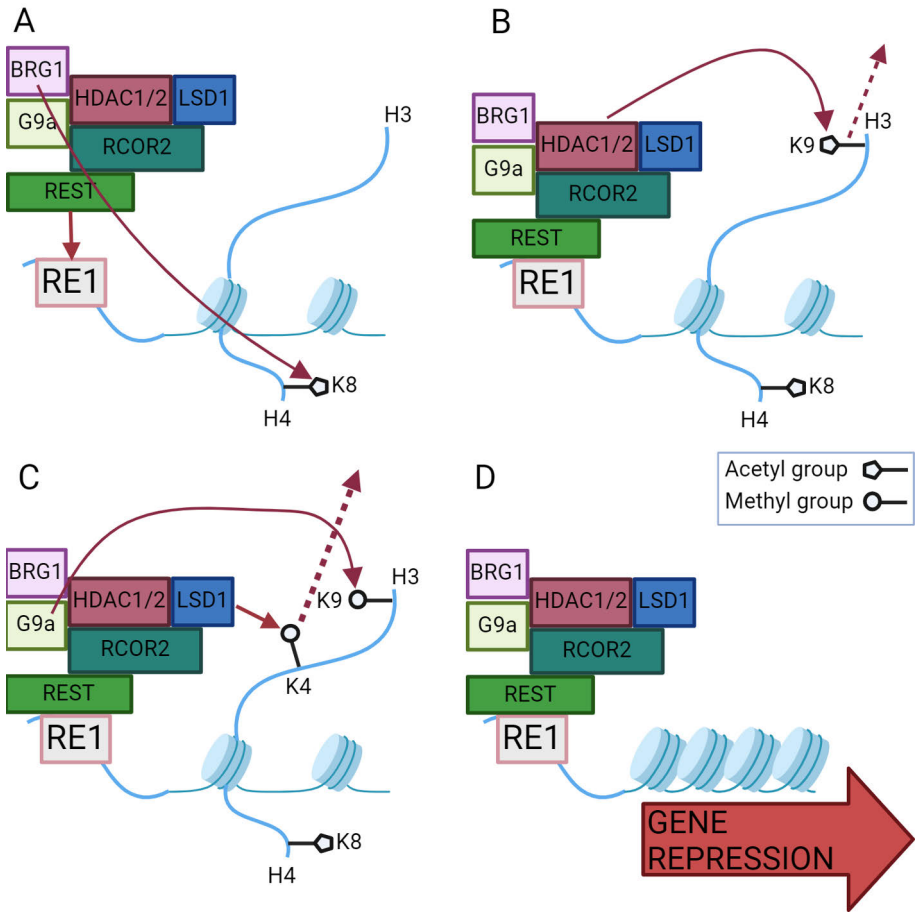

Figure 6. Simplified schematic representation of RCOR2 complex-mediated gene repression. RCOR2 forms a complex with REST, LSD1 and HDAC1/2 as well as BRG1 and G9a. A: Initially, REST binds its responsive element RE1 and BRG1 acetylates H4K8. B: HDAC1/2 deacetylates H3K9. C: LSD1 demethylates H3K4me1/2 and G9a methylates H3K9. D: Chromatin is condensed, thus repressing gene expression. Modified from Maksour et al., 2020. Created in BioRender.com

2.4.1 LSD1

LSD1, or KDM1A, is a structurally distinct member of the FAD-dependent lysine demethylase subfamily. LSD1 is expressed in a variety of tissues including bone, neural tissues, endocrine tissues, respiratory and digestive tissues as well as reproductive tissues, among others. LSD1 consists of a SWIRM domain, amine oxidase domain (AOD) and a tower domain (Maiques-Diaz & Somervaille, 2016). The AOD is the functional core of LSD1, divided into two units: the non-covalent FAD binding site and the substrate binding and recognition site (Polticelli et al., 2005). Mono- or dimethylated lysine residues are demethylated through an iminium cation subproduct using the hydride anion of the oxidized FAD. The iminium cation is then hydrolysed to a demethylated residue. LSD1 demethylation activity is dependent on the free electron pair of the ε-nitrogen of lysine and therefore LSD1 cannot demethylate the trimethylated form of lysine. Demethylation activity of LSD1 is not linked to the release of the substrate, allowing non-methylated and trimethylated histone tails to competitively bind LSD1 (Stavropoulos et al., 2006).

The SWIRM domain of LSD1, unlike traditional SWIRM domains, does not have DNA binding properties, but instead it allows for protein-protein interactions. This enables the recruitment of LSD1 to other binding partners, such as the androgen receptor (AR) (Metzger et al., 2005). Mutations in the SWIRM domain or in the histone tails can lead to changes in substrate interaction and catalysis efficiency (Stavropoulos et al., 2006).

The tower domain of LSD1 allows for RCOR protein interaction through the linker sequence between the SANT domains of RCOR proteins. This interaction between SANT2 and tower domain is mandatory for LSD1 demethylase activity. The conformability of the SANT domains, tower domain and AOD allow for adaptability to different substrates (M. Yang et al., 2006).

Changes in the complex formation can indeed lead to differences in substrate selectivity. Initially LSD1 was the first histone demethylase discovered, targeting only mono- or dimethylated H3K4 (H3K4me1/me2) (Tong et al., 1998; You et al., 2001). This finding was followed by the discovery of complex formation with the androgen receptor (AR), adding mono- or dimethylated H3K9 to the possible substrates (Cai et al., 2014; Metzger et al., 2005). Lastly, it has been discovered that LSD1 can directly demethylate non-histone protein targets (Huang et al., 2007). Histone methylation targets and their effectors can be found in **Table 3**.

2.4.1.1 H3K4 methylation

The traditional mechanism of action for LSD1 demethylating mono- or dimethylated H3K4 was originally discovered in the context of HDAC2 complex, where a previously unknown HDAC2 binding partner co-immunoprecipitated with HDAC2

(Tong et al., 1998). Further research discovered more binding partners (e.g. CoREST, ZNF217, PHF21A and HMG20B) and identified the complex as the CoREST transcription repressor complex (Lakowski et al., 2006). The CoREST complex has been shown to have H3K4me1/2 demethylation and H3 deacetylation activities, in a CoREST protein dependent manner (M. G. Lee et al., 2005).

LSD1 was later discovered to bind metastasis tumor antigens 1, 2 and 3 (MTA1, MTA2 and MTA3), HDAC1, HDAC2, methyl-CpG binding domain 3 (MBD3) and Retinoblastoma Associated Proteins 46 and 48 (RbAp46/48), all members of the nucleosome remodelling and deacetylase (NuRD) complex. Histone modification activity of the NuRD complex has been shown to include deacetylation of H3K9/K14, demethylation of H3K4me1/me2 but not H3K9me2 in specific gene promoters, such as the *TGFB1* promoter (Y. Wang et al., 2009).

The third complex, where LSD1 has been found in, is the mixed lineage leukemia (MLL) coactivator complex, with at least 28 different proteins present either as a part of this complex or as individual complexes recruited to the MLL complex. The complex both deacetylated and demethylated the target gene promoter (Nakamura et al., 2002), which could be a result of recruitment of NuRD complex as an entity to the MLL complex.

2.4.1.2 H3K9 methylation

Despite the original finding of the specificity to H3K4me1/2 demethylation, some studies have suggested that in the association with certain complex members LSD1 could also demethylate H3K9me1/2, leading to transcriptional activation. Signalling through both estrogen receptors (ERs) and AR have also been shown to activate LSD1 demethylation activity of mono- and dimethylated histone 3 lysine 9 (H3K9me1/2) in LNCaP and MCF-7 cells (Metzger et al., 2005; Perillo et al., 2008). The complexes were capable of demethylating both H3K9me1/2 but surprisingly not H3K4me1/2, and dependence on LSD1 activity was shown to be crucial. LSD1 has been shown to regulate the transcriptional activity of AR, ER, glucocorticoid receptor and mineralocorticoid receptor (Carnesecchi et al., 2017; Clark et al., 2019; Kohata et al., 2022; Metzger et al., 2005).

2.4.1.3 Direct protein interactions

Not only is LSD1 a key regulator of gene expression through histone methylation status, but it has also been found to directly demethylate non-histone proteins. The first non-histone target found for LSD1 in humans was the tumor suppressor protein p53. LSD1 demethylates both the and mono- and dimethylated forms of K370, which leads to p53 release from binding partner 53BP1 and repression of p53 activity

(Huang et al., 2007). Other similar LSD1 demethylation targets that have been found include MYPT1 (K442), DNMT1 (K1094) and E2F1 (K185) (Cho et al., 2011; Kontaki & Talianidis, 2010; J. Wang et al., 2009).

2.4.2 RCOR2

2.4.2.1 RCOR Family members

Rest Corepressor 2 (RCOR2) belongs to the three-membered family of RCORs (RCOR1-3 or CoREST1-3). RCOR1, RCOR2 and RCOR3 isoforms a, c and d are structurally homologous containing two SANT domains and one Egl-27 and MTA homology 2 (ELM2) domain. RCOR3 has been found to have 4 isoforms, RCOR3a-d (Maksour et al., 2020). Of the three family members, only RCOR2 is expressed consistently in osteoblasts.

The SANT domains most likely play a role in histone tail recognition as well as histone remodelling. The linker domain between the two SANT domains and the SANT2 domain itself act as a binding site for LSD1, except for RCOR3 isoform b which lacks the second SANT domain and is incapable of binding LSD1 (Barrios et al., 2014; Upadhyay et al., 2014). The SANT1 domain of RCOR2 instead has a different amino acid sequence, leading to impaired binding of HDAC1/2 (Barrios et al., 2014). The SANT2 domain has been suggested to have a role in mediating DNA binding. The SANT1 domain is also mandatory for the binding to REST, a property all RCOR family members possess (Barrios et al., 2014; M. G. Lee et al., 2005; Maksour et al., 2020).

The ELM2 domain together with SANT1 recruits and binds HDAC1/2 (Andrés et al., 1999). Structural analysis of ELM2 does not provide a consistent structure when unbound but forms a stable complex with HDACs. ELM2 in MTA proteins consists of two regions, the aminoterminal part, which interacts with HDACs and the carboxyterminal part, which forms homodimers with other ELM2 domains allowing the binding of both HDAC1 and HDAC2 to the complex (Millard et al., 2013). The protein structures of RCOR ELM2 domains differ to those of MTA proteins in the number of helices, which leads to loss of dimerization capability (Song et al., 2020).

2.4.2.2 Mechanism of action and complexes with LSD1 or other proteins

RCOR2 or other members of the RCOR family have not been shown to have intrinsic histone modification activities. Instead, RCOR proteins have binding sites to recruit functionally active complex members together to REST and to DNA target sites. RCOR2 has been found in various complexes first discovered with CoREST/RCOR1

such as in the BHC complex, HDAC1/2 complex and CoREST-HDAC complex (Dreher & Theisen, 2023; Lakowski et al., 2006; Song et al., 2020).

RCOR2 is expressed in multiple different cell types, with the highest detected expression levels in the brain, testis, ovaries, pancreas and liver (Fagerberg et al., 2014). RCOR2 is the only family member with specific functions in development, where it has a key role in maintaining the stem cell state of embryonic stem cells, as well as restoring pluripotency of reprogrammed fibroblasts (P. Yang et al., 2011), but also in the differentiation of embryonic stem cells to all 3 germ layers (Pei et al., 2022). RCOR2 has also been shown not only to locate inside the nuclear speckles, but also to actively regulate nuclear speckle morphology from the core of nuclear speckles (Rivera et al., 2021).

2.4.3 LSD1 and RCOR2 in bone

The role of LSD1 has been previously studied in all MSC derived cell types as well as in osteoclasts. The first studies on the effects of LSD1 on osteoblast differentiation reported LSD1 to repress human adipose-derived stem cell differentiation to osteoblasts, and that the lentiviral shRNA-mediated silencing and pharmacological repression using a non-selective MAO inhibitor pargyline or more specific LSD1 inhibitor CBB1007 led to increased osteoblast differentiation *in vitro* and osteoblast function and differentiation *in vivo* (Ge et al., 2014). Another study found that LSD1 inhibits BMP-2 and WNT7B signalling and thereby leads to decreased osteoblast differentiation in mouse primary calvarial osteoblast culture experiments, and this was overcome through conditional knockout of LSD1 in a $Lsd1^{-/-}_{Prrx1}$ mouse model as well as by treatment with non-specific small molecule inhibitor tranylcypromine *in vivo* (Sun et al., 2018). LSD1 has also been found to be targeted by miR-655-3p in MC3T3-E1 cells and in ovariectomized (OVX) mice, which led to BMP-2/Smad-mediated increase of osteoblast differentiation (X.-J. Wang et al., 2020). Similar effect was seen in miR-137-mediated downregulation of LSD1 in osteogenically differentiated human adipose-derived stem cells (Fan et al., 2021).

LSD1 has also been shown to modulate osteoclast differentiation and activity. LSD1 expression was found to be upregulated by RANKL in human osteoclast precursors *in vitro* and LSD1 inhibition by SP-2509, a LSD1 and JAK/STAT3 pathway inhibitor, led to decreased osteoclast differentiation through decreased destabilization of Hypoxia-inducible factor 1 and E2F Transcription Factor 1 *in vivo* (Doi et al., 2022). LSD1 has also recently been reported to increase Integrin subunit beta 3 expression during osteoclast differentiation, while downregulation of either of the two led to decreased osteoclast formation on THP1 cells (D. Yu et al., 2023). LSD1 has also been found to modulate the expression of NFAT1 in primary articular chondrocytes (Rodova et al., 2011), and is identified as a key regulator of

endochondral ossification in fracture healing through retinoic acid signalling in $Lsd1^{-/-}_{Prrx1}$ mice (Sun et al., 2020). Lastly, LSD1 has been shown to regulate the differentiation of 3T3-L1 preadipocytes through changes in the methylation levels of H3K4 and H3K9 of CCAAT/enhancer-binding protein alpha (*C/EBPa*), leading to increased adipocyte differentiation (Musri et al., 2010).

In contrast, RCOR2 has not been previously associated with the regulation of osteoblast differentiation or to have a role in osteoblast differentiation or function. Suppression of RCOR1 (J. Xiao et al., 2010) and RCOR2 expression have been associated with the changes of articular cartilage to osteoarthritic cartilage, possibly through decreased repression of Hairy and Enhancer of Split 1 (HES1) (Primrose et al., 2023). The knockdown of RCOR2 and LSD1 expression has also been shown to impair 3T3-L1 preadipocyte differentiation (Hanzu et al., 2013).

3 Aims

Emerging research on epigenetic regulation has provided novel insights on the regulatory mechanisms of target gene expression. Even though the role of epigenetic regulators and their co-regulators, such as LSD1 and RCOR2, have been studied more extensively in cancer and embryonic stem cell maintenance, the mechanisms are likely transferrable to the bone field. The roles of LSD1 and RCOR2 as transcriptional repressors of MSC differentiation and bone formation as well as the potential mechanisms behind these roles have been studied inconclusively.

Thus, the specific primary aims of this study were:

1. To study the expression dynamics of LSD1 and RCOR2 in MSCs and during osteoblast differentiation.
2. To evaluate the effects of LSD1 and RCOR2 downregulation on osteoblast differentiation.

The findings of these studies further directed us towards the secondary aims:

3. To elucidate the mechanisms by which LSD1 and RCOR2 bind the target gene promoters during osteoblast differentiation.
4. To analyze the bone phenotype of mice after pharmacological inhibition of LSD1, targeted knockdown of LSD1, or targeted or global knockdown of RCOR2.

4 Materials and Methods

4.1 Ethics statement (I, II)

All mouse studies were approved by the Finnish ethical committee for experimental animals (license numbers 5186/04.10.07/2017 and 14044/2020), complying with the international guidelines on the care and use of laboratory animals, and were conducted under the supervision of the trained staff at the Central Animal Laboratory, University of Turku. The protocols of animal experiments followed the 3Rs principle (Replace, Reduce and Refine).

4.2 Mouse strains (I, II)

All genetically modified, LSD1 inhibitor treated and surgically treated mice used in these experiments were housed in cages in standard laboratory conditions (housing temperature 22°C, lights from 06:00 to 18:00). Water and soy-free chow were available ad libitum, excluding an up-to four hour fasting period before euthanasia. Mice were injected with calcein and demeclocycline intraperitoneally either 3 days and 1 day before euthanasia for the 4 weeks timepoint, 7 days and 2 days before euthanasia for the 6 weeks timepoint or 9 days and 2 days before euthanasia for the 12 weeks timepoint. The age and sex of mice used in these studies are summarized in **Table 5**.

Table 5. Mice models used in this study.

EXPERIMENTAL / GENETICALLY MODIFIED MOUSE MODEL	TREATMENT / KNOCKOUT	AGE AT ANALYSIS	SEX ANALYSED	STUDY REFERENCE
LSD1$_{PRRX1}$	Prrx1-Cre	4 weeks	Males and females	Study I
LSD1 INHIBITOR TREATMENT	GSK-LSD1 1.5 mg/kg 4-on-3-off	10 weeks	Males	Study I
RCOR2$^{+/-}$	Global heterozygous	6 weeks 12 weeks	Males and females	Study II
RCOR2$_{PRRX1}$	Prrx1-Cre	6 weeks 12 weeks 26 weeks	6 and 12 weeks: males and females, 26 weeks: males	Study II
RCOR2$_{PRRX1}$	Ovariectomy	16 weeks	Females	Study II
RCOR2$_{PRRX1}$	Closed tibial fracture	14 weeks	Males and females	Study II

4.2.1 Limb-bud mesenchyme targeted LSD1 knockout mice (I)

Mice embryos carrying the floxed KDM1A/LSD1 alleles (Lsd1$^{fl/fl}$, stock #023969) were obtained from the Jackson laboratory. Lsd1$^{fl/fl}$ mice were crossed with paired related homeobox 1 promoter Cre (Prrx1-Cre) mice to create homozygous and heterozygous conditional LSD1-knockout mice (Lsd1$^{-/-}_{Prrx1}$, Lsd1$^{+/-}_{Prrx1}$ respectively). Prrx1-Cre targets the deletion of exons 5-6 of *LSD1* to early limb bud mesenchyme and a subset of craniofacial mesenchyme. Male and female mice were analysed separately at 4 weeks of age. Littermate Lsd1$^{fl/fl}$ mice were used as controls.

4.2.2 Pharmacological inhibition of LSD1 *in vivo* (I)

Ten 6-week-old C57BL/6NHsd male mice were treated with either 0.9% NaCl (vehicle) or 1.5 mg/kg GSK-LSD1 (a highly specific LSD1 inhibitor, Sigma SML1072) delivered by intraperitoneal injections in a 4-on-3-off schedule for four weeks. The weight of the animals was monitored twice a week and the overall wellbeing five times a week.

4.2.3 Global RCOR2 knockout mice (II)

The knockout-first (Tm1a) allele for *RCOR2* gene bearing C57Bl/6NTac-Rcor2tm1a(EUCOMM)Wtsi/Wtsieg mice (ID EM:05885) were obtained from European Mutant Mouse Archive (EMMA).

Tm1a-allele mice were crossed with mice expressing Cre under the control of CMV enhancer-chicken-beta-actin (CAG) promoter (CAG-Cre/2 mice). This led to deletion of exons 1-7 in all tissues, creating the global knockout Rcor2KO$^{+/+}$ and Rcor2KO$^{+/-}$ mice. Male and female mice were analysed at 6 and 12 weeks of age.

4.2.4 Limb-bud mesenchyme targeted RCOR2 knockout mice (II)

The knockout-first (Tm1a) allele for *RCOR2* gene bearing C57Bl/6NTac-Rcor2tm1a(EUCOMM)Wtsi/Wtsieg mice (ID EM:05885) were obtained from European Mutant Mouse Archive (EMMA).

Tm1a-allele mice were crossed with Flp Deleter mice expressing Flp recombinase under the control of CMV enhancer and CAG promoter. Mice crossed with the Flp Deleter mice were crossed with mice expressing Cre recombinase under the control of the Prrx1 promoter. This led to deletion of exons 1-7 in cells of the early limb bud mesenchyme and a subset of craniofacial mesenchyme -origin, creating RCOR2 conditional knockout, Rcor2$^{fl/fl}$ and Rcor2$^{-/-}_{Prrx1}$ mice. Male mice were analysed at 6, 12 and 26 weeks of age, and female mice at the age of 6 and 12 weeks.

4.2.5 Genotyping (I, II)

Genotyping was carried out from DNA extracted from the ear marks of 2- to 3-week-old mice. Sequences of the PCR primers used are listed in **Table 6.** Verification of downregulation of target genes was done using PCR run from genomic DNA extracted from femurs, from which bone marrow was removed to eliminate the background expression by excising the heads with scissors and centrifuging the femur briefly.

Table 6. PCR primers used to verify recombination.

PRIMERS	SEQUENCE	PRODUCT SIZE AFTER RECOMBINATION	USED TO VERIFY
LSD1 F **LSD1 R**	GCTGGATTGAGTTGGTTGTG CTGCTCCTGAAAGACCTGCT	300 bp	LSD1 floxed alleles in LSD1cKO mice
RCOR2KO-R1 **Rcor2_88510_F**	GTATGCACAGTACCCAGCACTT CTCTCATGGTGAGCCTGGTG	676 bp	Global RCOR2 deletion
RCOR2KO-R1 **RCOR2_CKO DELETED_F**	GTATGCACAGTACCCAGCACTT TAATGGAGAAGCCCAGTGCG	587 bp	Conditional RCOR2 deletion

4.3 Experimental mouse models

4.3.1 Ovariectomy-induced bone loss (II)

Ovariectomy (OVX) was performed on 12-week-old female mice (n = 9–10 per group). In brief, subcutaneous injections of carprofen (5 mg/kg) and buprenorphine (0.05 mg/kg) were given and the surgical procedure was performed under isoflurane anaesthesia (2.5% at 250-400 ml/min) and aseptic conditions. A midline incision was done in the mid-dorsum of the mouse. The ovary was gently raised and removed from the surrounding fat tissue by cauterization. The ovarian horn was then released back into the peritoneum. A self-resorbing suture was placed over the muscle layer and a non-resorbing suture was set on the skin. The procedure was repeated on the contralateral side (Heydarpour et al., 2013). The sham procedure was done as above except after raising the ovaries from their surroundings, they were gently put back into place and left intact. The mice were administered with post-operative injections of carprofen and monitored regularly for the next 2–3 days.

4.3.2 Tibial fracture healing (II)

The closed tibial fracture procedure has been described before (Hiltunen et al., 1993; Puolakkainen et al., 2017). In brief, 10-week-old male and female mice (n = 10 per group) were anesthetized with isoflurane 30 min after analgesia administration (buprenorphine 0.05 mg/kg and carprofen 5 mg/kg subcutaneously). A sterile stainless-steel rod (Ø 0.2 mm) was inserted to the intramedullary canal for support and a standardized, closed tibial fracture was performed using an in-house manufactured fracture apparatus. Mice were treated with buprenorphine for 2 days after the procedure and sacrificed 14 or 28 days after the fracture.

4.4 Mouse skeletal phenotype analysis

4.4.1 Micro-computed tomography (I, II)

After euthanization, femurs, tibias, calvarias and fracture calluses were immediately collected, cleaned of excess soft tissues and fixed with neutral buffered formalin (10%) overnight and transferred to and stored in 70% ethanol. Bone lengths were measured with a measuring calliper. Bones were cleaned of remaining soft tissue and analysed with X-ray microcomputed tomography (μCT) using either SkyScan 1070 or SkyScan 1072 equipment (Kontich Belgium). A custom-made plastic holder was used to ensure immobilization and repeatable positioning of samples. Cross-sectional images were reconstructed using NRecon 1.4 software (SkyScan) and

reoriented to ensure comparability using Dataviewer software (SkyScan). Regions of interest (ROI) were defined using CTan 1.4.4 software (SkyScan).

In Study I, cortical and trabecular bone structure of femurs was analysed with 8.37 μm resolution. The start of ROIs were located 210 layers (1050 μm) up from the proximal end of the distal growth plate for the trabecular bone, and 1000 layers (5000 μm) up for the cortical bone. The ROI were drawn on every tenth layer from 120 layers with a total height of ~1000 μm for trabecular bone, and from 100 layers with a total height of ~840 μm for cortical bone and the results were then quantified and analysed.

Tibias of the LSD1cKO-mice were analysed using 5 μm resolution. The ROI were drawn on every tenth layer from 100 layers 210 layers (1050 μm) down from the distal end of the proximal growth plate for the trabecular bone, and 1000 layers (5000 μm) down for the cortical bone and subsequently analysed.

In Study II, cortical and trabecular bone structure of the distal femur or proximal tibia was analysed using 8.37 μm resolution. The ROIs were drawn on every tenth layer of 120 layers, with a total height of ~1000 μm for trabecular bone, and of 100 layers with a total height of ~840 μm for cortical bone and the results were then quantified and analysed. The ROIs were drawn blinded for the treatment groups or genotypes and quantified. In the case of significant difference in the bone length between treatment groups or genotypes, ROIs were adjusted before analysis.

4.4.2 Histology and histomorphometry (I, II)

After euthanization, femurs, tibias, fracture calluses and inguinal white adipose tissue depots were immediately collected, cleaned of excess soft tissues and fixed with 10% neutral buffered formalin overnight and transferred to and stored in 70% ethanol.

In Study I, tibias were decalcified in 10% EDTA after fixation, embedded in paraffin and cut into 4 μm thick sections for histological analyses. Safranin-O staining was done using conventional staining protocols and imaged using the PANNORAMIC 250 slide scanner (3DHISTECH). Collagen was visualized using the Picro-Sirius Red Stain Kit for Collagen (Biosite), imaged using 90° polarized light visualizing thin collagen fibers as green and thick collagen fibers as yellow-red, and analysed using FIJI software.

For growth plate analysis in Study I, haematoxylin and eosin -stained (HE) sagittal sections of proximal tibial epiphysis were used. Average thickness of one medial and two marginal lines of the proliferative and hypertrophic growth plate zones were measured by ImageJ. Cell density of the proliferative and hypertrophic zones of proximal tibia were analysed by counting average cell number in 8 squares

(each 10,000 μm^2 in size) covering the entire zone. Heights of chondrocyte columns were measured from 10 representative columns in proliferative and hypertrophic zones across the growth plate.

To measure adiposity in the callus area in Study II, tibias from the fracture experiment were fixed in 3.7% formalin, decalcified in 10% EDTA, embedded in paraffin, and cut into 4 μm thick sections. HE-stained samples were scanned with PANNORAMIC 1000 slide scanner (3DHISTECH). Number of adipocyte 'ghosts' was counted manually from the fracture callus area in tibial sections using CaseViewer programme (3DHISTECH). Analysed area was standardized to 23 mm^2. Number of adipocyte 'ghosts' was normalized to the area and reported as adipocyte number/mm^2.

For histomorphometry in Studies I and II, tibias were embedded in methyl methacrylate (MMA) (Sigma-Aldrich, USA) after fixation. 5 μm sagittal sections were cut using a Leica RM2165 rotatory microtome and von Kossa, toluidine blue and tartrate-resistant acid phosphatase (TRACP) stainings were performed on deplastified sections with standard protocols. In brief, TRACP-staining visualizes osteoclasts based on the osteoclast-expressed acid phosphatase activity. The slides were analysed using Osteomeasure-histomorphometry workstation (OsteomeasureXP 3.1.0.1, Osteometrics, USA). The analysed area of the tibias was defined as 1.30 mm x 0.84 mm, starting 200 μm distally from the growth plate, excluding the cortical border areas with a 100 μm margin. Static parameters were measured from toluidine blue and TRACP stained slides and dynamic parameters from unstained slides according to standardized protocols. Subepiphyseal TRACP-staining and bone area were measured from an area defined as 1.00 mm x 0.20 mm starting immediately distally from the proximal growth plate of the tibia using FIJI software.

4.4.3 Biomechanical testing (II)

In study II, samples for biomechanical testing were carefully cleared of muscles to avoid damaging the calluses and stored in −20 °C wrapped in phosphate buffed saline (PBS) -soaked gauzes to avoid dehydration. Biomechanical testing was performed with a compression device (Lloyd Instruments, Fareham, UK) with a calibrated 100 N load cell. The samples were subjected to a three-point bending test, where the tibia was placed on a two-point sample holder 10 mm apart. Load was applied to the middle of the callus with the rate of 1 mm/min until fracture occurred. Stiffness, maximum load, post-yield displacement and amount of work-to-fracture were analysed using Nexygen (v.4.7 issue 10, Lloyd instrument Ltd., Fareham, UK). Maximum load, work-to-fracture, stiffness, and post-yield displacement were read from the load-displacement curve: Maximum load was read from the highest point

of the curve, work-to-fracture the area under the curve, stiffness was calculated as the slope of the linear rise in curve and post-yield displacement the measured displacement between yield-point and fracture-point.

4.4.4 Bone turnover marker analysis (I)

Blood samples were collected at sacrifice via cardiac puncture. Blood samples were allowed to clot, serum was collected after centrifugation and stored at -80 °C. Bone formation and resorption were assessed using serum levels of N-terminal propeptides of type I collagen (P1NP) and C-terminal telopeptides of type I collagen (CTX-1) using Rat/Mouse PINP EIA and RatLaps CTX-I EIA kits (IDS, UK), respectively.

4.5 Cell culture experiments

4.5.1 MC3T3-E1 cell line and primary cell cultures (I, II)

Mouse MC3T3-E1 osteoblastic cell line (CRL-2593, ATCC, USA) was maintained in αMEM medium supplemented with 10% fetal bovine serum (FBS, Gibco, Grand Island, NY, USA) and 100 U/ml penicillin-streptomycin (i.e., growth medium). Osteogenic differentiation was induced by osteogenic medium (OM) composed of growth medium supplemented with 5 mM Na-β-glycerophosphate, 50 μg/ml ascorbic acid and 10 nM dexamethasone at a cell density dependent on the yield at cell isolation. For LSD1 inhibition studies, cells were treated with selective LSD1 inhibitors RN-1 (IC50=70 nM) and GSK2780854A (GSK-LSD1, IC50=16 nM) or vehicle (DMSO) supplemented medium. The proliferation rate of MC3T3-E1 cells was measured by plating 1000 cells/well in a 96-well plate in maintenance medium and imaging the confluence with Incucyte S3 analyzer (Essen Bioscience, UK).

Primary calvarial cells in Study I and II were isolated from calvaria of new-born mice for differentiation cultures by sequential digestions. Cells were isolated with five consecutive 20 min digestions with 1% collagenase and 2% dispase in αMEM at 37 °C and obtained fractions 2–5 were pooled and plated for culturing. After one passage, cells were plated on 6-well plates in growth medium at a density dependent on the yield of cell isolation. Differentiation of osteoblasts was induced at confluency by OM for 7, 14 and 21 days.

For adipocyte differentiation cultures in Study II, primary calvarial cells were cultured on 6-well plates at a seeding density of 80 000 cells/well in growth medium. Two days post confluency, adipocyte differentiation was induced with adipocyte induction media (growth medium supplemented with 10 μg/ml insulin and 1.0 μM

dexamethasone), which represents day 0 of the adipocyte culture. After two days of induction, induction media was replaced with maintenance media (growth medium supplemented with 10 µg/ml insulin). Cultures were maintained until day 11 or day 14.

For osteoclast differentiation cultures in Study II, bone marrow cells were flushed from femur and tibia of 6-week-old to 9-week-old mice. 10 000 bone marrow cells were seeded at 100 µL/well in growth medium supplemented with 10 nM hPTH1-34 (Millipore, Billerica, MA, USA) in a 96-well plate.

Primary chondrocytes in Study II were digested from mice ribcages with 2 h digestion in 3 mg/ml collagenase D diluted in Dulbecco's Modified Eagle Medium (D-MEM) at 37 °C. Digestion solution was changed to 0.5 mg/ml collagenase D in D-MEM and ribcages were incubated at 37 °C for overnight. After filtering through 100 µm strainer, chondrocytes were seeded (3×10^6 cells/well) on six-well plates and cultured in DMEM supplemented with 100 U/ml penicillin-streptomycin, 10% FBS, 2 mM L-glutamine and Insulin-Transferrin-Selenium (ITS, Gibco).

4.5.2 Lentiviral silencing (I, II)

In Study I, lentiviral particles containing Sigma TRCI library small hairpin RNAs (shRNAs) against *LSD1* (TRCN0000071373–71377) and control shRNA (shScrambled, SHC002) were obtained from the Functional Genomics Unit at the University of Helsinki. Mouse MC3T3-E1 cells were transduced with 5 different clones of shLSD1 lentiviruses and shScrambled control vector on 6-well plates with 8 µg/ml polybrene overnight. Transduction of cells was confirmed with selection in puromycin (5 µg/ml) for 5 days. The efficiency of LSD1 mRNA and protein knockdown was confirmed using Reverse transcription quantitative polymerase chain reaction (RT-qPCR) and Western blotting, respectively.

In Study II, lentiviral particles containing Sigma TRCII library shRNAs against *RCOR2* (five constructs, TRC0000085518 - TRC0000085522, later abbreviated as shRCOR2-18 to shRCOR2-22) were obtained from the Functional Genomics Unit at the University of Helsinki. MC3T3-E1 were transduced by 750 µl of shRNA (p24 concentration 4.04–5.67 pg/ml), followed by selection in puromycin (3 µg/ml) for 2 days. The efficiency of *RCOR2* knockdown was confirmed using RT-qPCR.

4.5.3 Cytochemical analysis (I, II)

Cells in Study I and II were fixed for 15 min in 10% phosphate-buffered formalin and stained for alkaline phosphatase (ALP) activity for 45 min at room temperature (RT) with freshly filtered ALP staining solution (0.1 mg/ml Naphtol AS MX-PO4;

0.6 mg/ml Fast Blue RR salt; 0.4% DMF in 0.1 M Tris-HCl pH 8.3) and rinsed with water. For von Kossa staining, cells were stained with 2.5% silver nitrate at room temperature for 30 min and rinsed with water. Adipocytes in Study II were fixed as above, washed three times with PBS and stained with freshly filtered Oil Red O (Sigma) solution for five minutes. Stained culture wells were scanned with a tabletop scanner. All cytochemical staining experiments were repeated three times.

Representative images of the von Kossa or Oil Red O -stained wells (three wells per culture or genotype) were analysed with ImageJ software. Overall adipocyte or osteoblast area was defined by colour thresholding. Percentage of the positive stained area was expressed as the pixel area of Oil Red O-stained adipocytes or von Kossa -stained osteoblasts out of the total well area in pixels.

4.6 Molecular biology

4.6.1 Reverse transcription quantitative polymerase chain reaction (I, II)

RNA was extracted from cell culture samples with Nucleospin RNA Plus kit (Macherey-Nagel) after homogenization in RNA lysis buffer using Ultra-Turrax T25 homogenizer (Janke&Kunkel, Germany) and eluted to 2x30 µl aqua.

From bone samples, RNA was extracted using RNeasy Mini kit (Qiagen, USA) after pulverization of snap-frozen bones followed by homogenization in RNA lysis buffer using Ultra-Turrax T25 homogenizer. RNA concentrations were measured with NanoDrop OneC (Thermo Scientific) and the samples were stored at -80 °C.

For RT-qPCR, RNA was reverse transcribed to cDNA using the SensiFast cDNA synthesis kit (Bioline, USA) with 500 ng RNA per reaction. qPCR reactions were performed using SYBR Green master mix (Thermo Scientific) with the Bio-Rad CFX96 or CFX384 Real-Time PCR Detection System and software. Ct values were normalized to beta-actin (ACTB) levels and ΔΔ-Ct method was used to analyze relative gene expression levels. Primers used for RT-qPCR are listed in **Table 7**.

Table 7. RT-qPCR target genes and primer sequences.

TARGET	FORWARD PRIMER	REVERSE PRIMER
ADIPOQ	CGACACCAAAAGGGCTCAGG	CCAACCTGCACAAGTTCCCT
ALP	ACTCAGGGCAATGAGGTCAC	CACCCGAGTGGTAGTCACAA
ACTB	CGTGGGCCGCCCTAGGCACCA	TTGGCCTTAGGGTTCAGGGGG
BGLAP	GCAATAAGGTAGTGAACAGACTCC	CCATAGATGCGTTTGTAGGCGG
COL1A1	AGACATGTTCAGCTTTGTGGAC	GCAGCTGACTTCAGGGATG
CYCLB	GGGACCTAAAGTCACAGTCAAGG	GAAGCGCTCACCATAGATGC
DMP1	GGTTTTGACCTTGTGGGAAA	TTGGGATGCGATTCCTCTAC
IBSP	GAATGGCCTGTGCTTTCTCG	CCGGTACTTAAAGACCCCGTT
LSD1	AAGCCAGGGATCGAGTAGGT	GGAACAGCTTGTCCATTGGC
PPARG	AAGACAACGGACAAATCACCA	GGGGGTGATATGTTTGAACTTG
RCOR1	CCGACTTCGCTGCCAAA	AGCCTGCTCCATGTTGTACC
RCOR2	AGGGCATGTACCTGAGTCCT	TGGTCTGCTTCATGCTCTGG
RCOR3	TACCAAGCTCGGATCCCTGA	ATTCATCCAATTTGGCATCTGG
RUNX2	GCCCAGGCGTATTTCAGA	TGCCTGGCTCTTCTTACTGAG
SP7	GTCCTCTCTGCTTGAGGAAGAA	GGGCTGAAAGGTCAGCGTAT
TRACP	CGTCTCTGCACAGATTGCAT	AAGCGCAAACGGTAGTAAGG

4.6.2 RNA-sequencing and bioinformatic analysis (I, II)

MC3T3-E1 cells were plated in triplicates in 6-well plates at density of 100 000 cells per well. Cells were harvested at 80% confluence representing proliferative stage, as well as at confluency and after 24 h, 14 days and 21 days of osteogenic differentiation in OM. At indicated timepoints, the cells were washed once with PBS, lysed and RNA extracted by RNeasy mini kit (Qiagen) according to the manufacturer's instructions. Quality of RNA was analysed by Bioanalyzer, and RIN-value was measured to be >9 before sequencing. Based on the RIN-value of the three replicates, two samples were selected from each timepoint for RNA-seq library preparation.

RNA-seq was performed on the Illumina2000 platform as 51 bp paired-end reads and processed using a standardized bioinformatic pipeline. Gene expression is expressed in fragments/kilobase pair/million mapped reads (FPKM). RNA-seq data were deposited in the Gene Expression Omnibus of the National Institute for Biotechnology Information (GSE186832).

The raw reads were subjected to quality control using FastQC, a framework for fastq format sequencing data quality analysis. The reads were aligned to the latest version of UCSC mouse genome (mm10) using TopHat version 2.0.9 for 64bit Linux x86 with default parameters that have been optimized for mammalian genomes. The data were analysed using R version 3.0.1 for 64bit Linux x86 (http://www.r-

project.org/) for Euclidean distance, Pearson correlation and Principal component analysis. Differential expression between base time point T1 and all other time points was computed in R using DESeq2 version 1.2.8. P-values were corrected using Benjamini-Hochberg multiple testing adjustment procedure.

Collective biological properties of the differentially expressed (DE) genes were investigated using pathway enrichment analysis. The pathway set used consisted of the biological process, molecular function and cellular compartment categories of Gene Ontology version 2.10.1 (http://www.geneontology.org/). Statistically enriched pathways were determined with the TopGO R toolset using the classic algorithm with Fisher statistic. The pathway enrichment analysis was repeated for each set of DE genes, generating results using each of the three Gene Ontology (GO) categories. First hierarchical agglomerative clustering was applied to the expression values of most highly time variant genes. The distance metric used in the clustering is Dynamic Time Warping (DTW), a method specifically designed to be used with time series data.

In order to distinguish these trends more carefully, k-means clustering was performed (II, Fig. 4). To evaluate the correct number of clusters the Bayesian Information Criterion (BIC) was used to analyze the density of clustering results using different values of k. K-means clustering was performed using 6 clusters. Pathway enrichment analysis was performed to the clustered gene sets. Pathway enrichment using the Gene Ontology categories was computed for each gene cluster.

4.6.3 Chromatin immunoprecipitation sequencing and bioinformatic analysis (I)

MC3T3-E1 cells (10 000 cells/cm^2) were plated in 10 cm plates in growth medium. The cells were harvested by trypsin and analysed using a chromatin immunoprecipitation (ChIP) assay using LSD1, H3K4me1, H3K4me2, H3K4me3, H3K27me3 and control IgG antibodies. Antibody information can be found in **Table 8**. Sequencing libraries were prepared and massively parallel high throughput DNA sequencing was performed on an Illumina HiSeq2000 system. The alignment, quality assessment, peak calling, and visualization was performed with a standardized bioinformatic analysis pipeline (HiChIP). The mm10 reference genome was used to align 50 base paired-end with a custom script that only retains pairs with one or both ends uniquely mapped. The analysis was guided by the Burrows-Wheeler Aligner, Picard and SAMTools and the SICER package. ChIP-seq data were deposited with accession number GSE186665.

Table 8. Information on antibodies used in ChIP and Western blotting.

ANTIBODY	MANUFACTURER	CAT NO	APPLICATION
H3	Abcam	ab1791	Western blot
H3K4ME1	Diagenode	C15410037	Western blot
H3K4ME2	ActiveMotif	39679	Western blot
H3K9ME1	Abcam	ab9045	Western blot
H3K9ME2	Abcam	ab1220	Western blot
LSD1	Abcam	ab17721	Western blot
ANTI-MOUSE	Cell Signalling Technology	7076S	Western blot
ANTI-RABBIT	Cell Signalling Technology	7074S	Western blot
CHIP IGG	Sigma-Aldrich	12-370	ChIP-seq
CHIP H3K4ME1	Cell Signalling Technology	5326 Lot1	ChIP-seq
CHIP H3K4ME2	Abcam	ab7766	ChIP-seq
CHIP H3K4ME3	Diagenode	C15410003	ChIP-seq
CHIP H3K27ME3	Cell Signalling Technology	9733BC (C36B11)	ChIP-seq
CHIP LSD1	Abcam	ab17721	ChIP-seq

Peak data were read using custom R scripts, and exploratory analysis and peak annotation was done using R package ChIPseeker. Average profiles of ChIP-seq peaks binding to transcription start site (TSS) regions were inspected and visualized, using 3 kb upstream and downstream TSS flanking sequences for the mapping. Peaks were annotated to the nearest TSS, with TSS region defined from -3 kb to +3 kb (default). R package DiffBind was used for generation of the correlation heatmaps. The overlaps of the ChIP-seq peak intervals were inspected using R package ChIPpeakAnno with minimum overlap of 1 bp of the peak intervals required. Further exploratory analysis was performed using DiffBind package. Shortly, consensus peak sets were generated for each of the five ChIP-seq targets separately, consisting of all peaks detected at one or more time points. Reads overlapping these consensus peak sets were calculated and normalized using Trimmed Mean of M-values (TMM) method with control read counts subtracted and using full library sizes for normalization. The resulting ChIP-seq affinity data was used for principal component analysis using DiffBind functionality.

BEDTools multiIntersectBed and merge tools were used for detecting peak overlaps between the three time point samples, retaining the information on the peak existence in a sample, and for merging the overlapping peak intervals into continuous peak regions. TMM normalized read counts for the merged peaks were obtained using DiffBind. Log2 fold change of normalized read counts between day 7 and day 0 samples, day 14 and day 0 samples as well as day 14 and day 7 samples were calculated.

HOMER (Hypergeometric Optimization of Motif EnRichment) software was used for analyzing enrichment of known transcription factor (TF) motifs in ChIP-seq peaks and annotating the peaks with the known motifs.

Gene set enrichment of Gene Ontology Biological Process (GOBP) terms and Kyoto Encyclopedia of Genes and Genomes (KEGG) pathway terms was performed using R package CHiP-Enrich with the gene locus definition set to 1 kb.

Integration of differential expression analysis data and ChIP-seq data was done using custom Rscripts and package ggplot2 for visualization.

4.6.4 Western blotting (I)

MC3T3-E1 cells were cultured on 10 cm dishes in growth medium or OM. Protein lysates were collected from preconfluent and confluent cells, as well as from cells differentiated for 7, 10 or 14 days after 10-minute incubation on ice in mRIPA lysis buffer (50 mM Tris-HCl, pH 7.4; 0.5% NP-40; 0.25% sodium deoxycholate; 150 mM sodium chloride; 1 mM sodium orthovanadate; 0.5 mM phenylmethylsulfonyl fluoride) supplemented with Pierce Mini protease inhibitors (Thermo Scientific). Cell lysates were homogenized by purging through a 27 G needle and cell debris discarded by centrifuging for 15 minutes at 16 000 G at 4°C. Protein concentration was measured using Bradford Protein Assay (Bio-Rad).

Protein samples were separated using 4–20% gradient SDS-PAGE gels (Bio-Rad Mini-PROTEAN TGX) and transferred to 0.22 µm nitrocellulose membranes (Maine Manufacturing LLC). Membranes were blocked with either 5% non-fat dried milk in Tris-buffered saline with Tween (TBST) (150 mM NaCl, 0.05% Tween20, 10 mM Tris pH 7.5) and incubated with primary antibodies against H3, H3K4me1, H3K4me2, H3K9me1, H3K9me2 or with 5% bovine serum albumin (BSA) in TBST and incubated with anti-LSD1 primary antibody. Horseradish peroxidase conjugated anti–mouse (LSD1) or anti-rabbit (other antibodies) IgG was used as a secondary antibody. Proteins were visualized using WesternBright Quantum detection kit (Advansta). Antibody information can be found in **Table 8.**

4.7 Statistical analyses (I, II)

All results were analysed with the GraphPad Prism 8.3.0 software, except for the RNA-sequencing and ChIP-sequencing data described above. Results are expressed as mean ± standard deviation (SD). The limit for statistical significance was set to $p < 0.05$ using Bonferroni's multiple comparison correction where applicable. Statistical significances are expressed with asterisks, * $p < 0.05$, ** $p < 0.01$ and *** $p < 0.001$.

In Studies I and II, all results were tested for normal distribution with the Shapiro-Wilk normality test and outliers with the ROUT method with Q = 1%. Changes between groups were analysed using Student's two-tailed t-test, one-way ANOVA or Kruskall-Wallis test. Student’s two-tailed t-test was applied when normal distribution was determined and two groups were compared, One-way ANOVA when normal distribution was determined and there were more than two groups and Kruskal-Wallis test when normal distribution was not found.

5 Results

5.1 Effects of LSD1 on osteoblast differentiation (I)

5.1.1 LSD1 is highly expressed in osteoblasts and binds to loci enriched with RUNX2 binding motifs

Research on the role of histone demethylases in osteoblast differentiation has mostly focused on the JmjC-domain containing KDM-family, leaving the LSD subfamily with less focus. We collected RNA samples from mouse pre-osteoblast MC3T3-E1 cells before differentiation from non-confluent and confluent cells and after 24 hours, 14 days or 21 days of osteoblast differentiation induced with dexamethasone, ascorbic acid and Na-β-glycerophosphate and analysed the gene expression changes during the differentiation using RNA-sequencing. Our data shows that during osteoblast differentiation *LSD1* is not only expressed more abundantly than *LSD2*, the other monoamine oxidase domain containing histone demethylase, but its expression was also among the highest of all KDMs measured in FPKM read counts. mRNA expression of *LSD1* in differentiating MC3T3-E1 cells was consistently high in our RNA-sequencing (FPKM >10) and RT-qPCR experiments (>1.5-fold expression compared to undifferentiated cells), while the protein levels increased during osteoblast differentiation compared to subconfluent or confluent pre-osteoblasts in Western blotting analysis (I, Fig 1 C, S1 Fig A-C, **Figure 7A**).

ChIP-sequencing of MC3T3-E1 cell lysates collected at 0, 7 and 14 days of differentiation and incubated with LSD1, H3K4me1, H3K4me2, H3K4me3, H3K27me3 and control IgG antibodies revealed increasing LSD1 binding to chromatin over the differentiation time course. There were a significant number of unique LSD1 binding sites at each time point, further suggesting a dynamic binding pattern during osteoblast differentiation. LSD1 binding sites enriched near the transcription start sites as well as proximal promoter areas, and the majority of LSD1 peaks were found within 1000 bases from a transcription start site (I, Fig 6 A-D).

The association of different histone marks with LSD1 binding to chromatin was further studied using the ChIP-sequencing data of LSD1, H3K4me1, H3K4me2, H3K4me3, H3K27me3 bound DNA. LSD1 peaks were often lacking H3K4me1 (46% simultaneous occupancy) but overlapping with H3K4me2 (89% occupancy) and

H3K4me3 (64% occupancy) binding (I, Fig 7 C-D, **Figure 7C**). As both H3K4me1 and H3K4me2 are targets for LSD1 demethylation activity, this would suggest a target preference to H3K4me2 over H3K4me1 in osteoblasts. However, association of LSD1 with H3K4me1 was at some loci found to be dependent on genomic context, as promoter area of KDM7a lacked H3K4me1/LSD1 co-occupancy, but an upstream enhancer area did show binding of both H3K4me1 and LSD1 (I, Fig 8, S3).

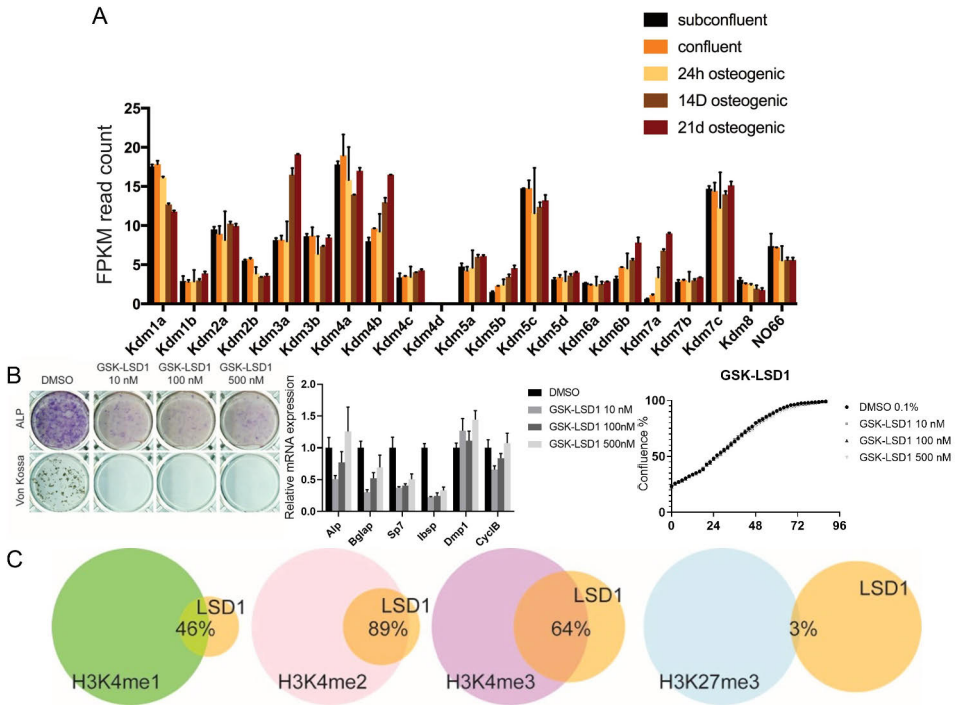

Figure 7. LSD1 is necessary for osteoblast differentiation. A: RNA-sequencing analysis of histone demethylases in MC3T3-E1 pre-osteoblasts during proliferation and differentiation. B: Inhibition of LSD1 demethylation activity with GSK-LSD1 inhibits MC3T3-E1 osteoblast differentiation *in vitro* but does not influence proliferation. C: LSD1 and histone modification peak overlaps in MC3T3-E1 cells differentiated for 14 days.

When comparing the RNA expression data and ChIP-sequencing data collected from the differentiating MC3T3-E1 osteoblasts, over 90% of genes with LSD1 binding at promoter area were expressed (log 2>1) both at confluency and at 14 days of differentiation (I, Fig 9 B). However when reversing the analysis, LSD1 binding at all expressed genes was more moderate, 20% and 33% at confluency and at 14 days of differentiation, respectively. Even though LSD1 has previously been defined as a member of a repressor complex, LSD1 binding was not predictive to the direction of the change when found in promoters of genes differentially expressed between the time points (I, Fig 9 C).

Previous research has not found a DNA targeting mechanism for LSD1 demethylating activity, but the binding has appeared to be non-specific (Pilotto et al., 2015; M. Yang et al., 2006). After revealing the high expression level of LSD1 and the colocalization of LSD1 with histone marks representing gene expression activation, our hypothesis was that LSD1 could be targeted to specific promoter areas by interactions with nuclear proteins. Therefore, LSD1 binding sites were searched for conserved binding motifs for transcription factors and indeed, consensus motifs for RUNX1/2 were found in 16-20% of LSD1 ChIP-sequencing peaks. LSD1 ChIP-sequencing peaks were also compared to previous RUNX2 ChIP-sequencing peak data (Tarkkonen et al., 2017), and 35% of the LSD1 peaks containing RUNX2 motifs were found to also be RUNX2 binding sites (I, Fig 6 E-F).

These results demonstrated a significant contribution of LSD1 to gene expression during osteoblast differentiation and correlation of LSD1 binding with increased gene expression, possibly through recruitment by RUNX2.

5.1.2 LSD1 inhibition and downregulation suppresses osteoblast function and differentiation *in vitro*

Previous results have suggested LSD1 to have a suppressive role for osteoblast differentiation (Sun et al., 2018). To further study the effect of loss of LSD1 activity on osteoblast differentiation, we inhibited both the demethylation activity of LSD1 using monoamine oxidase inhibitors RN-1 and GSK-LSD1, as well as silenced LSD1 expression with shRNA in MC3T3-E1 cells before differentiation and during differentiation in OM for 21 days.

Pharmacological inhibition of LSD1 demethylation activity in RN-1 and GSK-LSD1 treated cells differentiated in OM demonstrated that LSD1 function is important for osteoblast differentiation but it does not affect osteoblast proliferation measured by confluence analysis. Both inhibitors at nanomolar concentrations blocked osteoblast differentiation and mineralization detected by colour thresholding analysis of von Kossa staining in both MC3T3-E1 cells and calvarial primary cells at 21 days of differentiation in OM. Osteoblast differentiation blockage was also seen in the decreased gene expression of osteoblast markers *ALP*, osteocalcin, osterix and bone sialoprotein at 14 days of differentiation of LSD1 inhibitor treated MC3T3-E1 cells and calvarial primary cells in OM (I, Fig 2 A-C, **Figure 7B**).

Silencing of *LSD1* expression through shRNAs showed similar effects on osteoblast differentiation as pharmacological inhibition. Significant decrease of osteoblast differentiation and mineralization were detected by ALP and von Kossa stainings. Consistently, expression of osteoblast marker genes measured with RT-qPCR was decreased. However, global H3, H3K4me1 or H3K4me2 protein levels

measured with Western blotting were unchanged suggesting a more targeted than global demethylation effect for LSD1 (I, Fig 1 E-G).

These data show the key role on bone metabolism LSD1 demethylation activity plays by enabling osteoblast differentiation *in vitro*.

5.1.3 LSD1 inhibition suppresses osteoblast differentiation and function *in vivo*

To transfer the encouraging *in vitro* findings to a more translatable experimental setting, 6-week-old male C57BL/6NHsd male mice were treated with 1.5 mg/kg GSK-LSD1 or vehicle for 4 weeks. This LSD1 inhibitor treatment was well tolerated with no side effects such as symptoms of pain.

Effects of GSK-LSD1 inhibitor treatment were assessed using µCT as well as histomorphometric analysis and measurements of bone turnover markers. µCT analysis of the GSK-LSD1 treated proximal tibia showed significantly lower bone quantity measured as decreased bone volume per tissue volume (BV/TV), trabeculae number and trabecular thickness, as well as lower cortical thickness, when compared to vehicle treated mice (I, Fig 3, **Figure 8**).

Treatment	Control average ± SD	GSK-LSD1 average ± SD
µCT BV/TV (%)	11.33 ± 2.26	6.00 ± 2.56 ***
µCT Tb.Th (µm)	0.050 ± 0.0026	0.046 ± 0.0055 *
µCT Tb.n (#/mm)	2.24 ± 0.38	1.27 ± 0.45 ***
µCT Cort.Th (µm)	0.19 ± 0.016	0.17 ± 0.014 *
Histomorphometry BV/TV (%)	12.40 ± 3.04	5.25 ± 1.62 ***
Histomorphometry Tb.Th (µm)	35.06 ± 4.78	24.57 ± 3.84 ***
Histomorphometry n.Ob/B.Pm (#/mm)	4.13 ± 1.76	2.12 ± 0.98 *
Histomorphometry OS/BS (%)	5.77 ± 2.45	2.06 ± 1.00 **
Serum CTX-I (ng/ml)	31.10 ± 4.04	26.88 ± 4.77
Serum P1NP (ng/ml)	81.33 ± 24.79	57.45 ± 10.32 *

* = p<0.05, ** = p<0.01, *** = p<0.001

Figure 8. LSD1 inhibition with GSK-LSD1 *in vivo*. Left: Representative von Kossa stained methyl methacrylate sections of Control (top) and GSK-LSD1 treated (bottom) mouse tibias. Right: Most relevant µCT, histomorphometry and bone turnover marker data. (n=10/group)

To further investigate the mechanism behind the low bone quantity, histomorphometric analysis of methyl methacrylate embedded tibias was performed.

The analysis confirmed the same findings in GSK-LSD1 treated mice compared to controls, but also revealed a significantly lower number of osteoblasts as well as lower trabecular thickness and amount of osteoid (I, Fig 3, **Figure 8).** Relative number of osteoclasts was similar between the groups.

Analysis of bone turnover markers in serum did not reveal any differences in the levels of bone resorption marker CTX-I levels, but instead a significantly lower amount of bone formation marker P1NP, in line with the target cell population and results of histomorphometric analysis (I, Fig 3, **Figure 8**).

Collectively these results showed that the LSD1 demethylation activity is crucial for osteoblast activity and when LSD1 is inhibited, there is a significantly lower bone volume *in vivo.*

5.1.4 LSD1 downregulation disrupts growth plate organization and osteoblast differentiation *in vivo*

To fully demonstrate the effects of decreased LSD1 expression in bone *in vivo,* we created a conditional LSD1 knockout mouse line, where LSD1 is either heterozygously or homozygously deleted in the limb bud mesenchyme under the control of Prrx1-promoter, $Rcor2^{-/-}_{Prrx1}$.

LSD1 conditional knockout mice demonstrated a clear phenotype at already 4 weeks of age in both males and females, as the body mass of homozygous knockout mice was 42% lower than in control littermates and the body size was significantly smaller as measured by 35% shorter tibias in males. Heterozygous knockout mice were also smaller than control mice, but resembled control mice more closely than homozygous knockout mice. The overall appearance of bones in 2D X-ray analysis was reminiscent of Osteogenesis imperfecta with characteristic curvature of long bones. Other significant findings were the loss of secondary ossification centres and impaired union of the fibula to the tibia. 3D X-ray analysis also demonstrated unclosed calvarial sutures (I, Fig 4, **Figure 9 A**).

More detailed μCT analysis of the tibias and femurs revealed a dose-dependent decrease in bone volume and structural organization in decreased BV/TV, trabecular number, structural model index, cortical tissue volume and density (I, Fig 4, **Figure 9 B**).

Histomorphometrical analysis of the MMA-embedded tibias controversially revealed increased BV/TV and trabecular thickness, similar osteoblast numbers and activity and decreased osteoclast numbers in homozygous knockout male mice compared to controls. There were no differences in the levels of bone turnover markers CTX and P1NP between the groups (I, Fig 4, **Figure 9 C**). These conflicting results highlight the dysregulated status of bone metabolism. However, in the mRNA analysis of marrow-evacuated femurs of male mice, significant decrease in the expression of osteoblast marker genes *OSX*, *OPG*, *RUNX2* and *COL1A1* and

significantly increased adiponectin expression were observed. RT-qPCR analysis also showed 60% decrease in *LSD1* expression (I, Fig 4).

The distorted bone formation seen in 2D X-ray images was further analysed from the growth plates using Safranin-O stained tissue sections. Visual analysis of the sections revealed clear lack of organization and decreased cell number in the growth plates of knockout mice compared to controls. The proliferative zone was thinner, but the hypertrophic zone was comparable between groups. However, both cell density and mean column height were decreased in LSD1 knockout mice. Together with the decreased osteoclast number in the subepiphyseal bone, these results demonstrate the disorganization and lack of remodelling of the growth plates of conditional LSD1-knockout mice (I, Fig S2, **Figure 9 D**).

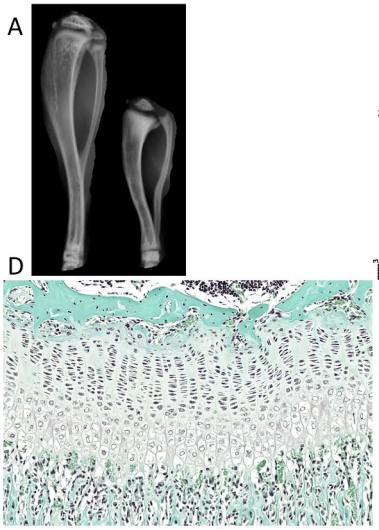

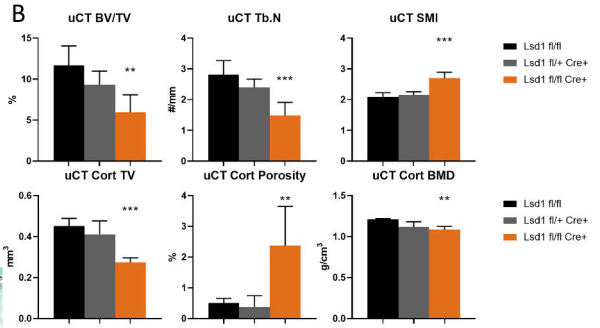

C

	$Lsd1^{fl/fl}$	$Lsd1^{+/-}_{Prrx1}$	$Lsd1^{-/-}_{Prrx1}$
BV/TV (%)	10,52 ± 0,89	10,24 ± 2,43	25,23 ± 3,35
Tb.Th (µm)	25,50 ± 1,78	24,47 ± 3,08	41,66 ± 3,11
OS/BS (%)	1,92 ± 1,25	2,37 ± 1,10	2,30 ± 1,22
n.Ob/B.Pm (#/mm)	2,37 ± 1,37	2,56 ± 1,09	2,30 ± 0,76
ES/BS (%)	2,62 ± 0,42	3,13 ± 1,27	2,42 ± 0,47
n.Oc/B.Pm (#/mm)	1,92 ± 0,31	2,24 ± 0,98	1,41 ± 0,34
MAR (µm/day)	4,42 ± 1,22	3,76 ± 0,69	4,93 ± 0,95
BFR/BV (%/year)	3,96 ± 0,94	3,44 ± 1,98	3,18 ± 0,80

* = p<0.05, ** = p<0.01, *** = p<0.001

Figure 9. LSD1 mesenchymal cell targeted conditional knockout *in vivo*. A: Representative 2D X-ray images of control (left) and LSD1 conditional knockout mouse (right) tibias. Loss of LSD1 leads to disturbed trabeculae distribution, non-union of the fibula and disturbed secondary ossification sites. B: µCT analysis of LSD1 conditional knockout mouse femurs show significant loss of bone quantity and bone mineral density. C: Histomorphometric analysis showed disturbed bone structure of LSD1 knockout mice (n=5-7/group). D: Safranin-O staining of control (top) and LSD1 knockout mouse (bottom) growth plates shows significant loss of organization.

These findings on the effects of LSD1 gene downregulation in mesenchymal limb bud cells highlight the importance of LSD1 on osteoblast differentiation, growth plate organization and bone remodelling *in vivo.*

5.2 Effects of RCOR2 on osteoblast differentiation (II)

5.2.1 Loss of RCOR2 delays osteoblast differentiation *in vitro*

The role of RCOR2 in bone environment has not been previously studied, except in osteoarthritic chondrocytes (Primrose et al., 2023). However, our RNA-sequencing analysis on OM-treated MC3T3-E1 cells showed a significantly increasing expression of *RCOR2* (but not *RCOR1* or *RCOR3*) during osteoblast differentiation *in vitro* (II, Fig 1 A). This expression pattern was further confirmed with RT-qPCR performed on RNA collected at start of differentiation or after 14 days of differentiation, showing increased *RCOR2* expression during differentiation of MC3T3-E1 cells, primary calvarial osteoblasts as well as primary calvarial adipocytes. Interestingly, RT-qPCR studies also showed increased *RCOR3* expression during MC3T3-E1 and primary calvarial osteoblast differentiation, a finding not seen in RNA-sequencing analysis (II, Fig 1 B-E). *RCOR2* was found to be expressed in all bone cells of mesenchymal origin (chondrocytes, adipocytes, primary osteoblasts and MC3T3-E1 cells), but not in osteoclasts derived from hematopoietic stem cells (II, Fig 1 F). *RCOR2* expression was further studied in a tissue panel of 14 mouse tissues using RT-qPCR, where *RCOR2* was found to be ubiquitously expressed in all tissues with highest expression levels in liver and pancreas, and surprisingly lowest in the femur (II, Fig 1 G).

Encouraged by the dynamic expression pattern of *RCOR2*, the role of RCOR2 in osteoblast differentiation was studied by silencing *RCOR2* expression using anti-*RCOR2* shRNA-constructs. Two different constructs with highest *RCOR2* silencing efficiency were selected (shRCOR2-18 and shRCOR2-21) and studied in both MC3T3-E1 cells and primary calvarial osteoblasts. Both shRNA constructs resulted in ~50% silencing of *RCOR2* in primary screening and silencing was reproducible and effective in MC3T3-E1 cells. Silencing of *RCOR2* led to significantly decreased osteoblast differentiation as seen by ALP staining at 14 and 21 days of differentiation in OM, as well as by osteoblast marker gene expression in RT-qPCR at 14 days, and loss of mineralization in von Kossa staining at 21 days of differentiation (II, Fig 2 A-C). These constructs efficiently silenced *RCOR2* also in the preliminary screening in primary calvarial osteoblasts, however the effects seen in MC3T3-E1 cells were only partly recapitulated. Osteoblast differentiation was decreased as seen by ALP staining at 14 and 21 days of differentiation, but mRNA expression data collected at

14 days using RT-qPCR was not consistent with either the ALP staining or the MC3T3-E1 cell data (II, Fig 2 D-F).

These results demonstrate the importance of RCOR2 expression in supporting osteoblast differentiation as evaluated by the regulation of osteoblast function and marker gene expression.

5.2.2 RCOR2 downregulation relieves target gene suppression

To further study the effects of RCOR2 during osteoblast differentiation, another RNA-sequencing analysis was done on shRCOR2-18-silenced MC3T3-E1 osteoblasts and shScrambled-treated control cells at confluency and after 24 hours or 7 days of osteogenic stimulation. This was performed to show differences in the initial response as well as at the early phases of osteogenic induction. Gene expression was compared between the constructs at each time point, separately for upregulated and downregulated genes compared to shScrambled. There were 438, 348 and 472 genes with differential expression at 0 hours, 24 hours and 7 days of osteogenic stimulation, respectively. Of the >2-fold differentially expressed (DE) genes, most were upregulated and the ratio of upregulated genes was increasing at each timepoint (II, Fig 3 A). This upregulation would support the previously suggested role of RCOR2 as a transcriptional repressor, now expanding also to include osteoblasts.

Next the DE genes between time points were studied and compared between constructs. When comparing the DE genes between 0 hours and 24 hours in shRCOR2 cells with shScrambled, there were nearly 700 genes in shScrambled of which 295 were common between groups, but only 167 unique genes in shRCOR2 cells. When comparing DE genes between 0 hours and 7 days, there was a similar number of DE genes in both groups (II, Fig 3 B). The DE genes from both 0 h/24 hours and 0 h/7 days comparisons were subjected to Pathway Enrichment analysis and the highlighted Gene Ontology terms included chromatin and chromosome organization and different metabolic processes (II, Fig 3 C).

The DE genes then underwent K-means clustering to form nine gene clusters of similar behaviour during differentiation. On average, more variation was seen in the gene expression at 24 hours than at 7 days of differentiation, highlighting the role of RCOR2 in the beginning of differentiation, during the transition from stem-like cells to differentiating cells. Cluster D, where gene expression increases at 24 hours and then decreases to 7 days, represents genes responding quickly to the introduction to osteogenic induction but reversing this response upon the onset of differentiation (II, Fig 4 D, Table S2). This cluster includes e.g. pathways related to interferon signalling, representing at least in part the response to dexamethasone present in osteogenic medium.

Due to the repressor role of RCOR2 in the REST complex, clusters with significant upregulation under RCOR2 silencing, clusters A, E, and H, were chosen for further pathway enrichment analysis. Cluster A represented genes with stable expression at 24 hours and increase to 7 days of differentiation. Genes of cluster A were associated with nucleotide biosynthesis and metabolic process pathways suggesting differences in cell proliferation/differentiation transition. Genes of TGF-β pathway were enriched in cluster A, supporting the early induction of osteoblast differentiation (II, Fig 4 A, Table S2). Cluster E includes genes with steadily increasing expression with levels not matched by control cells. These genes are linked to skeletal and limb morphogenesis, mesenchymal cell proliferation and neuronal differentiation (II, Fig 4 E, Table S2). Cluster H includes genes with similarly increasing expression as cluster E, but where the expression level at 7 days is the same as in control cells. These genes are considered mandatory for osteoblast differentiation (II, Fig 4 H, Table S2).

5.2.3 RCOR2 regulates osteoblast differentiation, but is not irreplaceable *in vivo*

To assess the role and function of RCOR2 in the complex regulatory environment of bone remodelling, we decided to study its effects by utilising knockout models, especially since there were no previous publications on the bone phenotype of RCOR2 knockout *in vivo*. To create global knockout mice, homozygous Tm1a knockout-first allele mice carrying LacZ-Neo insertion cassette upstream of the *RCOR2* gene were bred. These mice were found to be viable and fertile. However, after deletion of the LacZ-Neo cassette along with exons 1-7 of the *RCOR2* gene, all homozygous embryos were lost before E8.5, which could be linked to the previously reported role of RCOR2 in neuronal development (Y. Wang et al., 2016), as well as in the embryonic stem cell differentiation (Pei et al., 2022). Heterozygous RCOR2 knockout mice ($Rcor2KO^{+/-}$) were, however, viable and in terms of body weight indistinguishable of littermates.

The bone phenotype of $Rcor2KO^{+/-}$ mice was thus assessed at 6 and 12 weeks of age using µCT and histomorphometric analysis from both males and females. There were no significant differences between heterozygous and control mice in any of the µCT parameters analysed, except for an increased cortical thickness in males at 12 weeks of age. The histomorphometric analysis revealed a statistically significant 30% decrease in trabecular BV/TV ratio in males at 12 weeks of age (II, Fig 5 A-B, **Table 9**).

To further study the effect of homozygous deletion of RCOR2 *in vivo*, RCOR2 deletion was targeted to long bone mesenchymal progenitor cells by using Prrx1-Cre mouse strain. The $Rcor2^{-/-}_{Prrx1}$ mice were viable and had no issues with well-being,

fertility or bodyweight. The bone phenotype of both male and female mice was examined using µCT analysis at 6, 12 and 26 weeks of age. Increased cortical thickness was observed in femurs of 6-week-old females and 12-week-old males, as earlier seen in Rcor2KO$^{+/-}$ mice. 6-week-old females also had decreased marrow volume in the cortical bone analysis, and both 6- and 12-week-old females had decreased trabecular thickness. In males, the only statistically significant difference was increased cortical bone volume at 26 weeks of age (II, Fig 5 C-F, **Table 9**).

To further study the effect of conditional RCOR2 knockout on bone formation, we decided to induce rapid bone loss in mice by ovariectomy. Ovariectomy was performed on Rcor2$^{-/-}_{Prrx1}$ mice and Rcor2$^{fl/fl}$ control mice at the age of 12 weeks and samples were collected four weeks later. OVX led to similar overall loss of bone volume in both knockout and control mice, compared to sham-operated animals. The conditional deletion of RCOR2 led to increased trabeculae number as well as decreased cortical tissue and marrow volumes in the OVX-treated animals (II, Fig 6 A, **Table 9**).

Another method to highlight the potential differences in bone formation was the fracture healing model. Closed tibial fractures were performed on 8-week-old Rcor2$^{-/-}_{Prrx1}$ and Rcor2$^{fl/fl}$ male and female mice and samples collected 4 weeks later. µCT analysis did not reveal any significant differences in the fracture calluses. A subset of samples was frozen for biomechanic testing with the 3-point-bending test. No differences were found in the stiffness, maximum load or post-yield displacement properties, but the work-to-fracture value was significantly increased in the conditional knockout group (II, Fig 6 B-F, **Table 9**).

These *in vivo* findings suggest that although RCOR2 has a role in osteoblast differentiation and activity, the effects might be compensated by other RCOR family members or different mechanisms *in vivo*.

Table 9. Summary of µCT and biomechanic analysis of RCOR2 global and conditional knockout mice at different ages and when challenged with OVX or fracture. *p<0.05, **p<0.01, ***p<0.001. N/A, not analysed.

		FEMALES			**MALES**		
EXPERIMENTAL MODEL	Age	BV/TV (%)	Trab.Th (µm)	Cort.Th (µm)	BV/TV (%)	Trab.Th (µm)	Cort.Th (µm)
RCOR2KO	6 weeks	↔	↔	↔	↔	↔	↔
	12 weeks	↔	↔	↔	↔	↔	↑ **
RCOR2$_{PRRX1}$ TIBIAS	6 weeks	↔	↓ *	↔	↔	↔	↔
	12 weeks	↔	↔	↑ ***	↔	↔	↔
RCOR2$_{PRRX1}$ FEMURS	6 weeks	↔	↔	↑ ***	↔	↔	↔
	12 weeks	↔	↔	↔	↔	↔	↑ **
	26 weeks	N/A	N/A	N/A	↔	↔	↔
OVX	16 weeks	↔	↔	↔	N/A	N/A	N/A
		BV (mm^3)	TV (mm^3)	BMD (g/cm^3)	BV (mm^3)	TV (mm^3)	W-T-F (Nmm)
FRACTURE HEALING	12 weeks	↔	↔	↔	↔	↔	↑ ***

5.2.4 RCOR2 supports adipocyte differentiation *in vitro* and *in vivo*

As the initial differentiation experiments showed, RCOR2 expression was elevated in all bone-related mesenchymal cell types evaluated, including adipocytes (II, Fig 1 F). This raised the question, whether the downregulation of RCOR2 would impact adipocyte differentiation *in vitro* or *in vivo*. Calvarial cells were extracted from Rcor2KO$^{+/-}$ and control mice and differentiated to adipocytes using insulin and dexamethasone induction and insulin-supplemented differentiation medium. The heterozygous knockout of RCOR2 led to 45% decrease in Oil-Red-O stained area in adipocyte primary cell cultures (II, Fig 7 D-E) and the inguinal white adipose tissue accumulation was found to be significantly lower in female mice at the age of 16 weeks in Rcor2$^{-/-}_{Prrx1}$ mice compared to controls (II, Fig 7 C). Finally, the adiposity inside the fracture callus was evaluated from the H&E-stained sections and the number of adipocytes was found to be significantly lower in conditional knockout mice compared to control (II, Fig 7 A-B), suggesting that the mesenchymal cells inside the fracture callus were differentiating less to adipocytes and more to osteoblasts and chondrocytes. Taken together, the *in vitro* findings of impaired adipocyte differentiation were supported by *in vivo* findings.

6 Discussion

Increasing knowledge and data concerning the importance of epigenetic regulation of bone metabolism has led to more interest and emphasis on discovering the regulators and their cofactors. The variety of therapeutic options in treating bone diseases is still limited, giving rise to need for new treatment strategies. Current treatment options targeting osteoclast and osteoblast differentiation and function have left room for novel modes of action. One such approach could be treatment of osteoporosis through modifying epigenetic regulation of target genes.

This study aimed to demonstrate the roles of LSD1 and RCOR2 in osteoblast differentiation and investigate the mechanisms of action how they target and influence gene expression. In *Study I,* we demonstrated that the loss of LSD1 expression or demethylation function had an effect on osteoblast differentiation both *in vitro* and *in vivo,* and we linked the LSD1 DNA binding sites to previously published RUNX2 binding sites. The conditional knockout of LSD1 *in vivo* had detrimental effects on the structure and size of long bones, as well as closure of calvarial sutures and organization of growth plates. In *Study II,* we were able to show the impaired MC3T3-E1 pre-osteoblast differentiation when *RCOR2* expression was silenced, which was linked to decreased target gene suppression. However, these results were not entirely replicated in primary osteoblast differentiation culture experiments. Furthermore, the *in vitro* effects of decreased RCOR2 expression demonstrated limited replicability *in vivo* in both RCOR2 global and conditional knockout mice.

LSD1 in osteoblast differentiation

The effect of LSD1 on bone metabolism has been previously studied with different approaches, by studying the mechanisms in osteoclasts, osteoblasts and by using miRNAs. Our study design of targeting the LSD1 knockout to limb bud mesenchymal cells was preceded by two papers published by Sun et al in 2018 and 2020, although the studies were conducted simultaneously with ours. Surprisingly, our results on the effect of LSD1 knockout on bone metabolism were contradictory to their reports. Sun et al. demonstrated that *LSD1* silencing was reported to induce osteoblast differentiation *in vitro* and limb bud mesenchyme targeted LSD1

knockdown to cause increased bone formation *in vivo* through altered methylation of *WNT7B* and *BMP2B* promoter areas. Global H3K4me1/2 levels were higher in cells where LSD1 was knocked out. However, similar findings to ours, such as smaller body size, shorter bone length and changes in the calvarial suture closure were made (Sun et al., 2018). Their second paper described the effects of LSD1 knockdown on endochondral ossification, demonstrating impaired growth plate organization and osteogenesis imperfecta -like bone curvature (Sun et al., 2020) similar to the phenotype observed in our model. The findings of both of these papers were repeated in our findings of LSD1 binding near the promoter areas of target genes. We showed lack of H3K4me1 at LSD1 peaks and accordingly, Sun et al demonstrated enrichment of H3K4me1 after LSD1 downregulation. Another study has furthermore reported that overexpression of miR-655-3p induces osteoblast differentiation through BMP2 activation by silencing *LSD1* expression, as well as demonstrated that LSD1 expression was significantly elevated in OVX mice (X.-J. Wang et al., 2020), similarly to the data published by Sun et al.

LSD1 expression in osteoclasts has also been studied using different experimental models. Our data suggests that mesenchymal cell targeted LSD1 conditional knockout leads to a statistically non-significant decrease in osteoclast marker expression. Another study using small molecule inhibitors reported that LSD1 inhibition decreased osteoclast fusion and activity *in vitro*, as well as counteracted certain OVX-induced cortical bone effects *in vivo* when using significantly (up to 20x) higher doses than the ones used in our studies (Ding et al., 2023). In a study by Doi et al., LSD1 expression was significantly induced after RANKL stimulation in the synovium of rheumatoid arthritis patients. Silencing of LSD1 expression or treatment of osteoclast precursors with another LSD1 inhibitor has been reported to decrease osteoclast maturation (Doi et al., 2022). Astleford-Hopper et al. studied the effect of LSD1 on osteoclast differentiation *in vivo* in a myeloid lineage targeted conditional knockout mouse model. In that study, the conditional knockout female mice interestingly had a bone phenotype of increased trabecular bone and slightly larger diameter of cortical bone. There were no differences in the number of osteoclasts *in vivo*, but the osteoclasts were smaller and differentiated more poorly *in vitro* (Astleford-Hopper et al., 2022). LSD1 downregulation has also been shown to impair chondrocyte differentiation and marker gene expression, as well as impair endochondral ossification (Sun et al., 2020).

Post-translational methylation of H3K4 has been shown to have dose-specific effects on target gene expression. In general, unmethylated H3K4 presents silent chromatin, together with methylated DNA. Monomethylation of H3K4 commonly represents active enhancer areas even though these modifications are enriched further away from the TSS and are commonly found together with H3K27

acetylation of TSS. Dimethylated and trimethylated H3K4 are marks for active promoters and commonly found closer to the TSS than H3K4me. H3K4me3 has also been found enriched in the enhancer areas, though in smaller densities than H3K4me1. H3K9 methylation can represent either silenced areas (H3K9me3) or actively transcribed genes (H3K9me1) (Kimura, 2013; Sterling et al., 2021). Of these, H3K4me1/2 and H3K9me1/2 are LSD1 demethylation targets. Our data demonstrates that LSD1 binds target gene TSSs in an increasing manner during osteoblast differentiation, mainly within 1 kb of TSS. H3K4me1 binding was indeed enriched further from the TSS than H3K4me2/3 to other intron areas. LSD1 binding takes place closer to TSS results in overlapping binding more with H3K4me2/3 and less to H3K4me1 even though H3K4me3 is not a demethylation target. This would suggest that the interaction might take place with H3K4me3 as well but demethylation can mechanistically not take place, or that LSD1 binding is not actually targeted to H3K4me3 but data would present this as binding due to the overlap of H3K4me2 and H3K4me3 peaks.

LSD1 itself does not possess DNA-binding sites, which opens the targeting possibilities to context-specific complex member composition. Different complex members with DNA-binding capability, such as REST and transcription factors GFI1 and Snail have been identified to interact with LSD1 (Saleque et al., 2007), even though transcription factor interactions have not been extensively studied in osteoblasts. Our ChIP-sequencing data showed enrichment with different transcription factor binding motifs, most significantly with RUNX2 binding sites. This does not exclude the interaction with other transcription factors than RUNX1/2. Combining the transcriptional silencing effect of H3K4 demethylation and targeting to RUNX2 binding sites, our findings would collectively suggest a mechanism for inhibition of early osteoblast differentiation. Controversially, LSD1 inhibition or downregulation did not lead to increased osteoblast differentiation but instead impaired the differentiation and organization of osteoblasts and growth plate chondrocytes. In addition, of the differently expressed genes between the samples at day 0 and day 14, 37% were found as LSD1 binding sites at 14 days, which suggests a correlation between binding of LSD1 and change in gene expression level. LSD1 binding at the DE genes did not show significant preference for the direction of gene expression change, where only 53% of genes were downregulated and 47% were upregulated. This would suggest more dynamic effects for the LSD1 complex than the current paradigm of a repressor complex (Maiques-Diaz & Somervaille, 2016; Perillo et al., 2008).

RCOR2 in osteoblast differentiation

The role of RCOR2 is known best in the fields of neuronal development, stem cell maintenance and tumour immunity, and before our study no research had been published regarding the function of RCOR2 in osteoblasts. The ability to bind LSD1 and demethylate histones as a complex had been shown before (P. Yang et al., 2011) and our RNA-sequencing data tied RCOR2 expression to osteoblast differentiation. The expression of RCOR2 in chondrocytes has been previously studied and was found to be increasingly expressed in ATDC5 cells during chondrocyte differentiation and suggested to have a fate-deciding role due to its previously known function in gene silencing and neural differentiation (L. Chen et al., 2005). In osteoarthritic patient tissue samples, RCOR2 expression was significantly decreased in osteoarthritic cartilage compared to phenotypically healthy cartilage. On the other hand, RCOR2 overexpression has been shown to downregulate the expression of two cartilage-catabolizing enzymes, MMP13 and ADAMTS5 through silencing HES1 expression, suggesting a cartilage protective effect for RCOR2 (Primrose et al., 2023). In our study, no distinctive phenotypical changes were found in RCOR2 conditional or global knockout mice, but LSD1 conditional knockout mice showed significant cartilage phenotype after the loss of LSD1, which could be partly caused by a simultaneous loss of a complex member, RCOR2.

RCOR2 has been shown to control adipogenesis together with LSD1 (Hanzu et al., 2013). When expressed at the induction of differentiation, RCOR2 and LSD1 were shown to downregulate inflammatory gene expression and upregulate C/EBPβ and GLUT4 expression. Additionally, RCOR2 and LSD1 were both downregulated in the white adipose tissue of two different obesity mouse models: high-fat diet induced obesity and leptin-deficient ob/ob mice. Both models also demonstrated significantly increased expression of inflammation marker. Exposure of preadipocyte 3T3-L1 cells to TNFα led to significantly decreased LSD1 expression after 7 days (Hanzu et al., 2013). Our studies on RCOR2 conditional knockout mice showed similar results, since the amount of white adipose tissue depot as well as the adiposity within the fracture callus were significantly smaller in RCOR2 deficient mice. Correspondingly, primary cells extracted from calvarias of Rcor2KO$^{+/-}$ mice showed decreased differentiation to adipocytes compared to cells isolated from wildtype controls.

The effect of RCOR2 on stem/progenitor cell differentiation has been previously studied in various cell types, suggesting a role in controlling the switch between proliferation and differentiation (L. Chen et al., 2005; Hanzu et al., 2013; Monaghan et al., 2017; Saleque et al., 2007). Our results show significantly decreased differentiation of RCOR2 deficient osteoblasts at 14 and 21 days, which was demonstrated by ALP staining, as well as loss of *in vitro* mineralization at 21 days. Interestingly, when comparing the number of differentially expressed (DE) genes at

24 hours and 7 days compared to confluency (at day 0), there was a greater difference in unique DE genes between groups at 24 hours (401 and 167 genes in shScramble and shRCOR2 samples, respectively) than there were at 7 days (760 vs 707 genes in shScramble and shRCOR2 samples, respectively) (II, Figure 3 B-C). However, the total number of DE genes was the highest at seven days. This could suggest a slower transition from proliferation to differentiation as a response to osteogenic stimulation in shRCOR2 cells.

The CoREST/RCOR family consists of three structurally similar members, RCOR1-3. When comparing domain composition, RCOR2 and RCOR3 are closest to each other, although four different isoforms of RCOR3 with significant structural differences have been found (Maksour et al., 2020). All three family members bind LSD1. However, when comparing the complexes which different RCORs form, RCOR1 and RCOR3 share more similarities, with the key difference being RCOR2s reduced capacity to bind HDAC1/2. Different members of the RCOR family are also not observed to be bound in heterodimers (Barrios et al., 2014). Our RCOR2 knockout mouse models did not fully correspond to the extent of effects demonstrated with the shRCOR2 cell lines *in vitro*, thus raising the question whether RCOR2 could be compensated by other RCOR family members *in vivo*. We found a modest yet significant increase in *RCOR3* mRNA expression during osteoblast differentiation in MC3T3-E1 and calvarial osteoblast cells (II, Figure 1 C-D). As the complexes formed by RCOR1/3 differ from that of RCOR2, such compensation might have been detectable through different outcome of complex recruitment to target gene promoter areas. In addition, our RNA-sequencing data on shRCOR2 MC3T3-E1 cell line did not bring out significant changes in the gene expression of other RCOR family members as a compensation mechanism (II, Table S1).

These results provide novel information on the suggested interaction of LSD1 and RUNX2 to target histone demethylation to genes affecting osteoblast differentiation. Additional information on the effects of LSD1 on osteoblast differentiation and growth plate organization is provided. Lastly, the transcriptional effects that loss of RCOR2 causes in osteoblasts are described.

Limitations of the study

There are some limitations to this study. This study avoided the embryolethality of homozygous global knockouts by creating conditional knockout mice strains targeting the knockout to the limb bud mesenchyme using the Prrx1-Cre promoter. However, significant loss of calvarial suture closure was detected in the conditional LSD1 knockout mice, suggesting that Prrx1-Cre promoter does not exclusively target the deletion to limb bud mesenchyme. Another presumed non-bone target effect seen in Prrx1-Cre mice was the decreased inguinal adipose tissue depot size.

Similar changes of calvarial sutures have also been reported in the previous LSD1 conditional knockout models using Prrx1-Cre (Sun et al., 2018), and Prrx1 mutations have been linked to craniofacial defects in humans (Tooze et al., 2023). Labelling to detect murine Prrx1-Cre expression *in vivo* has demonstrated that subcutaneous white adipose tissue was observed to express Prrx1-Cre, thus subjecting also adipose depots to deletion of target genes (Sanchez-Gurmaches et al., 2015). This leaves open the possible effects of other non-targeted tissue LSD1 knockdown in bone through an unforeseen mechanism.

Similarly, the expression pattern of *RCOR2* in different tissues in our study did not correspond to previously published data. In our study, *RCOR2* expression was nearly unmeasurable in femur samples and comparable to other tissues such as the brain (II, Fig 1 G). The low expression of *RCOR2* in the femur samples could however be explained by the method for RNA extraction without removing the bone marrow, thus possibly masking the relatively low *RCOR2* mRNA expression in bone due to the abundance of mRNAs in bone marrow.

Future perspectives

This study demonstrates the limiting effect of LSD1 knockdown on the differentiation of all mesenchymal cells in bone, aligned with other reports on osteoclasts and chondrocytes (Doi et al., 2022; Rodova et al., 2011). An interesting aspect of LSD1 mechanism of action is although the role of LSD1 on regulation of embryonic stem cells has been studied (Adamo et al., 2011), the effect on other less totipotent stem cells remains to be characterized. LSD1 has been studied as a prognostic factor and therapeutic target in different cancers, also in clinical phases (Noce et al., 2023). If the modulation of LSD1 expression or activity affects the escape of cancer cells from immune cell response and recognition, anti-LSD1 combination therapy could open doors to epigenetic regulation in cancer cells. Another possibly utilisable finding is the downregulation of LSD1 in white adipose tissue of obese mice and in adipocytes treated with TNFα (Hanzu et al., 2013), which could be counteracted with upregulation of LSD1 expression or induced activity leading to normalized adipocyte function.

Our results partially contradict the previous studies of LSD1s effects on osteoblast differentiation. The overall outcome of LSD1 loss in our models was impaired osteoblast differentiation *in vitro* and *in vivo*, resulting in bone loss instead of increased bone formation, which has been reported by others (Sun et al., 2018; D. Yu et al., 2023). Some differences can be found between the experimental models, such as deletion of different exons in the knockout models or the use of less specific LSD1 inhibitors in higher doses, but the main difference for the conflicting results remains debatable. To further explain the mechanism behind the phenotype, the gene

expression differences between LSD1 knockdown and control cells should be investigated more thoroughly using different methods, such as assay for transposase-accessible chromatin with sequencing (ATAC-Seq) and RNA-sequencing. Our study suggested an osteoblast-specific targeting mechanism through binding site similarity with RUNX2 binding sites. The complex members of LSD1 in mesenchymal cells are still, however, poorly described and require further research by investigating different complex compositions with techniques such as co-immunoprecipitation or proximity ligation assay followed by mass spectrometry identification. The conditional knockout mouse models could also be extended to deletion of LSD1 under a different promoter to target the deletion to a later stage of differentiation, to induce deletion at a later stage in life with an inducible model or to an entirely another cell type.

Another interesting finding made was the decreased *RUNX2* expression in mRNA extracted from femurs of LSD1 conditional knockout mice. It was however not further investigated whether the decreased expression was linked to loss of osteoblast differentiation or whether there would be a direct regulation mechanism between *LSD1* and *RUNX2* gene expression leading to decreased osteoblast differentiation. The binding and effect of LSD1 in promoter areas of different genes of interest warrant for more research in future.

The *in vitro* results of RCOR2 downregulation were not completely transferrable to our *in vivo* models of RCOR2 global and conditional deletion. The global homozygous deletion of RCOR2 led to early embryolethality and our conditional homozygous deletion, although deleting RCOR2 efficiently in the target tissues, did not produce a pronounced skeletal phenotype. Although the expression of *RCOR1* or *RCOR3* were not significantly increased in the shRCOR2 RNA-sequencing samples at any time point, the possibility of compensation with another family member *in vivo* cannot be blatantly rejected, especially considering the increased expression of *RCOR3* in cell culture mRNA samples. Development of RCOR3 global and conditional knockout mouse lines could further demonstrate the effect of family members with previously reported higher binding efficiency to HDAC1/2. The RCOR3 conditional knockout mouse lines could also be crossbred with the RCOR2 conditional mouse line to further investigate the compound effect of a double RCOR2/RCOR3 knockout mouse. As RCOR3 is, similarly to RCOR2, expressed in neuronal, endocrine and respiratory tissues, the embryolethality of RCOR3 homozygous global knockout is likely. To overcome the embryolethality of RCOR2 and RCOR3, an inducible knockout model could be created e.g. using a tetracycline-inducible system.

Similar findings where the loss of RCOR2 leads to downregulation of differentiation in different cell types have been made in our study and by others (Monaghan et al., 2017; Pei et al., 2022; Y. Wang et al., 2016). Similarly to the role

of LSD1, also the role of RCOR2 on mesenchymal cell differentiation should be investigated through methods such as ATAC-sequencing and ChIP-sequencing. As RCOR2 is commonly found as a part of a repressor complex, one should study whether the effects of RCOR2 seen in mesenchymal cells are specific to mesenchymal lineage or applicable also to other cell types. The composition and dynamics of RCOR2 complex are still mostly unknown and relying on data obtained in different contexts. The members of the complex could be investigated using e.g. proximity-ligation assays or co-immunoprecipitation followed by mass spectrometry to identify the possible partners.

Regulation of bone metabolism through epigenetic mechanisms is an expanding field as more data of various regulators is published. The effects of different miRNAs and post-translational histone modifiers are revealed and brought to use also in the development of novel therapies for bone diseases (de Nigris et al., 2021). Loss of bone caused by aging, lack of mobility as well as due to pharmacological therapy of other conditions needs counterbalancing through treatments, which are developed to preserve bone mass by gaining new knowledge of the regulation of bone metabolism. These treatments should not solely rely on osteoblast/osteoclast differentiation signalling targets but also on the targeted epigenetic regulation of the key transcription factors. Results presented in this study thus provide data, which is necessary to further develop treatments to target the epigenetic regulation in osteoblasts and to enhance bone formation.

7 Conclusions

Based on the results and discussion presented in this thesis, the following conclusions can be made:

1. Both LSD1 and RCOR2 are expressed in mesenchymal stromal cells during osteoblast differentiation, and loss of either of them leads to severely impaired osteoblast differentiation and mineralization *in vitro*.
2. LSD1 binding to chromatin is enriched at known RUNX2 binding sites.
3. Inhibition of LSD1 demethylation activity leads to loss of bone volume and decreased osteoblast activity *in vivo*.
4. Mesenchymal cell targeted knockdown of LSD1 leads to osteogenesis imperfecta -like phenotype in mice with shorter, curved bones, loss of bone volume and disrupted ossification of primary spongiosa and growth plate organization.
5. Global knockdown or mesenchymal cell targeted knockdown of RCOR2 did not lead to similar osteoblast phenotype as observed *in vitro*, but resulted in decreased adipocyte differentiation *in vitro* and *in vivo*.

Acknowledgements

This thesis was carried out at the Department of Medical Biochemistry and Genetics, Institute of Biomedicine, University of Turku, Finland, during the years 2016–2025. I want to thank the present and former heads of the department, Professor Klaus Elenius and Professor Kati Elima for providing the research facilities to conduct these studies. I also want to acknowledge the Turku Doctoral Programme of Molecular Medicine (TuDMM) for valuable support and networking events to establish a platform for fellow doctoral researchers to discuss and share experiences about their studies and projects.

I want to express my deepest gratitude to my supervisors Riku Kiviranta, Terhi Heino and Kaisa Ivaska. You have provided me the opportunity and means to pursue my PhD studies, offered me your knowledge, advice and independence to learn and grow as a scientist. And when the time was right, you have steered me into the right direction to find the goal. I am thankful for all the time you have taken to mentor me and for the patience when it has been needed.

I want to sincerely thank Professor Marie Lagerquist and Adjunct Professor Kirsi Ketola for reviewing this thesis. Your comments were constructive, insightful and improved this thesis. I also want to thank my follow up committee members Kati Tarkkonen, Maria Sundvall and Riikka Lund for evaluating my progress and providing me with guidance and ideas on progressing my research and the structure of this thesis.

I also want to thank the collaborators in my original publications, Amel Dudakovich, Andre van Wijnen, Cristina Valensisi and David Hawkins, as well as the esteemed histomorphometric trainers and collaborators Dorothy Hu, Kenichi Nagano and Roland Baron.

The Skeletor Lab, our research group, was the academic home of mine. The other family of mine, with who we laughed and cried, discussed and debated. The group shared resemblance with other legendary houses of education where help is always given for those who ask for it, and it was never frowned upon to ask. Drs Vappu Nieminen-Pihala, Tero Puolakkainen, Fan Wang and Martina Pauk, you have all shown me example, been there to listen and give advice, shared your expertise in different experiments and when the experiments have required it, shown great taste

in music. Dr Kati Tarkkonen, you were the driving force of this thesis. You listened, had the answers I needed and carried the projects when times were rough. Rana Al Majidi, you set the foundations on everything presented here with all your hard work. Merja Lakkisto, you kept everything running when I did my best to mix things up in the lab, answered my endless questions and were always there when we needed you. Your work was irreplaceable for me and for all of us. I also want to thank all of the other members of the Skeletor lab I had the joy of working with: Julius Laine, Jemina Lehto, Paula Tiitta and Lauri Saastamoinen. I also want to thank Erica Nyman, Mika Savisalo and the whole staff of Central Animal Laboratory for your assistance in my research.

The members of BoneLab Turku. Docent Jorma Määttä, I want to thank you for the advice and instructions. Drs Liina Uusitalo-Kylmälä, Milja Arponen and Nataliia Petruk, Karoliina Kajander, Nicko Widjaja, Niki Jalava and Anja Hjelt, I want to thank you for all the journal clubs, Christmas parties, discussions and support.

Research is not always just cell culture or scanning bones. Sometimes it is also long lunch breaks or discussions over a cold drink. I would like to thank Anni Suominen, Veera Ojala, Olli Metsälä and Joni Merisaari for all of these fruitful discussions. I also want to thank the colleagues at my new employer, especially Leena Kytömäki, Katja Näreoja and Anna Ahonen for your support when times have been rough. I also want to thank Pia Tuominen, Anna-Marja Säämänen, Minna Santanen, Sauli Haataja, Annele Sainio, Hannu Järveläinen, Raili Salonen and Vuokko Loimaranta and everyone at Pharmatest for all the discussions and support. My gratitude goes also to my friends, who have listened to the pains and joys of this project patiently.

This thesis was financially supported by the Academy of Finland, Sigrid Juselius Foundation, Emil Aaltonen Foundation, Finnish Cultural Foundation and TuDMM.

Lastly and foremost, I want to show my deepest gratitude to my family. My parents, siblings Toni and Riikka, and their families Tiina, Helka and Oiva who have shown unwaivering support and interest in my projects and given me balance. My other family Tapani, Anne, Petri, Anni, Aki, Albert, Astrid, Nala and Nukka I want to thank for hearing my worries, supporting me and asking the important questions. And finally Noora, for all the support, endurance, guidance and perspective. For keeping my feet on the ground, chin up and spirit high.

Turku, May 2025
Petri Rummukainen

References

Adamo, A., Sesé, B., Boue, S., Castaño, J., Paramonov, I., Barrero, M. J., & Belmonte, J. C. I. (2011). LSD1 regulates the balance between self-renewal and differentiation in human embryonic stem cells. *Nature Cell Biology*, *13*(6), 652–659. https://doi.org/10.1038/ncb2246

Aguilar, R., Bustos, F. J., Nardocci, G., van Zundert, B., & Montecino, M. (2021). Epigenetic silencing of the osteoblast-lineage gene program during hippocampal maturation. *Journal of Cellular Biochemistry*, *122*(3–4), 367–384. https://doi.org/https://doi.org/10.1002/jcb.29865

Andrés, M. E., Burger, C., Peral-Rubio, M. J., Battaglioli, E., Anderson, M. E., Grimes, J., Dallman, J., Ballas, N., & Mandel, G. (1999). CoREST: A functional corepressor required for regulation of neural-specific gene expression. *Proceedings of the National Academy of Sciences*, *96*(17), 9873–9878. https://doi.org/10.1073/pnas.96.17.9873

Angelov, D., Vitolo, J. M., Mutskov, V., Dimitrov, S., & Hayes, J. J. (2001). Preferential interaction of the core histone tail domains with linker DNA. *Proceedings of the National Academy of Sciences*, *98*(12), 6599–6604. https://doi.org/10.1073/pnas.121171498

Astleford-Hopper, K., Bradley, E., & Mansky, K. C. (2022). Female LSD1 Conditional Knockout Mice Have an Increased Bone Mass. *BioRxiv*, 2022.06.25.497607. https://doi.org/10.1101/2022.06.25.497607

Barrios, Á. P., Gómez, A. V, Sáez, J. E., Ciossani, G., Toffolo, E., Battaglioli, E., Mattevi, A., & Andrés, M. E. (2014). Differential Properties of Transcriptional Complexes Formed by the CoREST Family. *Molecular and Cellular Biology*, *34*(14), 2760–2770. https://doi.org/10.1128/MCB.00083-14

Bauer, O., Sharir, A., Kimura, A., Hantisteanu, S., Takeda, S., & Groner, Y. (2015). Loss of Osteoblast Runx3 Produces Severe Congenital Osteopenia. *Molecular and Cellular Biology*, *35*(7), 1097–1109. https://doi.org/10.1128/MCB.01106-14

Bhardwaj, A., Sapra, L., Tiwari, A., Mishra, P., Sharma, S., & Srivastava, R. (2022). "Osteomicrobiology": The Nexus Between Bone and Bugs. *Frontiers in Microbiology*, *12*. https://doi.org/10.3389/fmicb.2021.812466

Bird, A. (2007). Perceptions of epigenetics. *Nature*, *447*(7143), 396–398. https://doi.org/10.1038/nature05913

Bord, S., Ireland, D. C., Beavan, S. R., & Compston, J. E. (2003). The effects of estrogen on osteoprotegerin, RANKL, and estrogen receptor expression in human osteoblasts. *Bone*, *32*(2), 136–141. https://doi.org/https://doi.org/10.1016/S8756-3282(02)00953-5

Bridi, M., & Abel, T. (2013). Chapter 2 - Histone Modifications in the Nervous System and Neuropsychiatric Disorders. In J. D. Sweatt, M. J. Meaney, E. J. Nestler, & S. Akbarian (Eds.), *Epigenetic Regulation in the Nervous System* (pp. 35–67). Academic Press. https://doi.org/https://doi.org/10.1016/B978-0-12-391494-1.00002-1

Buck, S. W., Gallo, C. M., & Smith, J. S. (2004). Diversity in the Sir2 family of protein deacetylases. *Journal of Leukocyte Biology*, *75*(6), 939–950. https://doi.org/10.1189/jlb.0903424

Cai, C., He, H. H., Gao, S., Chen, S., Yu, Z., Gao, Y., Chen, S., Chen, M. W., Zhang, J., Ahmed, M., Wang, Y., Metzger, E., Schüle, R., Liu, X. S., Brown, M., & Balk, S. P. (2014). Lysine-Specific Demethylase 1 Has Dual Functions as a Major Regulator of Androgen Receptor Transcriptional Activity. *Cell Reports*, *9*(5), 1618–1627. https://doi.org/10.1016/j.celrep.2014.11.008

Canalis, E., Economides, A. N., & Gazzerro, E. (2003). Bone Morphogenetic Proteins, Their Antagonists, and the Skeleton. *Endocrine Reviews*, *24*(2), 218–235. https://doi.org/10.1210/er.2002-0023

Carnesecchi, J., Forcet, C., Zhang, L., Tribollet, V., Barenton, B., Boudra, R., Cerutti, C., Billas, I. M. L., Sérandour, A. A., Carroll, J. S., Beaudoin, C., & Vanacker, J.-M. (2017). ERRα induces H3K9 demethylation by LSD1 to promote cell invasion. *Proceedings of the National Academy of Sciences*, *114*(15), 3909–3914. https://doi.org/10.1073/pnas.1614664114

Carninci, P., Sandelin, A., Lenhard, B., Katayama, S., Shimokawa, K., Ponjavic, J., Semple, C. A. M., Taylor, M. S., Engström, P. G., Frith, M. C., Forrest, A. R. R., Alkema, W. B., Tan, S. L., Plessy, C., Kodzius, R., Ravasi, T., Kasukawa, T., Fukuda, S., Kanamori-Katayama, M., … Hayashizaki, Y. (2006). Genome-wide analysis of mammalian promoter architecture and evolution. *Nature Genetics*, *38*(6), 626–635. https://doi.org/10.1038/ng1789

Celil, A. B., Hollinger, J. O., & Campbell, P. G. (2005). Osx transcriptional regulation is mediated by additional pathways to BMP2/Smad signalling. *Journal of Cellular Biochemistry*, *95*(3), 518–528. https://doi.org/https://doi.org/10.1002/jcb.20429

Chan, W. C. W., Tan, Z., To, M. K. T., & Chan, D. (2021). Regulation and Role of Transcription Factors in Osteogenesis. *International Journal of Molecular Sciences*, *22*(11). https://doi.org/10.3390/ijms22115445

Chen, D., Zhao, M., & Mundy, G. R. (2004). Bone Morphogenetic Proteins. *Growth Factors*, *22*(4), 233–241. https://doi.org/10.1080/08977190412331279890

Chen, L., Fink, T., Zhang, X.-Y., Ebbesen, P., & Zachar, V. (2005). Quantitative transcriptional profiling of ATDC5 mouse progenitor cells during chondrogenesis. *Differentiation*, *73*(7), 350–363. https://doi.org/https://doi.org/10.1111/j.1432-0436.2005.00038.x

Cho, H.-S., Suzuki, T., Dohmae, N., Hayami, S., Unoki, M., Yoshimatsu, M., Toyokawa, G., Takawa, M., Chen, T., Kurash, J. K., Field, H. I., Ponder, B. A. J., Nakamura, Y., & Hamamoto, R. (2011). Demethylation of RB Regulator MYPT1 by Histone Demethylase LSD1 Promotes Cell Cycle Progression in Cancer Cells. *Cancer Research*, *71*(3), 655–660. https://doi.org/10.1158/0008-5472.CAN-10-2446

Clark, E. A., Wu, F., Chen, Y., Kang, P., Kaiser, U. B., Fang, R., & Shi, Y. G. (2019). GR and LSD1/KDM1A-Targeted Gene Activation Requires Selective H3K4me2 Demethylation at Enhancers. *Cell Reports*, *27*(12), 3522-3532.e3. https://doi.org/10.1016/j.celrep.2019.05.062

Clarke, S. G. (2013). Protein methylation at the surface and buried deep: thinking outside the histone box. *Trends in Biochemical Sciences*, *38*(5), 243–252. https://doi.org/https://doi.org/10.1016/j.tibs.2013.02.004

Cohen-Armon, M., Visochek, L., Rozensal, D., Kalal, A., Geistrikh, I., Klein, R., Bendetz-Nezer, S., Yao, Z., & Seger, R. (2007). DNA-Independent PARP-1 Activation by Phosphorylated ERK2 Increases Elk1 Activity: A Link to Histone Acetylation. *Molecular Cell*, *25*(2), 297–308. https://doi.org/10.1016/j.molcel.2006.12.012

Dahlman-Wright, K., Cavailles, V., Fuqua, S. A., Jordan, V. C., Katzenellenbogen, J. A., Korach, K. S., Maggi, A., Muramatsu, M., Parker, M. G., & Gustafsson, J.-Å. (2006). International Union of Pharmacology. LXIV. Estrogen Receptors. *Pharmacological Reviews*, *58*(4), 773. https://doi.org/10.1124/pr.58.4.8

Daluiski, A., Engstrand, T., Bahamonde, M. E., Gamer, L. W., Agius, E., Stevenson, S. L., Cox, K., Rosen, V., & Lyons, K. M. (2001). Bone morphogenetic protein-3 is a negative regulator of bone density. *Nature Genetics*, *27*(1), 84–88. https://doi.org/10.1038/83810

Datta, N. S., & Abou-Samra, A. B. (2009). PTH and PTHrP signalling in osteoblasts. *Cellular Signalling*, *21*(8), 1245–1254. https://doi.org/https://doi.org/10.1016/j.cellsig.2009.02.012

Delaisse, J.-M. (2014). The reversal phase of the bone-remodeling cycle: cellular prerequisites for coupling resorption and formation. *BoneKEy Reports*, *3*. https://doi.org/10.1038/bonekey.2014.56

de Nigris, F., Ruosi, C., Colella, G., & Napoli, C. (2021). Epigenetic therapies of osteoporosis. *Bone*, *142*, 115680. https://doi.org/https://doi.org/10.1016/j.bone.2020.115680

Derynck, R., Zhang, Y., & Feng, X.-H. (1998). Transcriptional Activators of TGF-β Responses: Smads. *Cell*, *95*(6), 737–740. https://doi.org/https://doi.org/10.1016/S0092-8674(00)81696-7

Ding, M., Chen, Z., Cho, E., Park, S.-W., & Lee, T.-H. (2023). Crucial Role of Lysine-Specific Histone Demethylase 1 in RANKL-Mediated Osteoclast Differentiation. *International Journal of Molecular Sciences*, *24*(4), 3605. https://doi.org/10.3390/ijms24043605

Doi, K., Murata, K., Ito, S., Suzuki, A., Terao, C., Ishie, S., Umemoto, A., Murotani, Y., Nishitani, K., Yoshitomi, H., Fujii, T., Watanabe, R., Hashimoto, M., Murakami, K., Tanaka, M., Ito, H., Park-Min, K.-H., Ivashkiv, L. B., Morinobu, A., & Matsuda, S. (2022). Role of Lysine-Specific Demethylase 1 in Metabolically Integrating Osteoclast Differentiation and Inflammatory Bone Resorption Through Hypoxia-Inducible Factor 1α and E2F1. *Arthritis & Rheumatology*, *74*(6), 948–960. https://doi.org/https://doi.org/10.1002/art.42074

Dominici, M., Le Blanc, K., Mueller, I., Slaper-Cortenbach, I., Marini, F. C., Krause, D. S., Deans, R. J., Keating, A., Prockop, D. J., & Horwitz, E. M. (2006). Minimal criteria for defining multipotent mesenchymal stromal cells. The International Society for Cellular Therapy position statement. *Cytotherapy*, *8*(4), 315–317. https://doi.org/https://doi.org/10.1080/14653240600855905

Dou, C., Li, N., Ding, N., Liu, C., Yang, X., Kang, F., Cao, Z., Quan, H., Hou, T., Xu, J., & Dong, S. (2016). HDAC2 regulates FoxO1 during RANKL-induced osteoclastogenesis. *American Journal of Physiology-Cell Physiology*, *310*(10), C780–C787. https://doi.org/10.1152/ajpcell.00351.2015

Dreher, R. D., & Theisen, E. R. (2023). Lysine specific demethylase 1 is a molecular driver and therapeutic target in sarcoma. *Frontiers in Oncology*, *12*. https://doi.org/10.3389/fonc.2022.1076581

Du, J., Zhou, Y., Su, X., Yu, J. J., Khan, S., Jiang, H., Kim, J., Woo, J., Kim, J. H., Choi, B. H., He, B., Chen, W., Zhang, S., Cerione, R. A., Auwerx, J., Hao, Q., & Lin, H. (2011). Sirt5 Is a NAD-Dependent Protein Lysine Demalonylase and Desuccinylase. *Science*, *334*(6057), 806–809. https://doi.org/10.1126/science.1207861

Edwards, J. R., & Mundy, G. R. (2011). Advances in osteoclast biology: old findings and new insights from mouse models. *Nature Reviews Rheumatology*, *7*(4), 235–243. https://doi.org/10.1038/nrrheum.2011.23

Elhamamsy, A. R. (2017). Role of DNA methylation in imprinting disorders: an updated review. *Journal of Assisted Reproduction and Genetics*, *34*(5), 549–562. https://doi.org/10.1007/s10815-017-0895-5

Fagerberg, L., Hallström, B. M., Oksvold, P., Kampf, C., Djureinovic, D., Odeberg, J., Habuka, M., Tahmasebpoor, S., Danielsson, A., Edlund, K., Asplund, A., Sjöstedt, E., Lundberg, E., Szigyarto, C. A.-K., Skogs, M., Takanen, J. O., Berling, H., Tegel, H., Mulder, J., … Uhlén, M. (2014). Analysis of the Human Tissue-specific Expression by Genome-wide Integration of Transcriptomics and Antibody-based Proteomics*. *Molecular & Cellular Proteomics*, *13*(2), 397–406. https://doi.org/https://doi.org/10.1074/mcp.M113.035600

Fan, C., Ma, X., Wang, Y., Lv, L., Zhu, Y., Liu, H., & Liu, Y. (2021). A NOTCH1/LSD1/BMP2 co-regulatory network mediated by miR-137 negatively regulates osteogenesis of human adipose-derived stem cells. *Stem Cell Research & Therapy*, *12*(1), 417. https://doi.org/10.1186/s13287-021-02495-3

Friedlaender, G. E., Perry, C. R., Cole, J. D., Cook, S. D., Cierny, G., Muschler, G. F., Zych, G. A., Calhoun, J. H., LaForte, A. J., & Yin, S. (2001). Osteogenic protein-1 (bone morphogenetic protein-7) in the treatment of tibial nonunions. *The Journal of Bone and Joint Surgery. American Volume*, *83-A Suppl 1*(Pt 2), S151-8.

Frost, H. M. (1994). Wolff's Law and bone's structural adaptations to mechanical usage: an overview for clinicians. *The Angle Orthodontist*, *64*(3), 175–188. https://doi.org/10.1043/0003-3219(1994)064<0175:WLABSA>2.0.CO;2

Fuggle, N. R., Laskou, F., Harvey, N. C., & Dennison, E. M. (2022). A review of epigenetics and its association with ageing of muscle and bone. *Maturitas*, *165*, 12–17. https://doi.org/10.1016/j.maturitas.2022.06.014

Fyodorov, D. V, Zhou, B.-R., Skoultchi, A. I., & Bai, Y. (2018). Emerging roles of linker histones in regulating chromatin structure and function. *Nature Reviews Molecular Cell Biology*, *19*(3), 192–206. https://doi.org/10.1038/nrm.2017.94

Gao, L., Cueto, M. A., Asselbergs, F., & Atadja, P. (2002). Cloning and Functional Characterization of HDAC11, a Novel Member of the Human Histone Deacetylase Family*. *Journal of Biological Chemistry*, *277*(28), 25748–25755. https://doi.org/https://doi.org/10.1074/jbc.M111871200

Gardiner-Garden, M., & Frommer, M. (1987). CpG Islands in vertebrate genomes. *Journal of Molecular Biology*, *196*(2), 261–282. https://doi.org/https://doi.org/10.1016/0022-2836(87)90689-9

Ge, W., Liu, Y., Chen, T., Zhang, X., Lv, L., Jin, C., Jiang, Y., Shi, L., & Zhou, Y. (2014). The epigenetic promotion of osteogenic differentiation of human adipose-derived stem cells by the genetic and chemical blockade of histone demethylase LSD1. *Biomaterials*, *35*(23), 6015–6025. https://doi.org/http://dx.doi.org/10.1016/j.biomaterials.2014.04.055

GOVENDER, S., CSIMMA, C., GENANT, H. K., & VALENTIN-OPRAN, A. (2002). RECOMBINANT HUMAN BONE MORPHOGENETIC PROTEIN-2 FOR TREATMENT OF OPEN TIBIAL FRACTURES. *The Journal of Bone and Joint Surgery-American Volume*, *84*(12), 2123–2134. https://doi.org/10.2106/00004623-200212000-00001

Guennewig, B., & Cooper, A. A. (2014). Chapter Seven - The Central Role of Noncoding RNA in the Brain. In R. Hitzemann & S. Mcweeney (Eds.), *International Review of Neurobiology* (Vol. 116, pp. 153–194). Academic Press. https://doi.org/https://doi.org/10.1016/B978-0-12-801105-8.00007-2

Guntur, A. R., & Rosen, C. J. (2012). Bone As An Endocrine Organ. *Endocrine Practice*, *18*(5), 758–762. https://doi.org/https://doi.org/10.4158/EP12141.RA

Hakimi, M.-A., Bochar, D. A., Chenoweth, J., Lane, W. S., Mandel, G., & Shiekhattar, R. (2002). A core–BRAF35 complex containing histone deacetylase mediates repression of neuronal-specific genes. *Proceedings of the National Academy of Sciences*, *99*(11), 7420–7425. https://doi.org/10.1073/pnas.112008599

Hamilton, J. P. (2011). Epigenetics: Principles and Practice. *Digestive Diseases*, *29*(2), 130–135. https://doi.org/10.1159/000323874

Hanzu, F. A., Musri, M. M., Sánchez-Herrero, A., Claret, M., Esteban, Y., Kaliman, P., Gomis, R., & Párrizas, M. (2013). Histone demethylase KDM1A represses inflammatory gene expression in preadipocytes. *Obesity*, *21*(12), E616–E625. https://doi.org/https://doi.org/10.1002/oby.20479

Hashimoto, H., Liu, Y., Upadhyay, A. K., Chang, Y., Howerton, S. B., Vertino, P. M., Zhang, X., & Cheng, X. (2012). Recognition and potential mechanisms for replication and erasure of cytosine hydroxymethylation. *Nucleic Acids Research*, *40*(11), 4841–4849. https://doi.org/10.1093/nar/gks155

Hassan, A. H., Prochasson, P., Neely, K. E., Galasinski, S. C., Chandy, M., Carrozza, M. J., & Workman, J. L. (2002). Function and Selectivity of Bromodomains in Anchoring Chromatin-Modifying Complexes to Promoter Nucleosomes. *Cell*, *111*(3), 369–379. https://doi.org/https://doi.org/10.1016/S0092-8674(02)01005-X

Hemming, S., Cakouros, D., Isenmann, S., Cooper, L., Menicanin, D., Zannettino, A., & Gronthos, S. (2014). EZH2 and KDM6A Act as an Epigenetic Switch to Regulate Mesenchymal Stem Cell Lineage Specification. *Stem Cells*, *32*(3), 802–815. https://doi.org/10.1002/stem.1573

Hensley, A. P., & McAlinden, A. (2021). The role of microRNAs in bone development. *Bone*, *143*, 115760. https://doi.org/https://doi.org/10.1016/j.bone.2020.115760

Hershko, A., & Ciechanover, A. (1998). THE UBIQUITIN SYSTEM. *Annual Review of Biochemistry*, *67*(Volume 67, 1998), 425–479. https://doi.org/https://doi.org/10.1146/annurev.biochem.67.1.425

Heydarpour, P., Salehi-Sadaghiani, M., Javadi-Paydar, M., Rahimian, R., Fakhfouri, G., Khosravi, M., Khoshkish, S., Gharedaghi, M. H., Ghasemi, M., & Dehpour, A. R. (2013). Estradiol reduces depressive-like behavior through inhibiting nitric oxide/cyclic GMP pathway in ovariectomized mice. *Hormones and Behavior*, *63*(2), 361–369. https://doi.org/https://doi.org/10.1016/j.yhbeh.2012.12.005

Hiltunen, A., Vuorio, E., & Aro, H. T. (1993). A standardized experimental fracture in the mouse tibia. *Journal of Orthopaedic Research : Official Publication of the Orthopaedic Research Society*, *11*(2), 305–312. https://doi.org/10.1002/jor.1100110219

Huang, J., Sengupta, R., Espejo, A. B., Lee, M. G., Dorsey, J. A., Richter, M., Opravil, S., Shiekhattar, R., Bedford, M. T., Jenuwein, T., & Berger, S. L. (2007). p53 is regulated by the lysine demethylase LSD1. *Nature*, *449*(7158), 105–108. https://doi.org/10.1038/nature06092

Hu, L., Chen, W., Qian, A., & Li, Y.-P. (2024). Wnt/β-catenin signalling components and mechanisms in bone formation, homeostasis, and disease. *Bone Research*, *12*(1), 39. https://doi.org/10.1038/s41413-024-00342-8

Husmann, D., & Gozani, O. (2019). Histone lysine methyltransferases in biology and disease. *Nature Structural & Molecular Biology*, *26*(10), 880–889. https://doi.org/10.1038/s41594-019-0298-7

Irizarry, R. A., Ladd-Acosta, C., Wen, B., Wu, Z., Montano, C., Onyango, P., Cui, H., Gabo, K., Rongione, M., Webster, M., Ji, H., Potash, J. B., Sabunciyan, S., & Feinberg, A. P. (2009). The human colon cancer methylome shows similar hypo- and hypermethylation at conserved tissue-specific CpG island shores. *Nature Genetics*, *41*(2), 178–186. https://doi.org/10.1038/ng.298

Jack, A. P. M., Bussemer, S., Hahn, M., Pünzeler, S., Snyder, M., Wells, M., Csankovszki, G., Solovei, I., Schotta, G., & Hake, S. B. (2013). H3K56me3 Is a Novel, Conserved Heterochromatic Mark That Largely but Not Completely Overlaps with H3K9me3 in Both Regulation and Localization. *PLOS ONE*, *8*(2), e51765-. https://doi.org/10.1371/journal.pone.0051765

Jansen, I. D. C., Vermeer, J. A. F., Bloemen, V., Stap, J., & Everts, V. (2012). Osteoclast Fusion and Fission. *Calcified Tissue International*, *90*(6), 515–522. https://doi.org/10.1007/s00223-012-9600-y

Jilka, R. L., O'Brien, C. A., Bartell, S. M., Weinstein, R. S., & Manolagas, S. C. (2010). Continuous elevation of PTH increases the number of osteoblasts via both osteoclast-dependent and -independent mechanisms. *Journal of Bone and Mineral Research*, *25*(11), 2427–2437. https://doi.org/10.1002/jbmr.145

Joshi, P., Greco, T. M., Guise, A. J., Luo, Y., Yu, F., Nesvizhskii, A. I., & Cristea, I. M. (2013). The functional interactome landscape of the human histone deacetylase family. *Molecular Systems Biology*, *9*(1), 672. https://doi.org/https://doi.org/10.1038/msb.2013.26

Kang, J. S., Alliston, T., Delston, R., & Derynck, R. (2005). Repression of Runx2 function by TGF-β through recruitment of class II histone deacetylases by Smad3. *The EMBO Journal*, *24*(14), 2543-2555–2555. https://doi.org/https://doi.org/10.1038/sj.emboj.7600729

Kang, J.-Y., Kim, J.-Y., Kim, K.-B., Park, J. W., Cho, H., Hahm, J. Y., Chae, Y.-C., Kim, D., Kook, H., Rhee, S., Ha, N.-C., & Seo, S.-B. (2018). KDM2B is a histone H3K79 demethylase and induces transcriptional repression via sirtuin-1-mediated chromatin silencing. *The FASEB Journal*, *32*(10), 5737–5750. https://doi.org/https://doi.org/10.1096/fj.201800242R

Kanzawa, M., Sugimoto, T., Kanatani, M., & Chihara, K. (2000). Involvement of osteoprotegerin/osteoclastogenesis inhibitory factor in the stimulation of osteoclast formation by parathyroid hormone in mouse bone cells. *European Journal of Endocrinology*, *142*(6), 661–664. https://doi.org/10.1530/eje.0.1420661

Kao, H.-Y., Downes, M., Ordentlich, P., & Evans, R. M. (2000). Isolation of a novel histone deacetylase reveals that class I and class II deacetylases promote SMRT-mediated repression. *Genes & Development*, *14*(1), 55–66. https://doi.org/10.1101/gad.14.1.55

Khosla, S., & Monroe, D. G. (2018). Regulation of Bone Metabolism by Sex Steroids. *Cold Spring Harbor Perspectives in Medicine*, *8*(1). http://perspectivesinmedicine.cshlp.org/content/8/1/a031211.abstract

Kim, J.-M., Lin, C., Stavre, Z., Greenblatt, M. B., & Shim, J.-H. (2020). Osteoblast-Osteoclast Communication and Bone Homeostasis. *Cells*, *9*(9). https://doi.org/10.3390/cells9092073

Kimura, H. (2013). Histone modifications for human epigenome analysis. *Journal of Human Genetics*, *58*(7), 439–445. https://doi.org/10.1038/jhg.2013.66

Kitase, Y., & Prideaux, M. (2023). Targeting osteocytes vs osteoblasts. *Bone*, *170*, 116724. https://doi.org/https://doi.org/10.1016/j.bone.2023.116724

Kitaura, H., Marahleh, A., Ohori, F., Noguchi, T., Shen, W.-R., Qi, J., Nara, Y., Pramusita, A., Kinjo, R., & Mizoguchi, I. (2020). Osteocyte-Related Cytokines Regulate Osteoclast Formation and Bone Resorption. *International Journal of Molecular Sciences*, *21*(14). https://doi.org/10.3390/ijms21145169

Kobayashi, Y., Maeda, K., & Takahashi, N. (2008). Roles of Wnt signalling in bone formation and resorption. *Japanese Dental Science Review*, *44*(1), 76–82. https://doi.org/https://doi.org/10.1016/j.jdsr.2007.11.002

Kohata, N., Kurihara, I., Yokota, K., Kobayashi, S., Murai-Takeda, A., Mitsuishi, Y., Nakamura, T., Morisaki, M., Kozuma, T., Torimitsu, T., Kawai, M., & Itoh, H. (2022). Lysine-specific demethylase 1 as a corepressor of mineralocorticoid receptor. *Hypertension Research*, *45*(4), 641–649. https://doi.org/10.1038/s41440-022-00859-7

Komori, T., Yagi, H., Nomura, S., Yamaguchi, A., Sasaki, K., Deguchi, K., Shimizu, Y., Bronson, R. T., Gao, Y.-H., Inada, M., Sato, M., Okamoto, R., Kitamura, Y., Yoshiki, S., & Kishimoto, T. (1997). Targeted Disruption of Cbfa1 Results in a Complete Lack of Bone Formation owing to Maturational Arrest of Osteoblasts. *Cell*, *89*(5), 755–764. https://doi.org/https://doi.org/10.1016/S0092-8674(00)80258-5

Kontaki, H., & Talianidis, I. (2010). Lysine Methylation Regulates E2F1-Induced Cell Death. *Molecular Cell*, *39*(1), 152–160. https://doi.org/https://doi.org/10.1016/j.molcel.2010.06.006

Kuo, M.-H., & Allis, C. D. (1998). Roles of histone acetyltransferases and deacetylases in gene regulation. *BioEssays*, *20*(8), 615–626. https://doi.org/https://doi.org/10.1002/(SICI)1521-1878(199808)20:8<615::AID-BIES4>3.0.CO;2-H

Lakowski, B., Roelens, I., & Jacob, S. (2006). CoREST-like complexes regulate chromatin modification and neuronal gene expression. *Journal of Molecular Neuroscience*, *29*(3), 227–239. https://doi.org/10.1385/JMN:29:3:227

Lee, K.-S., Hong, S.-H., & Bae, S.-C. (2002). Both the Smad and p38 MAPK pathways play a crucial role in Runx2 expression following induction by transforming growth factor-β and bone morphogenetic protein. *Oncogene*, *21*(47), 7156–7163. https://doi.org/10.1038/sj.onc.1205937

Lee, M. G., Wynder, C., Cooch, N., & Shiekhattar, R. (2005). An essential role for CoREST in nucleosomal histone 3 lysine 4 demethylation. *Nature*, *437*(7057), 432–435. https://doi.org/10.1038/nature04021

Lee, M.-H., Kwon, T.-G., Park, H.-S., Wozney, J. M., & Ryoo, H.-M. (2003). BMP-2-induced Osterix expression is mediated by Dlx5 but is independent of Runx2. *Biochemical and Biophysical Research Communications*, *309*(3), 689–694. https://doi.org/https://doi.org/10.1016/j.bbrc.2003.08.058

Lee, S.-J., Lee, E.-H., Park, S.-Y., & Kim, J.-E. (2017). Induction of fibrillin-2 and periostin expression in Osterix-knockdown MC3T3-E1 cells. *Gene*, *596*, 123–129. https://doi.org/https://doi.org/10.1016/j.gene.2016.10.018

Lian, J. B., Balint, E., Javed, A., Drissi, H., Vitti, R., Quinlan, E. J., Zhang, L., van Wijnen, A. J., Stein, J. L., Speck, N., & Stein, G. S. (2003). Runx1/AML1 hematopoietic transcription factor contributes to skeletal development in vivo. *Journal of Cellular Physiology*, *196*(2), 301–311. https://doi.org/https://doi.org/10.1002/jcp.10316

Liu, Z., Tang, Y., Qiu, T., Cao, X., & Clemens, T. L. (2006). A Dishevelled-1/Smad1 Interaction Couples WNT and Bone Morphogenetic Protein Signalling Pathways in Uncommitted Bone Marrow Stromal Cells*. *Journal of Biological Chemistry*, *281*(25), 17156–17163. https://doi.org/https://doi.org/10.1074/jbc.M513812200

Li, X., Zhang, Y., Kang, H., Liu, W., Liu, P., Zhang, J., Harris, S. E., & Wu, D. (2005). Sclerostin Binds to LRP5/6 and Antagonizes Canonical Wnt Signalling. *Journal of Biological Chemistry*, *280*(20), 19883–19887. http://www.jbc.org/content/280/20/19883.abstract

Li, Y., & Sasaki, H. (2011). Genomic imprinting in mammals: its life cycle, molecular mechanisms and reprogramming. *Cell Research*, *21*(3), 466–473. https://doi.org/10.1038/cr.2011.15

Li, Y., Williams, J. N., Kambrath, A. V., & Sankar, U. (2018). The Generation of Closed Femoral Fractures in Mice: A Model to Study Bone Healing. *JoVE*, *138*, e58122. https://doi.org/doi:10.3791/58122

Long, C. L., & Humphrey, M. B. (2012). Osteoimmunology: the expanding role of immunoreceptors in osteoclasts and bone remodeling. *BoneKEy Reports*, *1*(4). https://doi.org/10.1038/bonekey.2012.59

Luger, K., Mäder, A. W., Richmond, R. K., Sargent, D. F., & Richmond, T. J. (1997). Crystal structure of the nucleosome core particle at 2.8 Å resolution. *Nature*, *389*(6648), 251–260. https://doi.org/10.1038/38444

Ma, D. K., Guo, J. U., Ming, G., & Song, H. (2009). DNA excision repair proteins and Gadd45 as molecular players for active DNA demethylation. *Cell Cycle*, *8*(10), 1526–1531. https://doi.org/10.4161/cc.8.10.8500

Maiques-Diaz, A., & Somervaille, T. C. P. (2016). LSD1: biologic roles and therapeutic targeting. *Epigenomics*, *8*(8), 1103–1116. https://doi.org/10.2217/epi-2016-0009

Maksour, S., Ooi, L., & Dottori, M. (2020). More than a Corepressor: The Role of CoREST Proteins in Neurodevelopment. *Eneuro*, *7*(2), ENEURO.0337-19.2020. https://doi.org/10.1523/ENEURO.0337-19.2020

Mannstadt, M., Jüppner, H., & Gardella, T. J. (1999). Receptors for PTH and PTHrP: their biological importance and functional properties. *American Journal of Physiology-Renal Physiology*, *277*(5), F665–F675. https://doi.org/10.1152/ajprenal.1999.277.5.F665

Martineau, X., Abed, É., Martel-Pelletier, J., Pelletier, J.-P., & Lajeunesse, D. (2017). Alteration of Wnt5a expression and of the non-canonical Wnt/PCP and Wnt/PKC-Ca2+ pathways in human osteoarthritis osteoblasts. *PLOS ONE*, *12*(8), e0180711-. https://doi.org/10.1371/journal.pone.0180711

Marushige, K. (1976). Activation of chromatin by acetylation of histone side chains. *Proceedings of the National Academy of Sciences*, *73*(11), 3937–3941. https://doi.org/10.1073/pnas.73.11.3937

Massagué, J., Seoane, J., & Wotton, D. (2005). Smad transcription factors. *Genes & Development*, *19*(23), 2783–2810. https://genesdev.cshlp.org/content/19/23/2783.abstract

McDonald, M. M., Khoo, W. H., Ng, P. Y., Xiao, Y., Zamerli, J., Thatcher, P., Kyaw, W., Pathmanandavel, K., Grootveld, A. K., Moran, I., Butt, D., Nguyen, A., Corr, A., Warren, S., Biro, M., Butterfield, N. C., Guilfoyle, S. E., Komla-Ebri, D., Dack, M. R. G., … Phan, T. G. (2021). Osteoclasts recycle via osteomorphs during RANKL-stimulated bone resorption. *Cell*, *184*(5), 1330-1347.e13. https://doi.org/https://doi.org/10.1016/j.cell.2021.02.002

McGee-Lawrence, M. E., & Westendorf, J. J. (2011). Histone deacetylases in skeletal development and bone mass maintenance. *Gene*, *474*(1), 1–11. https://doi.org/https://doi.org/10.1016/j.gene.2010.12.003

Melis, S., Trompet, D., Chagin, A. S., & Maes, C. (2024). Skeletal stem and progenitor cells in bone physiology, ageing and disease. *Nature Reviews Endocrinology*. https://doi.org/10.1038/s41574-024-01039-y

Mercer, T. R., Dinger, M. E., & Mattick, J. S. (2009). Long non-coding RNAs: insights into functions. *Nature Reviews Genetics*, *10*(3), 155–159. https://doi.org/10.1038/nrg2521

Metzger, E., Wissmann, M., Yin, N., Müller, J. M., Schneider, R., Peters, A. H. F. M., Günther, T., Buettner, R., & Schüle, R. (2005). LSD1 demethylates repressive histone marks to promote androgen-receptor-dependent transcription. *Nature*, *437*(7057), 436–439. https://doi.org/10.1038/nature04020

Millard, C. J., Watson, P. J., Celardo, I., Gordiyenko, Y., Cowley, S. M., Robinson, C. V., Fairall, L., & Schwabe, J. W. R. (2013). Class I HDACs Share a Common Mechanism of Regulation by Inositol Phosphates. *Molecular Cell*, *51*(1), 57–67. https://doi.org/https://doi.org/10.1016/j.molcel.2013.05.020

Mizzen, C. A., Yang, X.-J., Kokubo, T., Brownell, J. E., Bannister, A. J., Owen-Hughes, T., Workman, J., Wang, L., Berger, S. L., Kouzarides, T., Nakatani, Y., & Allis, C. D. (1996). The TAFII250 Subunit of TFIID Has Histone Acetyltransferase Activity. *Cell*, *87*(7), 1261–1270. https://doi.org/https://doi.org/10.1016/S0092-8674(00)81821-8

Monaghan, C. E., Nechiporuk, T., Jeng, S., McWeeney, S. K., Wang, J., Rosenfeld, M. G., & Mandel, G. (2017). REST corepressors RCOR1 and RCOR2 and the repressor INSM1 regulate the proliferation-differentiation balance in the developing brain. *Proceedings of the National Academy of Sciences of the United States of America*, *114*(3), E406–E415. https://doi.org/10.1073/pnas.1620230114

Moore, L. D., Le, T., & Fan, G. (2013). DNA Methylation and Its Basic Function. *Neuropsychopharmacology*, *38*(1), 23–38. https://doi.org/10.1038/npp.2012.112

Morcos, L., Ge, B., Koka, V., Lam, K. C. L., Pokholok, D. K., Gunderson, K. L., Montpetit, A., Verlaan, D. J., & Pastinen, T. (2011). Genome-wide assessment of imprinted expression in human cells. *Genome Biology*, *12*(3), R25. https://doi.org/10.1186/gb-2011-12-3-r25

Mullender, M., El Haj, A. J., Yang, Y., van Duin, M. A., Burger, E. H., & Klein-Nulend, J. (2004). Mechanotransduction of bone cellsin vitro: Mechanobiology of bone tissue. *Medical and Biological Engineering and Computing*, *42*(1), 14–21. https://doi.org/10.1007/BF02351006

Murn, J., & Shi, Y. (2017). The winding path of protein methylation research: milestones and new frontiers. *Nature Reviews Molecular Cell Biology*, *18*(8), 517–527. https://doi.org/10.1038/nrm.2017.35

Muslin, A. J., & Xing, H. (2000). 14-3-3 proteins: regulation of subcellular localization by molecular interference. *Cellular Signalling*, *12*(11), 703–709. https://doi.org/https://doi.org/10.1016/S0898-6568(00)00131-5

Musri, M. M., Carmona, M. C., Hanzu, F. A., Kaliman, P., Gomis, R., & Párrizas, M. (2010). Histone Demethylase LSD1 Regulates Adipogenesis*. *Journal of Biological Chemistry*, *285*(39), 30034–30041. https://doi.org/https://doi.org/10.1074/jbc.M110.151209

Nagano, T., & Fraser, P. (2009). Emerging similarities in epigenetic gene silencing by long noncoding RNAs. *Mammalian Genome*, *20*(9), 557–562. https://doi.org/10.1007/s00335-009-9218-1

Nakamura, T., Mori, T., Tada, S., Krajewski, W., Rozovskaia, T., Wassell, R., Dubois, G., Mazo, A., Croce, C. M., & Canaani, E. (2002). ALL-1 Is a Histone Methyltransferase that Assembles a Supercomplex of Proteins Involved in Transcriptional Regulation. *Molecular Cell*, *10*(5), 1119–1128. https://doi.org/https://doi.org/10.1016/S1097-2765(02)00740-2

Nakashima, K., Zhou, X., Kunkel, G., Zhang, Z., Deng, J. M., Behringer, R. R., & de Crombrugghe, B. (2002). The Novel Zinc Finger-Containing Transcription Factor Osterix Is Required for Osteoblast Differentiation and Bone Formation. *Cell*, *108*(1), 17–29. https://doi.org/https://doi.org/10.1016/S0092-8674(01)00622-5

Narla, R. R., & Ott, S. M. (2018). Bones and the sex hormones. *Kidney International*, *94*(2), 239–242. https://doi.org/https://doi.org/10.1016/j.kint.2018.03.021

NC3Rs. (2024, September 15). *Replacement, Reduction and Refinement*. Https://Nc3rs.Org.Uk/.

Niehrs, C. (2006). Function and biological roles of the Dickkopf family of Wnt modulators. *Oncogene*, *25*(57), 7469–7481. https://doi.org/10.1038/sj.onc.1210054

Nieminen-Pihala, V., Tarkkonen, K., Laine, J., Rummukainen, P., Saastamoinen, L., Nagano, K., Baron, R., & Kiviranta, R. (2021). Early B-cell Factor1 (Ebf1) promotes early osteoblast differentiation but suppresses osteoblast function. *Bone*, *146*, 115884. https://doi.org/https://doi.org/10.1016/j.bone.2021.115884

Niziolek, P. J., Bullock, W., Warman, M. L., & Robling, A. G. (2015). Missense Mutations in LRP5 Associated with High Bone Mass Protect the Mouse Skeleton from Disuse- and Ovariectomy-Induced Osteopenia. *PLOS ONE*, *10*(11), e0140775-. https://doi.org/10.1371/journal.pone.0140775

Noce, B., Di Bello, E., Fioravanti, R., & Mai, A. (2023). LSD1 inhibitors for cancer treatment: Focus on multi-target agents and compounds in clinical trials. *Frontiers in Pharmacology*, *14*. https://doi.org/10.3389/fphar.2023.1120911

O, H. P., S, H. S., Michael, E., & O, H. M. (2006). Nuclear ADP-Ribosylation Reactions in Mammalian Cells: Where Are We Today and Where Are We Going? *Microbiology and Molecular Biology Reviews*, *70*(3), 789–829. https://doi.org/10.1128/mmbr.00040-05

Onizuka, S., Iwata, T., Park, S.-J., Nakai, K., Yamato, M., Okano, T., & Izumi, Y. (2016). ZBTB16 as a Downstream Target Gene of Osterix Regulates Osteoblastogenesis of Human Multipotent Mesenchymal Stromal Cells. *Journal of Cellular Biochemistry*, *117*(10), 2423–2434. https://doi.org/https://doi.org/10.1002/jcb.25634

Pal, D., Ghatak, S., & Sen, C. K. (2015). Chapter 3 - Epigenetic Modification of MicroRNAs. In C. K. Sen (Ed.), *MicroRNA in Regenerative Medicine* (pp. 77–109). Academic Press. https://doi.org/https://doi.org/10.1016/B978-0-12-405544-5.00003-4

Pan, Q., Wu, Y., Lin, T., Yao, H., Yang, Z., Gao, G., Song, E., & Shen, H. (2009). Bone Morphogenetic Protein-2 induces chromatin remodeling and modification at the proximal promoter of Sox9 gene.

Biochemical and Biophysical Research Communications, *379*(2), 356–361. https://doi.org/https://doi.org/10.1016/j.bbrc.2008.12.062

Park, S.-Y., & Kim, J.-S. (2020). A short guide to histone deacetylases including recent progress on class II enzymes. *Experimental & Molecular Medicine*, *52*(2), 204–212. https://doi.org/10.1038/s12276-020-0382-4

Pei, L., Zhang, H., Zhang, M., Wang, Y., & Wei, K. (2022). Rcor2 Is Required for Somatic Differentiation and Represses Germline Cell Fate. *Stem Cells International*, *2022*(1), 5283615. https://doi.org/https://doi.org/10.1155/2022/5283615

Peng, Y., Kang, Q., Cheng, H., Li, X., Sun, M. H., Jiang, W., Luu, H. H., Park, J. Y., Haydon, R. C., & He, T.-C. (2003). Transcriptional characterization of bone morphogenetic proteins (BMPs)-mediated osteogenic signalling. *Journal of Cellular Biochemistry*, *90*(6), 1149–1165. https://doi.org/https://doi.org/10.1002/jcb.10744

Perillo, B., Ombra, M. N., Bertoni, A., Cuozzo, C., Sacchetti, S., Sasso, A., Chiariotti, L., Malorni, A., Abbondanza, C., & Avvedimento, E. V. (2008). DNA Oxidation as Triggered by H3K9me2 Demethylation Drives Estrogen-Induced Gene Expression. *Science*, *319*(5860), 202–206. https://doi.org/10.1126/science.1147674

Pilotto, S., Speranzini, V., Tortorici, M., Durand, D., Fish, A., Valente, S., Forneris, F., Mai, A., Sixma, T. K., Vachette, P., & Mattevi, A. (2015). Interplay among nucleosomal DNA, histone tails, and corepressor CoREST underlies LSD1-mediated H3 demethylation. *Proceedings of the National Academy of Sciences*, *112*(9), 2752–2757. https://doi.org/10.1073/pnas.1419468112

Pokholok, D. K., Harbison, C. T., Levine, S., Cole, M., Hannett, N. M., Lee, T. I., Bell, G. W., Walker, K., Rolfe, P. A., Herbolsheimer, E., Zeitlinger, J., Lewitter, F., Gifford, D. K., & Young, R. A. (2005). Genome-wide Map of Nucleosome Acetylation and Methylation in Yeast. *Cell*, *122*(4), 517–527. https://doi.org/https://doi.org/10.1016/j.cell.2005.06.026

Polticelli, F., Basran, J., Faso, C., Cona, A., Minervini, G., Angelini, R., Federico, R., Scrutton, N. S., & Tavladoraki, P. (2005). Lys300 Plays a Major Role in the Catalytic Mechanism of Maize Polyamine Oxidase. *Biochemistry*, *44*(49), 16108–16120. https://doi.org/10.1021/bi050983i

Ponzetti, M., & Rucci, N. (2021). Osteoblast Differentiation and Signalling: Established Concepts and Emerging Topics. *International Journal of Molecular Sciences*, *22*, 6651. https://doi.org/10.3390/ijms22136651

Poulard, C., Corbo, L., & Le Romancer, M. (2016). Protein arginine methylation/demethylation and cancer. *Oncotarget*, *7*(41), 67532–67550. https://doi.org/10.18632/oncotarget.11376

Primrose, J. G. B., Jain, L., Alhilali, M., Bolam, S. M., Monk, A. P., Munro, J. T., Dalbeth, N., & Poulsen, R. C. (2023). REST, RCOR1 and RCOR2 expression is reduced in osteoarthritic chondrocytes and contributes to increasing MMP13 and ADAMTS5 expression through upregulating HES1. *Cellular Signalling*, *109*, 110800. https://doi.org/https://doi.org/10.1016/j.cellsig.2023.110800

Puolakkainen, T., Rummukainen, P., Lehto, J., Ritvos, O., Hiltunen, A., Saamanen, A.-M., & Kiviranta, R. (2017). Soluble activin type IIB receptor improves fracture healing in a closed tibial fracture mouse model. *PloS One*, *12*(7), e0180593. https://doi.org/10.1371/journal.pone.0180593

Rakyan, V. K., Preis, J., Morgan Hugh D, & Whitelaq, E. (2001). The marks, mechanisms and memory of epigenetic states in mammals. *Biochemical Journal*, *356*(1), 1–10. https://doi.org/10.1042/bj3560001

Rashid, H., Chen, H., & Javed, A. (2021). Runx2 is required for hypertrophic chondrocyte mediated degradation of cartilage matrix during endochondral ossification. *Matrix Biology Plus*, *12*, 100088. https://doi.org/https://doi.org/10.1016/j.mbplus.2021.100088

Rauner, M., Taipaleenmäki, H., Tsourdi, E., & Winter, E. M. (2021). Osteoporosis Treatment with Anti-Sclerostin Antibodies—Mechanisms of Action and Clinical Application. *Journal of Clinical Medicine*, *10*(4). https://doi.org/10.3390/jcm10040787

Rechache, N. S., Wang, Y., Stevenson, H. S., Killian, J. K., Edelman, D. C., Merino, M., Zhang, L., Nilubol, N., Stratakis, C. A., Meltzer, P. S., & Kebebew, E. (2012). DNA Methylation Profiling Identifies Global Methylation Differences and Markers of Adrenocortical Tumors. *The Journal of Clinical Endocrinology & Metabolism*, *97*(6), E1004–E1013. https://doi.org/10.1210/jc.2011-3298

Redman, M., King, A., Watson, C., & King, D. (2016). What is CRISPR/Cas9? *Archives of Disease in Childhood - Education &Amp; Practice Edition*, *101*(4), 213. https://doi.org/10.1136/archdischild-2016-310459

Rivera, C., Verbel-Vergara, D., Arancibia, D., Lappala, A., González, M., Guzmán, F., Merello, G., Lee, J. T., & Andrés, M. E. (2021). Revealing RCOR2 as a regulatory component of nuclear speckles. *Epigenetics & Chromatin*, *14*(1), 51. https://doi.org/10.1186/s13072-021-00425-4

Rodova, M., Lu, Q., Li, Y., Woodbury, B. G., Crist, J. D., Gardner, B. M., Yost, J. G., Zhong, X., Anderson, H. C., & Wang, J. (2011). Nfat1 regulates adult articular chondrocyte function through its age-dependent expression mediated by epigenetic histone methylation. *Journal of Bone and Mineral Research*, *26*(8), 1974–1986. https://doi.org/10.1002/jbmr.397

Rougeulle, C., Glatt, H., & Lalande, M. (1997). The Angelman syndrome candidate gene, UBE3AIE6-AP, is imprinted in brain. *Nature Genetics*, *17*(1), 14–15. https://doi.org/10.1038/ng0997-14

Rutkovskiy, A., Stensløkken, K.-O., & Vaage, I. J. (2016). Osteoblast Differentiation at a Glance. *Medical Science Monitor Basic Research*, *22*, 95–106. https://doi.org/https://dx.doi.org/10.12659/MSMBR.901142

Salari, N., Ghasemi, H., Mohammadi, L., Behzadi, M. hasan, Rabieenia, E., Shohaimi, S., & Mohammadi, M. (2021). The global prevalence of osteoporosis in the world: a comprehensive systematic review and meta-analysis. *Journal of Orthopaedic Surgery and Research*, *16*(1), 609. https://doi.org/10.1186/s13018-021-02772-0

Saleque, S., Kim, J., Rooke, H. M., & Orkin, S. H. (2007). Epigenetic regulation of hematopoietic differentiation by Gfi-1 and Gfi-1b is mediated by the cofactors CoREST and LSD1. *Molecular Cell*, *27*(4), 562–572. https://doi.org/S1097-2765(07)00483-2 [pii]

Sanchez-Gurmaches, J., Hsiao, W.-Y., & Guertin, D. A. (2015). Highly Selective In Vivo Labeling of Subcutaneous White Adipocyte Precursors with Prx1-Cre. *Stem Cell Reports*, *4*(4), 541–550. https://doi.org/https://doi.org/10.1016/j.stemcr.2015.02.008

Sato, K., Suematsu, A., Nakashima, T., Takemoto-Kimura, S., Aoki, K., Morishita, Y., Asahara, H., Ohya, K., Yamaguchi, A., Takai, T., Kodama, T., Chatila, T. A., Bito, H., & Takayanagi, H. (2006). Regulation of osteoclast differentiation and function by the CaMK-CREB pathway. *Nature Medicine*, *12*(12), 1410–1416. https://doi.org/10.1038/nm1515

Sauer, B., & Henderson, N. (1988). Site-specific DNA recombination in mammalian cells by the Cre recombinase of bacteriophage P1. *Proceedings of the National Academy of Sciences*, *85*(14), 5166–5170. https://doi.org/10.1073/pnas.85.14.5166

Schafrum Macedo, A., Cezaretti Feitosa, C., Yoiti Kitamura Kawamoto, F., Vinicius Tertuliano Marinho, P., dos Santos Dal-Bó, Í., Fiuza Monteiro, B., Prado, L., Bregadioli, T., Antonio Covino Diamante, G., & Ricardo Auada Ferrigno, C. (2019). Animal modeling in bone research—Should we follow the White Rabbit? *Animal Models and Experimental Medicine*, *2*(3), 162–168. https://doi.org/https://doi.org/10.1002/ame2.12083

Sepulveda, H., Aguilar, R., Prieto, C. P., Bustos, F., Aedo, S., Lattus, J., van Zundert, B., Palma, V., & Montecino, M. (2017). Epigenetic Signatures at the RUNX2-P1 and Sp7 Gene Promoters Control Osteogenic Lineage Commitment of Umbilical Cord-Derived Mesenchymal Stem Cells. *Journal of Cellular Physiology*, *232*(9), 2519–2527. https://doi.org/https://doi.org/10.1002/jcp.25627

Shahbazian, M. D., & Grunstein, M. (2007). Functions of Site-Specific Histone Acetylation and Deacetylation. *Annual Review of Biochemistry*, *76*(Volume 76, 2007), 75–100. https://doi.org/https://doi.org/10.1146/annurev.biochem.76.052705.162114

Sharma, G., Sultana, A., Abdullah, K. M., Pothuraju, R., Nasser, M. W., Batra, S. K., & Siddiqui, J. A. (2024). Epigenetic regulation of bone remodeling and bone metastasis. *Seminars in Cell & Developmental Biology*, *154*, 275–285. https://doi.org/https://doi.org/10.1016/j.semcdb.2022.11.002

Shiama, N. (1997). The p300/CBP family: integrating signals with transcription factors and chromatin. *Trends in Cell Biology*, *7*(6), 230–236. https://doi.org/https://doi.org/10.1016/S0962-8924(97)01048-9

Shigehara, K., Izumi, K., Kadono, Y., & Mizokami, A. (2021). Testosterone and Bone Health in Men: A Narrative Review. *Journal of Clinical Medicine*, *10*(3). https://doi.org/10.3390/jcm10030530

Shi, Y. (2007). Histone lysine demethylases: emerging roles in development, physiology and disease. *Nature Reviews Genetics*, *8*(11), 829–833. https://doi.org/10.1038/nrg2218

Silva, B. C., & Bilezikian, J. P. (2015). Parathyroid hormone: anabolic and catabolic actions on the skeleton. *Current Opinion in Pharmacology*, *22*, 41–50. https://doi.org/https://doi.org/10.1016/j.coph.2015.03.005

Slack, J. M. W. (2014). Chapter 7 - Molecular Biology of the Cell. In R. Lanza, R. Langer, & J. Vacanti (Eds.), *Principles of Tissue Engineering (Fourth Edition)* (pp. 127–145). Academic Press. https://doi.org/https://doi.org/10.1016/B978-0-12-398358-9.00007-0

Smith, S., & Stillman, B. (1991). Stepwise assembly of chromatin during DNA replication in vitro. *The EMBO Journal*, *10*(4), 971-980–980. https://doi.org/https://doi.org/10.1002/j.1460-2075.1991.tb08031.x

Song, Y., Dagil, L., Fairall, L., Robertson, N., Wu, M., Ragan, T. J., Savva, C. G., Saleh, A., Morone, N., Kunze, M. B. A., Jamieson, A. G., Cole, P. A., Hansen, D. F., & Schwabe, J. W. R. (2020). Mechanism of Crosstalk between the LSD1 Demethylase and HDAC1 Deacetylase in the CoREST Complex. *Cell Reports*, *30*(8), 2699-2711.e8. https://doi.org/https://doi.org/10.1016/j.celrep.2020.01.091

Soung, D. Y., Dong, Y., Wang, Y. J., Zuscik, M. J., Schwarz, E. M., O'Keefe, R. J., & Drissi, H. (2007). Runx3/AML2/Cbfa3 Regulates Early and Late Chondrocyte Differentiation*. *Journal of Bone and Mineral Research*, *22*(8), 1260–1270. https://doi.org/10.1359/jbmr.070502

St-Arnaud, R., & Hekmatnejad, B. (2011). Combinatorial control of ATF4-dependent gene transcription in osteoblasts. *Annals of the New York Academy of Sciences*, *1237*(1), 11–18. https://doi.org/https://doi.org/10.1111/j.1749-6632.2011.06197.x

Stavropoulos, P., Blobel, G., & Hoelz, A. (2006). Crystal structure and mechanism of human lysine-specific demethylase-1. *Nature Structural & Molecular Biology*, *13*(7), 626–632. https://doi.org/10.1038/nsmb1113

Sterling, J., Menezes, S. V, Abbassi, R. H., & Munoz, L. (2021). Histone lysine demethylases and their functions in cancer. *International Journal of Cancer*, *148*(10), 2375–2388. https://doi.org/https://doi.org/10.1002/ijc.33375

Streicher, C., Heyny, A., Andrukhova, O., Haigl, B., Slavic, S., Schüler, C., Kollmann, K., Kantner, I., Sexl, V., Kleiter, M., Hofbauer, L. C., Kostenuik, P. J., & Erben, R. G. (2017). Estrogen Regulates Bone Turnover by Targeting RANKL Expression in Bone Lining Cells. *Scientific Reports*, *7*(1), 6460. https://doi.org/10.1038/s41598-017-06614-0

Sun, J., Ermann, J., Niu, N., Yan, G., Yang, Y., Shi, Y., & Zou, W. (2018). Histone demethylase LSD1 regulates bone mass by controlling WNT7B and BMP2 signalling in osteoblasts. *Bone Research*, *6*(1), 14. https://doi.org/10.1038/s41413-018-0015-x

Sun, J., Feng, H., Xing, W., Han, Y., Suo, J., Yallowitz, A. R., Qian, N., Shi, Y., Greenblatt, M. B., & Zou, W. (2020). Histone demethylase LSD1 is critical for endochondral ossification during bone fracture healing. *Science Advances*, *6*(45). https://doi.org/10.1126/sciadv.aaz1410

Sweatt, J. D., Nestler, E. J., Meaney, M. J., & Akbarian, S. (2013). Chapter 1 - An Overview of the Molecular Basis of Epigenetics. In J. D. Sweatt, M. J. Meaney, E. J. Nestler, & S. Akbarian (Eds.), *Epigenetic Regulation in the Nervous System* (pp. 3–33). Academic Press. https://doi.org/https://doi.org/10.1016/B978-0-12-391494-1.00001-X

TAKADA, I., SUZAWA, M., MATSUMOTO, K., & KATO, S. (2007). Suppression of PPAR Transactivation Switches Cell Fate of Bone Marrow Stem Cells from Adipocytes into Osteoblasts. *Annals of the New York Academy of Sciences*, *1116*(1), 182–195. https://doi.org/https://doi.org/10.1196/annals.1402.034

Tang, C.-Y., Chen, W., Luo, Y., Wu, J., Zhang, Y., McVicar, A., McConnell, M., Liu, Y., Zhou, H.-D., & Li, Y.-P. (2020). Runx1 up-regulates chondrocyte to osteoblast lineage commitment and promotes bone formation by enhancing both chondrogenesis and osteogenesis. *Biochemical Journal*, *477*(13), 2421–2438. https://doi.org/10.1042/BCJ20200036

Thrasivoulou, C., Millar, M., & Ahmed, A. (2013). Activation of Intracellular Calcium by Multiple Wnt Ligands and Translocation of β-Catenin into the Nucleus: A CONVERGENT MODEL OF Wnt/Ca2+ AND Wnt/β-CATENIN PATHWAYS*. *Journal of Biological Chemistry*, *288*(50), 35651–35659. https://doi.org/https://doi.org/10.1074/jbc.M112.437913

Tong, J. K., Hassig, C. A., Schnitzler, G. R., Kingston, R. E., & Schreiber, S. L. (1998). Chromatin deacetylation by an ATP-dependent nucleosome remodelling complex. *Nature*, *395*(6705), 917–921. https://doi.org/10.1038/27699

Tooze, R. S., Miller, K. A., Swagemakers, S. M. A., Calpena, E., McGowan, S. J., Boute, O., Collet, C., Johnson, D., Laffargue, F., de Leeuw, N., Morton, J. V, Noons, P., Ockeloen, C. W., Phipps, J. M., Tan, T. Y., Timberlake, A. T., Vanlerberghe, C., Wall, S. A., Weber, A., … Wilkie, A. O. M. (2023). Pathogenic variants in the paired-related homeobox 1 gene (PRRX1) cause craniosynostosis with incomplete penetrance. *Genetics in Medicine*, *25*(9), 100883. https://doi.org/https://doi.org/10.1016/j.gim.2023.100883

Tsukada, Y., Fang, J., Erdjument-Bromage, H., Warren, M. E., Borchers, C. H., Tempst, P., & Zhang, Y. (2006). Histone demethylation by a family of JmjC domain-containing proteins. *Nature*, *439*(7078), 811–816. https://doi.org/10.1038/nature04433

Uccelli, A., Moretta, L., & Pistoia, V. (2008). Mesenchymal stem cells in health and disease. *Nature Reviews Immunology*, *8*(9), 726–736. https://doi.org/10.1038/nri2395

Valcourt, U., Gouttenoire, J., Moustakas, A., Herbage, D., & Mallein-Gerin, F. (2002). Functions of Transforming Growth Factor-β Family Type I Receptors and Smad Proteins in the Hypertrophic Maturation and Osteoblastic Differentiation of Chondrocytes*. *Journal of Biological Chemistry*, *277*(37), 33545–33558. https://doi.org/https://doi.org/10.1074/jbc.M202086200

Vanderschueren, D., Vandenput, L., Boonen, S., Lindberg, M. K., Bouillon, R., & Ohlsson, C. (2004). Androgens and Bone. *Endocrine Reviews*, *25*(3), 389–425. https://doi.org/10.1210/er.2003-0003

Verreault, A., Kaufman, P. D., Kobayashi, R., & Stillman, B. (1998). Nucleosomal DNA regulates the core-histone-binding subunit of the human Hat1 acetyltransferase. *Current Biology*, *8*(2), 96–108. https://doi.org/10.1016/S0960-9822(98)70040-5

Waddington, C. H. (1957). *The Strategy of the Genes* (1st Edition).

Wang, J., Hevi, S., Kurash, J. K., Lei, H., Gay, F., Bajko, J., Su, H., Sun, W., Chang, H., Xu, G., Gaudet, F., Li, E., & Chen, T. (2009). The lysine demethylase LSD1 (KDM1) is required for maintenance of global DNA methylation. *Nature Genetics*, *41*(1), 125–129. https://doi.org/10.1038/ng.268

Wang, L., You, X., Ruan, D., Shao, R., Dai, H.-Q., Shen, W., Xu, G.-L., Liu, W., & Zou, W. (2022). TET enzymes regulate skeletal development through increasing chromatin accessibility of RUNX2 target genes. *Nature Communications*, *13*(1), 4709. https://doi.org/10.1038/s41467-022-32138-x

Wang, X.-J., Liu, J.-W., & Liu, J. (2020). MiR-655-3p inhibits the progression of osteoporosis by targeting LSD1 and activating BMP-2/Smad signalling pathway. *Human & Experimental Toxicology*, *39*(10), 1390–1404. https://doi.org/10.1177/0960327120924080

Wang, Y., Belflower, R. M., Dong, Y., Schwarz, E. M., O'Keefe, R. J., & Drissi, H. (2005). Runx1/AML1/Cbfa2 Mediates Onset of Mesenchymal Cell Differentiation Toward Chondrogenesis*. *Journal of Bone and Mineral Research*, *20*(9), 1624–1636. https://doi.org/10.1359/JBMR.050516

Wang, Y., Wu, Q., Yang, P., Wang, C., Liu, J., Ding, W., Liu, W., Bai, Y., Yang, Y., Wang, H., Gao, S., & Wang, X. (2016). LSD1 co-repressor Rcor2 orchestrates neurogenesis in the developing mouse brain. *Nature Communications*, *7*, 10481. https://doi.org/10.1038/ncomms10481 [doi]

Wang, Y., Zhang, H., Chen, Y., Sun, Y., Yang, F., Yu, W., Liang, J., Sun, L., Yang, X., Shi, L., Li, R., Li, Y., Zhang, Y., Li, Q., Yi, X., & Shang, Y. (2009). LSD1 Is a Subunit of the NuRD Complex and Targets the Metastasis Programs in Breast Cancer. *Cell*, *138*(4), 660–672. https://doi.org/https://doi.org/10.1016/j.cell.2009.05.050

Wei, J., Shimazu, J., Makinistoglu, M. P., Maurizi, A., Kajimura, D., Zong, H., Takarada, T., Iezaki, T., Pessin, J. E., Hinoi, E., & Karsenty, G. (2015). Glucose Uptake and Runx2 Synergize to Orchestrate Osteoblast Differentiation and Bone Formation. *Cell*, *161*(7), 1576–1591. https://doi.org/10.1016/j.cell.2015.05.029

Wein, M. N., & Kronenberg, H. M. (2018). Regulation of Bone Remodeling by Parathyroid Hormone. *Cold Spring Harbor Perspectives in Medicine*, *8*(8). http://perspectivesinmedicine.cshlp.org/content/8/8/a031237.abstract

Weitzmann, M. N., & Pacifici, R. (2006). Estrogen deficiency and bone loss: an inflammatory tale. *The Journal of Clinical Investigation*, *116*(5), 1186–1194. https://doi.org/10.1172/JCI28550

Wilkinson, L. S., Davies, W., & Isles, A. R. (2007). Genomic imprinting effects on brain development and function. *Nature Reviews Neuroscience*, *8*(11), 832–843. https://doi.org/10.1038/nrn2235

Winkler, D. G., Sutherland, M. K., Geoghegan, J. C., Yu, C., Hayes, T., Skonier, J. E., Shpektor, D., Jonas, M., Kovacevich, B. R., Staehling-Hampton, K., Appleby, M., Brunkow, M. E., & Latham, J. A. (2003). Osteocyte control of bone formation via sclerostin, a novel BMP antagonist. *The EMBO Journal*, *22*(23), 6267–6276. https://doi.org/10.1093/emboj/cdg599

Wolffe, A. P., & Hayes, J. J. (1999). Chromatin disruption and modification. *Nucleic Acids Research*, *27*(3), 711–720. https://doi.org/10.1093/nar/27.3.711

Wu, M., Chen, G., & Li, Y.-P. (2016). TGF-β and BMP signalling in osteoblast, skeletal development, and bone formation, homeostasis and disease. *Bone Research*, *4*(1), 16009. https://doi.org/10.1038/boneres.2016.9

Xiao, G., Jiang, D., Ge, C., Zhao, Z., Lai, Y., Boules, H., Phimphilai, M., Yang, X., Karsenty, G., & Franceschi, R. T. (2005). Cooperative Interactions between Activating Transcription Factor 4 and Runx2/Cbfa1 Stimulate Osteoblast-specific Osteocalcin Gene Expression*. *Journal of Biological Chemistry*, *280*(35), 30689–30696. https://doi.org/https://doi.org/10.1074/jbc.M500750200

Xiao, J., Li, T., Wu, Z., Shi, Z., Chen, J., Lam, S. K. L., Zhao, Z., Yang, L., & Qiu, G. (2010). REST corepressor (CoREST) repression induces phenotypic gene regulation in advanced osteoarthritic chondrocytes. *Journal of Orthopaedic Research*, *28*(12), 1569–1575. https://doi.org/https://doi.org/10.1002/jor.21151

Xiong, B., Lu, S., & Gerton, J. L. (2010). Hos1 Is a Lysine Deacetylase for the Smc3 Subunit of Cohesin. *Current Biology*, *20*(18), 1660–1665. https://doi.org/https://doi.org/10.1016/j.cub.2010.08.019

Xu, F., Li, W., Yang, X., Na, L., Chen, L., & Liu, G. (2021). The Roles of Epigenetics Regulation in Bone Metabolism and Osteoporosis. *Frontiers in Cell and Developmental Biology*, *8*. https://www.frontiersin.org/journals/cell-and-developmental-biology/articles/10.3389/fcell.2020.619301

Yamashiro, T., Åberg, T., Levanon, D., Groner, Y., & Thesleff, I. (2002). Expression of Runx1, -2 and -3 during tooth, palate and craniofacial bone development. *Mechanisms of Development*, *119*, S107–S110. https://doi.org/https://doi.org/10.1016/S0925-4773(03)00101-1

Yang, M., Gocke, C. B., Luo, X., Borek, D., Tomchick, D. R., Machius, M., Otwinowski, Z., & Yu, H. (2006). Structural Basis for CoREST-Dependent Demethylation of Nucleosomes by the Human LSD1 Histone Demethylase. *Molecular Cell*, *23*(3), 377–387. https://doi.org/https://doi.org/10.1016/j.molcel.2006.07.012

Yang, P., Wang, Y., Chen, J., Li, H., Kang, L., Zhang, Y., Chen, S., Zhu, B., & Gao, S. (2011). RCOR2 is a subunit of the LSD1 complex that regulates ESC property and substitutes for SOX2 in reprogramming somatic cells to pluripotency. *Stem Cells*, *29*(5), 791–801. https://doi.org/10.1002/stem.634

Yang, X.-J., Ogryzko, V. V, Nishikawa, J., Howard, B. H., & Nakatani, Y. (1996). A p300/CBP-associated factor that competes with the adenoviral oncoprotein E1A. *Nature*, *382*(6589), 319–324. https://doi.org/10.1038/382319a0

Yang, X., & Karsenty, G. (2002). Transcription factors in bone: developmental and pathological aspects. *Trends in Molecular Medicine*, *8*(7), 340–345. https://doi.org/https://doi.org/10.1016/S1471-4914(02)02340-7

You, A., Tong, J. K., Grozinger, C. M., & Schreiber, S. L. (2001). CoREST is an integral component of the CoREST- human histone deacetylase complex. *Proceedings of the National Academy of Sciences*, *98*(4), 1454–1458. https://doi.org/10.1073/pnas.98.4.1454

Yu, D., Li, Z., Cao, J., Wei, G., & Shen, F. (2023). LSD1 knockdown confers protection against osteoclast formation by reducing histone 3 lysine 9 monomethylation and dimethylation in ITGB3 promoter. *Acta Histochemica*, *125*(7), 152073. https://doi.org/https://doi.org/10.1016/j.acthis.2023.152073

Yu, J., Li, Y., Ishizuka, T., Guenther, M. G., & Lazar, M. A. (2003). A SANT motif in the SMRT corepressor interprets the histone code and promotes histone deacetylation. *The EMBO Journal*, *22*(13), 3403-3410–3410. https://doi.org/https://doi.org/10.1093/emboj/cdg326

Yu, S., Franceschi, R. T., Luo, M., Fan, J., Jiang, D., Cao, H., Kwon, T.-G., Lai, Y., Zhang, J., Patrene, K., Hankenson, K., Roodman, G. D., & Xiao, G. (2009). Critical Role of Activating Transcription

Factor 4 in the Anabolic Actions of Parathyroid Hormone in Bone. *PLOS ONE*, *4*(10), e7583-. https://doi.org/10.1371/journal.pone.0007583

Zawel, L., Le Dai, J., Buckhaults, P., Zhou, S., Kinzler, K. W., Vogelstein, B., & Kern, S. E. (1998). Human Smad3 and Smad4 Are Sequence-Specific Transcription Activators. *Molecular Cell*, *1*(4), 611–617. https://doi.org/https://doi.org/10.1016/S1097-2765(00)80061-1

Zhang, W., Zhang, K., Ma, Y., Song, Y., Qi, T., Xiong, G., Zhang, Y., Kan, C., Zhang, J., Han, F., & Sun, X. (2023). Secreted frizzled-related proteins: A promising therapeutic target for cancer therapy through Wnt signalling inhibition. *Biomedicine & Pharmacotherapy*, *166*, 115344. https://doi.org/https://doi.org/10.1016/j.biopha.2023.115344

Zhu, S., Chen, W., Masson, A., & Li, Y.-P. (2024). Cell signalling and transcriptional regulation of osteoblast lineage commitment, differentiation, bone formation, and homeostasis. *Cell Discovery*, *10*(1), 71. https://doi.org/10.1038/s41421-024-00689-6

TURUN
YLIOPISTO
UNIVERSITY
OF TURKU

Painosalama, Turku, Finland 2025

ISBN 978-952-02-0104-3 (PRINT)
ISBN 978-952-02-0105-0 (PDF)
ISSN 0355-9483 (Print)
ISSN 2343-3213 (Online)